UNIVERSITÀ DEGLI STUDI DI PADOVA

UNIVERSITÀ DEGLI STUDI DI PADOVA

DEPARTMENT OF PHARMACEUTICAL AND PHARMACOLOGICAL SCIENCES

Doctoral School in Molecular Sciences

Curriculum in Pharmaceutical Sciences

Cycle XXVII

STUDIES ON POLYMER CONJUGATION OF THERAPEUTIC PROTEINS AND PEPTIDES

SCHOOL DEAN: Ch.mo Prof. Antonino Polimeno

COORDINATOR: Ch.mo Prof. Stefano Moro

SUPERVISOR: Ch.mo Prof. Gianfranco Pasut

PhD Student: Antonella Grigoletto

February 2nd, 2015

INDEX

ABBREVIATIONS AND SYMBOLS

°C	Celsius degrees
^{1}H-NMR	Nuclear magnetic resonance of the hydrogen
aa	amino acid/s
Abs	absorbance
$Abs_{0.1\%}$	absorbance of a solution 1g/L or 1mg/mL
ACN	acetonitrile
βGlu	β-Glutamic acid
Da	Dalton
DCC	N,N'-dicyclohexylcarbodiimide
DCI	N,N'-diisopropylcarbodimmide
DCM	dichloromethane
DDSs	drug delivery systems
DMF	dimethylformamide
DMSO	dimethylsulfoxide
DNA	desossiribonucleic acid
EtAOc	ethyl acetate
EtOH	ethanol
FDA	Food and Drug Administration
g	grams
GCSF	granulocyte colony-stimulating factor
h	hours
HCl	chloridic acid
HOBT	1-Hydroxybenzotriazole
kDa	kilo Dalton (10^{3} Da, equal to ≈ 1,66053886 * 10^{-24} g)
L	liters
m	meters
M	Molarity (mol/liter)
m	multiplet, multiplicity
MeOH	methanol
mg	milli grams (10^{-3} grams)
min	minute
mL	milli liters (10^{-3} liters)
mM	milli Molar (10^{-3} moles/liters)
mmol	milli moli (10^{-3} moles)
MW	molecular weight
$NaBH_3CN$	sodium cyanoborohydride
NaCl	sodium chloride
NaOH	sodium hydroxide

NHS	N-Hydroxysuccinimide
nm	nano meters (10^{-9} meters)
nmol	nano moli (10^{-9} moles)
o.n.	over nigth
PAGE	polyacrylamide gel electrophoresis
PBS	Phosfate Buffered Solution
PEG	polyethylene glycole
pH	$- \log_{10} [H_3O^+]$
PK	pharmacokinetic
ppm	parts per million
RP-HPLC	Reverse Phase - High Performance Liquid Chromatography
RT	room temperature
s	seconds
s	singlet, multiplicity
SEC-HPLC	Size Exlusion Chromatography - High Performance Liquid Chromatography
t	time
t	triplet, multiplicity
TFA	trifluoroacetic acid
THF	tetrahydrofuran
TLC	Thin Layer Chromatography
t_R	retention time
UV-Vis	ultraviolet-visible
v/v	volume per volume
w/v	weight per volume
μg	micro grams (10^{-6} grams)
μL	micro liters (10^{-6} liters)
μm	micro meters (10^{-6} meters)
μmol	micro moles (10^{-6} moles)

1 ABSTRACT

Since the introduction of recombinant insulin in 1979 and thanks to the advances in pharmaceutical biotechnology, therapeutic proteins and peptides have gained significant importance in the treatment of many diseases and after they represent the only therapeutic option. However, such growing success is not devoid of potential pitfalls like short half-life, easy enzymatic degradation and immunogenicity. PEGylation, namely the attachment of polyethylene glycol (PEG) chain(s) to a bioactive molecule, is nowadays one of the most commonly used strategies to overcome the inherent limits of therapeutic proteins.

The studies reported in this thesis are focused on the design and preparation of conjugates of therapeutic proteins and peptides with optimized polymeric carriers, in order to obtain improved performances in both pharmacokinetic and pharmacodynamic profiles of a conjugated biologic. The proteins and the peptide used are recombinant human granulocyte colony-stimulating factor (G-CSF), recombinant human growth hormone (hGH) and KR14, an anti-HIV triazole peptide (PT). G-CSF, hGH and KR14, owing to their low molecular weights, are rapidly excreted from the body and are subject to proteolytic degradation, resulting in low bioavailability and therefore requiring frequent administration schedule.

The first part of this PhD thesis was focused on: i) transglutaminase-mediated conjugation of common non charged or new multicarboxylic PEGs to G-CSF, ii) characterization and stability studies of the conjugates, iii) pharmacokinetic studies in animals, to allow the comparison between the conjugates and with the reference G-CSF. In this study, the aim was to test multicarboxylic PEG derivatives for evaluating the contribution of negative charges on protein half-life prolongation thanks to the charge-selective property of the glomerular filtration barrier. PEGylation with high molecular weight PEGs, by increasing the hydrodynamic volume of a protein, decreases the glomerular filtration rate, but may constitute a steric hindrance and reduce the binding affinity between the therapeutic protein and its target. The charge selectivity concept of the glomerular filtration barrier can be exploited with the new polyanionic polymers, which with low molecular weights, can still extend the PK profile of the protein and achieve also a better preservation of protein activity.

The investigated polyanionic PEG derivatives were i) $H_2N\text{-}PEG_{5k}\text{-}(COOH)_7$, a heterobifunctional PEG that was derivatized on one end with β-glutamic acid units to contain 7 carboxyl groups and ii) $H_2N\text{-}PEG_{3.4k}\text{-b-}PLE_{50}$, a linear polyanionic polymer that consists of a PEG linked to a PLE with the pendant ϒ-carboxyl groups of glutamic acid monomers. In addition to these two multicarboxylic PEGs, two classic uncharged PEGs with molecular weights of 5 kDa and 20 kDa were also used. After PEGylation, all the G-CSF-PEG conjugates were characterized by MALDI-TOF mass spectrometry, SDS-PAGE and circular dichroism and the pharmacokinetic studies were carried out in rats.

The second part of this PhD thesis focused on the comparison of the biological activity (stimulation of somatic growth) of three hGH conjugates differing for the

polymeric carrier (multicarboxylic or neutral) and for the site of polymer conjugation. The aim of this study was to evaluate if the protein stability and the protein/receptor recognition were influenced by the site of conjugation of the polymer and to assess the impact of polyanionic carriers on the pharmacodynamic behaviour of the protein.

Conjugation of the multicarboxylic polymer, poly(L-glutamic acid), resulted in an increase of the final negative charge of the conjugate. Based on the charge selectivity concept of glomerular filtration, polyanionic polymers having relatively low molecular weights may provide a half-life extension of a given protein, similar to that provided by higher molecular weight neutral polymers. Two different site-specific mono-PEGylated forms of hGH were prepared exploiting an enzymatic PEGylation (PEG-Gln141-hGH) via transglutaminase (TGase) and a chemical *N*-terminal PEGylation (PEG-Nter-hGH), using neutral 20kDa PEGs. Interestingly the conjugates showed an increased thermal stability and the ability to refold after thermal denaturation.

The third monoconjugate of hGH was prepared by chemical *N*-terminal conjugation, using poly(L-glutamic acid) with 50 glutamic acid units and with an aldehyde function at one end (PLE_{50ald}). The glutamic acid monomers confer to this polymer a polyanionic characteristic. hGH-PLE_{50ald} was characterized by MALDI-TOF mass spectrometry, SDS-PAGE, circular dichroism and the pharmacokinetic studies were carried out in rats. The bioactivities of a single dose of hGH-PLE_{50ald}, PEG-Gln141-hGH and PEG-Nter-hGH were similar or even better to that of a daily injection of hGH, by testing the somatic growth in hypophysectomized rats.

The third section of this work has dealt with: synthesis and characterization of KR14 peptide and its conjugation with PEG_{20kDa}-Mal, pharmacokinetic studies of the conjugate in mice and SPR affinity binding experiments. A part of this work was developed at the Department of Biochemistry and Molecular Biology of the Drexel University College of Medicine in Philadelphia, under the supervision of Professor Irwin Chaiken, whose laboratory is focused on the design and realization of peptide drugs that inhibit the entry of HIV-1 in the target cells. This initial step of HIV-1 entry is characterized by the binding of envelope glycoprotein gp120 on to the cellular receptor CD4 and co-receptor. The triazole peptide KR14 derive from a previously known family of PT's that has great therapeutic potential as it exhibits high affinity binding to gp120 and inhibits interactions of gp120 with both CD4 and the co-receptor surrogate mAb17b. KR14 was designed to contain a free thiol group at position 16 that has been exploited to achieve selective PEGylation with a PEG-maleimide of 20 kDa. The identity and purity of the conjugate were confirmed by SEC-HPLC and MALDI-TOF. Pharmacokinetic studies in mice demonstrated that PEGylation extended the t1/2 of the peptide from 44 min to 289 min. Even more remarkably the conjugate did not show the typical loss in bioactivity, common to most PEGylated drugs. In fact SPR studies demonstrated that PEG-KR14 is only about 1.5, 1.6 fold less active than KR14, a relevant result. In conclusion the studies

of this PhD thesis further demonstrated the potential of PEGylation in the delivery of protein and peptides. Although PEGylation is already a mature technology that yielded several products in clinical use, we demonstrated that there are still reasons for implementation and new discoveries by pursing also the renal filtration charge selectivity and not only the size selectivity as done so far in this field.

1 RIASSUNTO

Sin dall'introduzione dell'insulina ricombinante, nel 1979 e grazie ai progressi della biotecnologia farmaceutica, proteine e peptidi terapeutici hanno raggiunto una significativa importanza nel trattamento di molte patologie e rappresentano l'unica opzione terapeutica. Questo crescente successo non è comunque, privo di potenziali ostacoli come una breve emivita, una facile degradazione enzimatica e l'immunogenicità. La PEGhilazione, ovvero il legame di catene di polietilenglicole (PEG) a molecole bioattive, è oggigiorno una delle più comuni strategie usate per superare i limiti inerenti alle proteine terapeutiche.

Gli studi riportati in questa tesi di dottorato sono focalizzati sulla progettazione e preparazione di coniugati di proteine e peptidi terapeutici con carrier polimerici ottimizzati, in modo da ottenere migliori prestazioni dell'entità coniugata, sia dal punto di vista del profilo farmacocinetico che farmacodinamco. Le proteine e il peptide usati in questo lavoro sono G-CSF, o fattore di crescita umano ricombinante stimolante la formazione di colonie granulocitiche, hGH, o ormone della crescita umano ricombinante e KR14, un peptide anti-HIV. G-CSF, hGH e KR14, a causa del loro basso peso molecolare, sono rapidamente eliminati dall'organismo e sono soggetti a degradazione proteolitica, con conseguente bassa biodisponibilità e necessità di somministrazioni frequenti.

La prima parte di questa tesi di dottorato è focalizzata su: i) PEGhilazione enzimatica via transglutaminasi di G-CSF a PEG non carichi e a nuovi PEG multicarbossilati, ii) caratterizzazione e studi di stabilità dei coniugati ottenuti, iii) studi farmacocinetici in ratti, per avere un confronto tra i coniugati e la proteina nativa come riferimento. Lo scopo di questo studio è stato quello di testare i PEG multicarbossilati per valutare il contributo delle cariche negative sul prolungamento dell'emivita della proteina, grazie alle proprietà di selezione della carica della barriera di filtrazione del glomerulo. La PEGhilazione con PEG ad alto peso molecolare, aumentando il volume idrodinamico della proteina, riduce la velocità di filtrazione glomerulare, ma può costituire un impedimento sterico e ridurre l'affinità di legame tra la proteina terapeutica e il suo target. Il concetto di selettività della carica della barriera di filtrazione glomerulare può essere sfruttato con i nuovi polimeri polianionici, che, con un basso peso molecolare, possono mantenere un profilo farmacocinetico della proteina esteso e raggiungere anche una migliore conservazione dell'attività della proteina. I PEG polianionici usati per questo lavoro sono stati i) $H_2N\text{-}PEG_{5k}\text{-}(COOH)_7$, un PEG eterobifunzionale che è stato derivatizzato ad un'estremità con unità di acido β-glutammico e che possiede 7 gruppi carbossilici e ii) $H_2N\text{-}PEG_{3.4k}\text{-b-}PLE_{50}$, un polimero polianionico lineare costituito da PEG legato a PLE, il quale possiede i gruppi pendenti ϒ-carbossilici dei monomeri dell'acido glutammico. Oltre a questi due PEG multicarbossilati, sono stati usati anche due PEG non carichi, di peso molecolare 5 e 20 kDa. Dopo PEGhilazione, tutti i coniugati di G-CSF sono stati caratterizzati tramite MALDI-TOF, SDS-PAGE e dicroismo circolare e gli studi farmacocinetici sono stati condotti in ratti.

La seconda parte di questa tesi di dottorato si focalizza sul confronto dell'attività biologica (stimolazione della crescita somatica) di tre coniugati dell'ormone della crescita che si differenziano per il carrier polimerico (multicarbossilato o neutro) e per il sito di coniugazione del polimero. Lo scopo di questo studio è stato valutare se la stabilità della proteina e il riconoscimento proteina/recettore sono stati influenzati dal sito di coniugazione del polimero e verificare l'impatto di carrier polianionici sul profilo farmacodinamico della proteina. La coniugazione del polimero multicarbossilato, acido (poli)glutammico, risulta in un aumento della carica negativa netta del coniugato. Sulla base del concetto di selettività della carica della filtrazione glomerulare, polimeri polianionici aventi pesi molecolari relativamente bassi, possono fornire un'estensione dell'emivita di una proteina simile a quella ottenuta con polimeri neutri di alto peso molecolare. Due diverse forme di hGH mono-PEGhilato in maniera sito-specifica sono state preparate sfruttando una PEGhilazione enzimatica (PEG-Gln141-hGH) via tranglutaminase (TGase) e una PEGhilazione chimica all'*N*-terminale (PEG-Nter-hGH), usando PEG neutri di peso molecolare 20 kDa. Interessante è il fatto che i coniugati hanno mostrato una stabilità termica aumentata e la capacità di refold dopo denaturazione termica.

Il terzo monoconiugato di hGH è stato preparato tramite coniugazione all'N-terminale, usando un acido (poli)glutammico con 50 unità di acido glutammico e con una funzione aldeidica ad un'estremità (PLE50ald). I monomeri di acido glutammico conferiscono al polimero la caratteristica di polianionico. hGH-PLE50ald è stato caratterizzato tramite MALDI-TOF, SDS-PAGE, dicroismo circolare e gli studi farmacocinetici sono stati condotti in ratti. La bioattività di una dose singola di hGH-PLE50ald, PEG-Gln141-hGH e PEG-Nter-hGH si è dimostrata simile o migliore rispetto a iniezioni giornaliere di hGH, misurando la crescita somatica in ratti ipofisectomizzati.

La terza parte di questo lavoro tratta di: sintesi e caratterizzazione di KR14 e coniugazione di KR14 a PEG20kDa-Mal, studi farmacocinetici del coniugato in topi e studi di affinità di legame tramite SPR. Una parte di questo lavoro è stata sviluppata al Dipartimento di Biochimica e Biologia Molecolare presso Drexel University College of Medicine a Philadelphia, sotto la supervisione del Professor Irwin Chaiken, il cui laboratorio è focalizzato sulla progettazione e realizzazione di farmaci peptidici che inibiscono l'entrata del virus HIV-1 nelle cellule target. Questo passaggio iniziale di entrata del virus è caratterizzato dal legame della glicoproteina di membrana gp120 al recettore cellulare CD4 e al co-recettore. Il peptide KR14 proviene da una famiglia già nota di peptidi, modificati con triazolo, che ha un considerevole potenziale terapeutico, esibendo alta affinità di legame per la gp120 e inibendo le interazioni di gp120 con CD4 e con il surrogato del co-recettore mAb17b.

KR14 è stato progettato in modo da comprendere un gruppo tiolico libero in posizione 16, che è stato utilizzato per la PEGhilazione selettiva con un PEG-maleimide di 20 kDa. L'identità e la purezza del coniugato sono state confermate

tramite SEC-HPLC e MALDI-TOF. Gli studi farmacocinetici in topi hanno dimostrato che la PEGhilazione ha prolungato l'emivita del peptide da 44 minuti a 289 minuti. Ancora più interessante, il coniugato non ha mostrato la tipica perdita di bioattività, comune alla maggior parte dei farmaci PEGhilati. Infatti gli studi SPR hanno dimostrato che PEG-KR14 è solo 1,5, 1,6 volte meno attivo di KR14, un risultato rilevante.

In conclusione gli studi di questa tesi di dottorato hanno dimostrato ulteriormente il potenziale della PEGhilazione nella veicolazione di proteine e peptidi. Anche se la PEGhilazione è già una tecnologia matura che ha portato diversi prodotti in uso clinico, abbiamo dimostrato che ci sono ancora motivi per l'implementazione e le nuove scoperte, perseguendo anche la selettività di carica della filtrazione renale e non solo la selettività per dimensioni, come fatto finora in questo campo.

2 INTRODUCTION

2.1 THERAPEUTIC PROTEINS

The growing knowledge in disciplines such as molecular biology and proteomics, and the recent developments in biotechnology in the past few decades, have resulted in a great interest in biotechnological drugs and discoveries on the role and activity of new proteins. Many of these proteins might be involved in pathological conditions, might represent new targets for highly specific therapies, or might even, themselves, become new drugs. Furthermore, a considerable number of proteins as therapeutic agents are approved drugs, currently on the market and have had great success in treating various diseases that were not possible to treat with conventional drugs [1].

The high structural complexity and certain physico-chemical characteristics of proteins limit their use in therapy. Proteins are very sensitive to variations in temperature, pH, and ionic force and are easily degraded by microbial agents. Moreover the therapeutic application of a new protein is hampered by unexpected shortcomings and/or poor therapeutic outcomes. Among these potential limits it is possible to list rapid body clearance, immunogenicity, physical and chemical instabilities (e.g. aggregation, adsorption, deamination, clipping, oxidation, etc.), and enzymatic degradation. In particular, a short half-life in blood, common for proteins having a molecular weight below the kidney excretion threshold, is of itself a significant problem because is reflected in frequent administrations of therapeutics or in administrations at high doses, to reach the desired effect, thus also simultaneously aggravating side effects.

Several tools for the development of better therapeutic proteins, can be exploited, such as genetic engineering [2], advanced protein formulation, and delivery [3]. Genetic engineering is strictly at the base of some delivery approaches like the expression of fusion or hyper-glycosylated proteins. Drug delivery systems (DDSs) are particularly promising in improving the *in vivo* efficacy of active molecules as they can prolong the in vivo half-life and protect the drug from enzymatic degradation, thus enhancing the in vivo bioactivity. Various drug delivery approaches have been proposed and investigated to overcome the over mentioned limitations, including incorporation into micro/nanoparticles, liposomes or hydrogels and chemical modification with small molecules or polymers. Among others, conjugation of polymers to proteins surface has been a successful technology. Either natural or synthetic polymers have been tested for this purpose, but only poly(ethyleneglycol) (PEG) resulted in conjugates of great therapeutic and clinical success and therefore is widely used for the delivery of therapeutic proteins.

2.2 PEGYLATION OF PROTEINS AND PEPTIDES

PEGylation is defined as the covalent attachment of poly(ethylene glycol) (PEG) chains to bioactive molecules. This technique has become the leading approach for overcoming most of the aforementioned limits of biologics and the number of PEGylated products on the market is continuously increasing, together with the number of new conjugates entering clinical trials [4].

2.2.1 Characteristic of polymeric carrier

Several polymers of natural and synthetic origin have been studied. This resulted in the identification of requirements for an ideal carrier:

- the polymer must be biocompatible and not induce significant toxicity or immunogenicity;
- must be biodegradable by hydrolytic or enzymatic activity or have a molecular weight below the kidney excretion threshold;
- posses a low polydispersity;
- must be found in large-scale, low cost and made by simple economic processes;
- must be hydrophilic;
- must possess the functional groups that allow binding of the drug.

2.2.2 Poly(ethylene glycol) (PEG)

PEG is a synthetic and amphiphilic polymer composed of repeated oxyethylene units with molecular weight of 44 Da (figure 2.1).

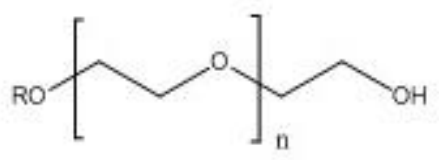

Figure 2.1: Structural formula of PEG.

PEG is synthesized by anionic ring opening polymerization of ethylene oxide, initiated by nucleophilic attack of an anion on the epoxide ring. The three phases of the synthesis of PEG, shown in figure 2.2, are as follows:

I. Initiation: it begins with the nucleophile attack of OH^- to ethylene oxide cyclic opening the epoxy ring and the formation of oxygen reactive alcohol;
II. Propagation: the reaction propagation continues with the addition of other ethylene oxide molecules;
III. Termination: the reaction is stopped by the action of a terminator.

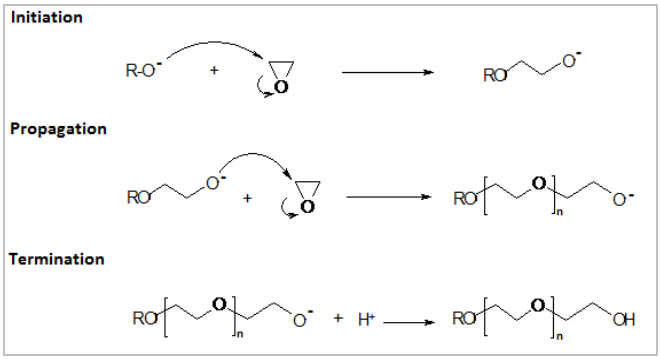

Figure 2.2: Synthesis of PEG.

The initiator anion (RO^-) can be a hydroxide (OH^-) or methoxide (CH_3O^-); the former results in the formation of a bifunctional diol, whereas the latter results in the formation of a monomethoxy PEG (figure 2.3). The main advantage of monomethoxy PEG (mPEG) is the presence of only one functional group, preventing the cross-linking phenomenon. For polypeptide modification, mPEG is widely applied because of its negligible in vivo toxicity and ease of activation.

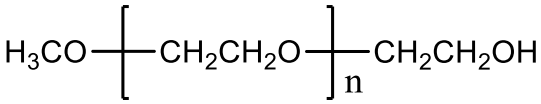

Figure 2.3: Structural formula of PEG.

Appropriate modulation of the polymerization reaction allows the attainment of polymeric chains of different molecular weights (300-50000 Da) characterized by a low polydispersity index. Physical properties of the polymer depends on the average length of the chain: the polymer is in the liquid form when its molecular weight is below 1 kDa, and in the solid form when above 1 kDa.

PEG is a polymer suitable for bioconjugation thanks to many characteristics: is non-toxic, biocompatible, non-antigenic, and non-immunogenic. It is soluble in water and many organic solvents such as dichloromethane, chloroform, and benzene, whereas insoluble in ethanol and hexane. Being a non-biodegradable polymer, it must be used at molecular weights below 40 kDa to avoid body accumulation and it is available in the market in a wide range of molecular weights and structures at low cost. These characteristics allow the use of PEG in various applications in biomedical field. It has been approved by the American Food and Drug

Administration (FDA) as a constituent of food, cosmetic products and pharmaceutical formulations.

Moreover, PEG has a great capacity of coordinating water molecules, allowing to increase its hydrodynamic volume up to 5-10 fold. The glomerular filtration limit for PEG, therefore, is not 66 kDa as it is for proteins, but is 20 kDa. Consequently, elimination of PEGs having molecular weights greater than 20 kDa is mainly via biliary route. PEGs of molecular weights higher than 40 kDa should not be used, as PEG is not biodegradable and would accumulate in the body.

2.2.3 Advantages of PEGylation

PEG is one of the most commonly used polymers in the field of drug delivery, due to its physico-chemical characteristics such as high flexibility, hydrataion, and biocompatibility. PEGylation of therapeutic proteins results in conjugates with improved physico-chemical and pharmacokinetic characteristics.

Among the main advantages of therapeutic protein PEGylation are:

- reduction of the rapid kidney clearance of the PEGylated protein by increasing its hydrodynamic volume,
- protection from chemical and enzymatic degradation, due to the masking of amino acid sequences or critical sites that are sensitive to degradation,
- prevention of immunogenicity, by masking of critical sites recognized by antibodies,
- increasing of thermal stability of proteins [5],
- reduction of protein aggregation owing to a repulsion between PEGylated surfaces [6]
- reduction of administration and dosages (Figure 2.4)

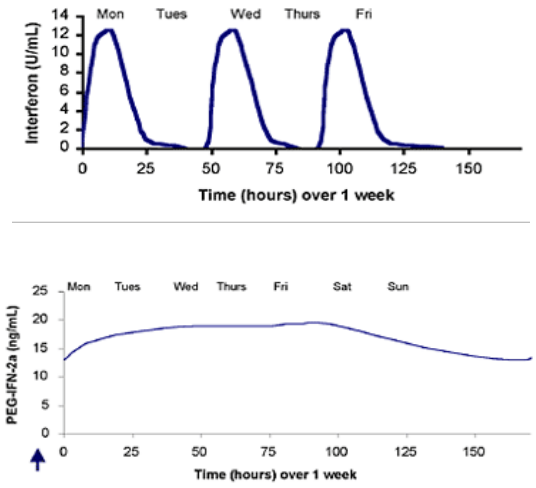

Figure 2.4: Interferon and PEG-IFN-2a administration.

Many studies on this technology report that the secondary and tertiary structures of the conjugated proteins were unchanged after PEGylation [7, 8]. Nevertheless, a reduction in biological potency is usual after PEGylation due to the steric entanglement of polymer chains during protein/receptor recognition process.

2.2.4 Chemistry of PEGylation

A linear PEG derivative, used for PEGylation, has two unique ends. For the coupling of PEG to a molecule (i.e. proteins, peptides), it is necessary to activate the PEG through derivatization with a functional group at one or both ends. The choice of the functional group depends on the available target reactive group on the molecule to be PEGylated. The most commonly selected PEGylation sites in proteins are *N*-terminal amino group or the ε-amino group of lysines and thiol group of cysteines, due to their relatively high chemical reactivity under mild conditions with respect to other amino acid residues.
Various PEG derivatives used for PEGylation reactions are as follows:

- PEG derivatives reactive towards amino groups: include alkylating PEGs (Figure 2.5) which result in the formation of a secondary amine upon coupling to a protein and acylating PEGs such as PEG-carboxylates (Figure 2.6) and PEG-carbonates (Figure 2.7) that generate amides or urethanes.
- PEG derivatives reactive towards thiol groups: include PEG–pyridildisulphide, PEG–maleimide, PEG–vinylsulfone, and PEG–iodo acetamide (Figure 2.8).

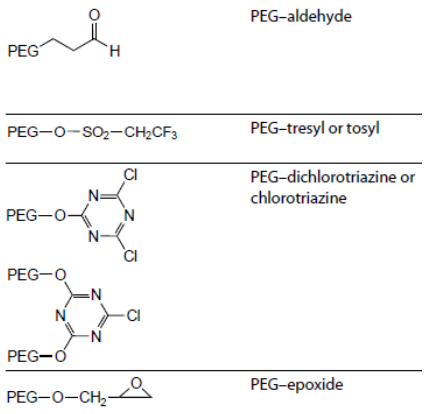

Figure 2.5: Alkylating PEGs.

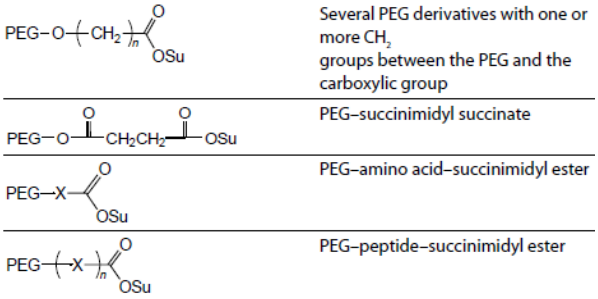

Figure 2.6: PEG-carboxylates.

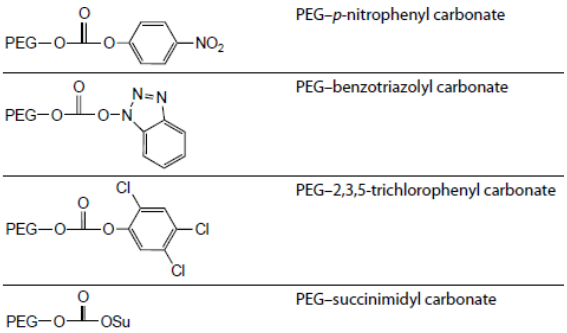

Figure 2.7: PEG-carbonates.

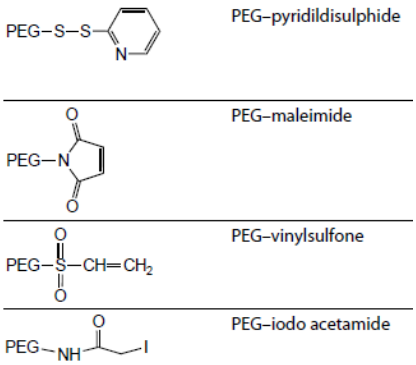

Figure 2.8: Thiol reactive PEGs.

Recently, PEGs having particular structures and/or functions have been designed to improve the characteristics of the bioconjugates, including branched, dendritic and multi-arm PEGs. Figure 2.9 demonstrates several different PEG structures.

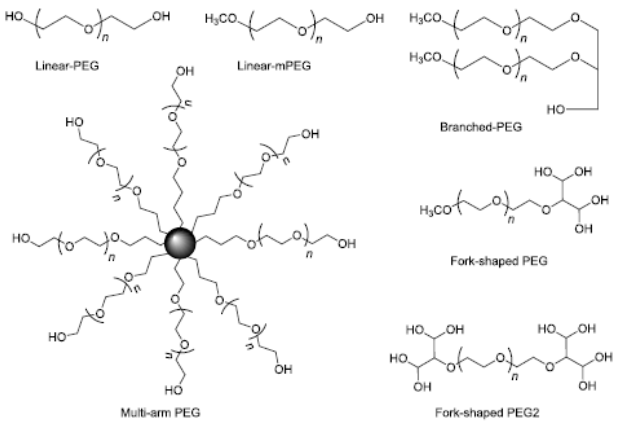

Figure 2.9: Various PEG structures [9].

2.2.5 PEGylation strategies

An ideal PEGylation strategy must ensure the preservation of protein's biologic activity to a high extent and this can be achieved by coupling the polymer to the amino acid residues that are not essential for the biological activity of the protein or the peptide. Moreover, it should shield the amino acid sequences that are subject to proteolytic degradation and those that are epitopes for antibodies. To this extent, the important parameters to take into consideration for PEGylation of therapeutic proteins and peptides are the molecular weight of PEG to be used, the type of its activating group and the conjugation method.

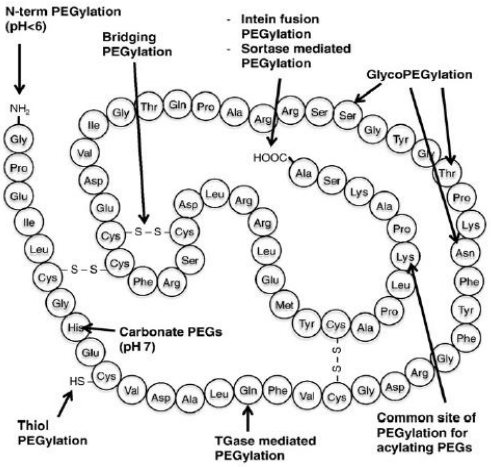

Figure 2.10: Drawing of amino acids and sites in a protein that can be modified by PEGylation.

Several FDA-approved PEGylated therapeutic proteins currently in the market are products of non-specific conjugation. Amine PEGylation, where the polymer is coupled to the ε-amine of lysine residues, is the most widely used technique among the non-specific ones. Due to the abundance of lysine residues in proteins, however,

this technique has low selectivity and results in complex mixtures with different degrees of PEGylation, compromising the bioactivity of proteins. The final product, given its heterogeneity, is relatively hard to purify and characterize. More recently, with the aim of overcoming these limitations, researchers have developed site-specific PEGylation techniques including N-terminal PEGylation, thiol PEGylation, bridging PEGylation, and enzymatic PEGylation. In figure 2.10, the different sites of PEGylation are shown.

N-terminal PEGylation. *N*-terminal PEGylation takes advantage of the different *pKa* values between the ε-amino residue of lysines, about 9.3–9.5, and the α-amino group at the protein *N*-terminus, about 7.6–8. In mildly acidic conditions (pH 6–6.5) the reaction at the *N*-terminus is selective because, at that pH, the ε-amino groups are protonated and consequently no reactive toward PEGylating agents while the α-amino group is still partially present as free base and available for the coupling reaction. Low-reactivity PEGylating agents such as PEG-aldehyde should be used for this type of conjugation, otherwise the polymer might be coupled to lysine residues as well.

The conjugation reaction proceeds as follows (Figure 2.11):

1. formation of a Schiff base intermediate (R_1-N=CH-R_2) between the aldehyde and *N*-terminal
2. Reduction of the Schiff base to secondary amine with $NaCNBH_3$

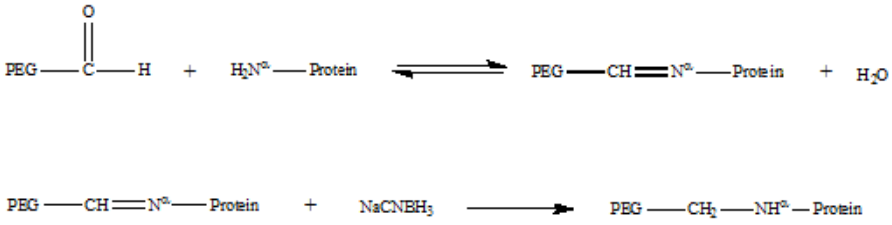

Figure 2.11: Site-specific conjugation of PEG-aldehyde to protein *N*-terminal.

Thiol PEGylation. Cysteine, in its reduced form, is rarely present in proteins because it is usually paired with another cysteine, forming a disulfide bridge. Proteins with a single free cysteine can be site-specifically PEGylated using a PEG derivative reactive toward this residue. Moreover, thanks to genetic engineering, thiol PEGylation is not limited only to those proteins having a free cysteine but can be virtually applied to any biologics. PEG maleimide is the most common used thiol reactive PEGylating agent. A thioether bond is formed by Michael's addition between the double bond of the maleimide ring and the thiol group of cysteine (figure 2.12).

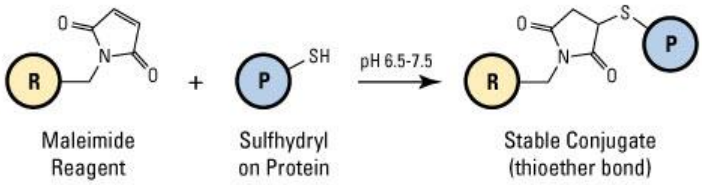

Figure 2.12: Thiol PEGylation.

Bridging PEGylation. Disulfide bridges are found in small numbers in therapeutic proteins, therefore can be considered for site-selective PEGylation. In this technique, a bifunctional PEGylating agent is linked to a reduced disulfide bridge in the protein. The scheme of reaction is shown in figure 2.12.

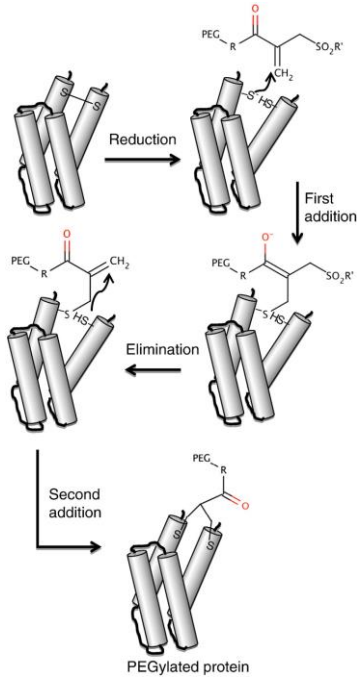

Figure 2.12: Bridging PEGylation.

Enzymatic PEGylation. Enzymes have been considered as tools for site-specific PEGylation of proteins, especially for coupling PEGs to amino acid residues that are usually not modified with chemical methods. Due to the high specificity and selectivity of the enzymes, the yield of the synthesis is generally high. Microbial transglutaminase (mTGase) and sortase A are among the enzymes that have been investigated for this purpose.

2.2.5.1 mTGase-mediated PEGylation

TGases are a large family of enzymes detected in several organisms, including mammals, invertebrates, plants and microorganisms [10]. These enzymes are widely distributed in most tissues and body fluids, including liver, hair follicles, epidermis,

prostate and blood and are thought to be involved in a variety of physiological functions. TGase(s) catalyze the acyl transfer between the γ-carboxamide group of a protein-bound glutamine (Gln) residue and an aliphatic primary amine, generally the ε-amino group of a lysine (Lys) residue [11] (Figure 2.13). A typical example of a TGase-catalyzed protein crosslinking reaction is the termination of bleeding in wound healing (blood coagulation) by factor XIIIa, an activated form of plasma TGase catalysing crosslinking between fibrin molecules [12].

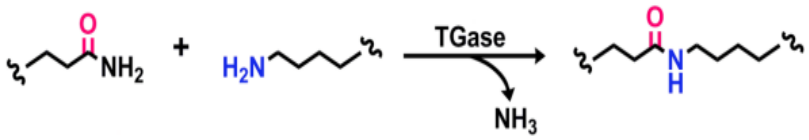

Figure 2.13: Amide bond formation catalyzed by TGase [13].

Among all the types of TGase(s), the most useful is a microbial TGase derived from a variant of *Streptomyces mobaraense* (Figure 2.14). mTGase has a molecular weight of 37.9 kDa, a high reaction rate and consists of a compact domain with the Cys64, the residue essential for the catalytic activity, located at the bottom of a deep cleft [14] (Figure 2.15).

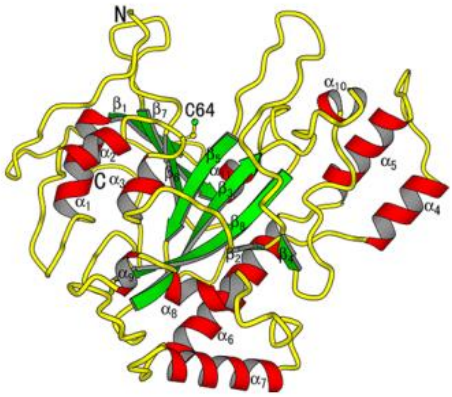

Figure 2.14: Overall structure of microbial TGase. Side chain of Cys64 is presented with ball-and-stick model [15].

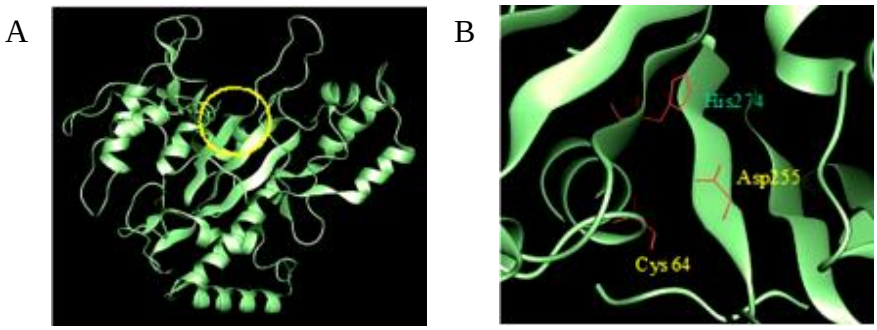

Figure 2.15: A) Overall structure of mTGase. Region in yellow circle: active site. B) Structure around the active site of mTGase. The catalytic triad of mTGase (Cys64, Asp255, His274) is presented with red wire model.

For protein PEGylation, an amino-derivative of PEG (PEG-NH_2) can be used as an amino donor in a TGase-mediated reaction to covalently attach a PEG moiety to protein-bound Gln residues of proteins of clinical utility [16]. The key step for catalysis involves the interaction of a γ-carboxamide group of a Gln residue of a polypeptide substrate with the TGases active site, forming a reactive thioacyl-moiety at the level of the Cys64 residue and then reaction with an amino donor, thus leading to a new isopeptide amide bond.

mTGase has been studied and employed for bioactive drug application and in particular for covalent binding of PEG to a pharmaceutical protein, where its glutamine (Gln) residue(s) serves as acyl donor and an amino-derivative of PEG (PEG-NH_2) serves as acyl acceptor (Figure 2.16). mTGase-mediated PEGylation presents two important advantages:

i) the modification of glutamine, a residue that otherwise cannot be modified with chemical methods, and
ii) the obtainment of highly homogenous conjugate isomer mixtures because usually only one or two glutamines, of all those present in a protein, are a substrate for the enzyme.

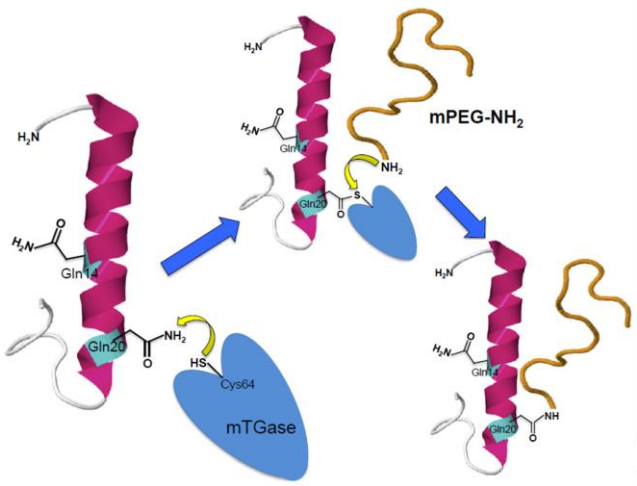

Figure 2.16: Site-specific enzymatic PEGylation via mTGase.

The conjugation reaction occurs in a highly site-specific manner; even when the protein contains more than one glutamine residue, usually only one or two are the substrates for the enzyme.

Mero et al [17] conjugated a monodisperse Boc-PEG-NH2 via mTGase to three model proteins containing 17, 11, and 6 Gln residues (human G-CSF, human growth hormone, and horse heart apomyoglobin, respectively) and identified the glutamine

residues that were covalently attached to PEG by mass spectrometry. The results showed that, mTGase-mediated PEGylation of these three model proteins led to the production of only mono- and bi-conjugates.

Several studies have been conducted to investigate the substrate specificity of TGases and the results revealed that there is no obvious consensus sequence around the Gln residues modified by TGase [18]. Fontana et al [19] observed that there is a notable correlation between the sites of enhanced chain flexibility and the sites of TGase attack. They concluded that the main feature directing the site-specific modification of a protein-bound Gln residue by TGase in a globular protein, is the flexibility or local unfolding of the chain region encompassing that Gln residue.

When only one glutamine residue of a protein is substrate for mTGase, the resulting conjugate is homogenous. However, if the protein to be PEGylated contains more than one Gln residue as substrate for mTGase, the reaction results in a mixture of isomers. In that case, the selectivity of mTGase can be further increased by performing the reaction in the presence of organic co-solvents that would modify the flexibility of the chain encompassing the substrate Gln residue [20]. The organic co-solvent acts as structure modifier and changes the native folding of the protein, reducing the flexibility of some regions. If a Gln residue found in these regions is substrate for mTGase in physiological conditions, it would lose its accessibility to mTGase upon the conformation change. Only the formerly substrate Gln residues encompassed in regions that are not affected by the presence of the organic co-solvent will be substrates for mTGase in these new conditions.

This strategy has been successfully applied to two model therapeutic proteins, salmon calcitonin and human growth hormon, with ethanol used as organic co-solvent. Both proteins, possessing two glutamine residues as mTGase substrate and therefore yielding a mixture of isomers when PEGylated via mTGase in physiological buffers, yielded pure mono-PEGylated isomers when PEGylated in the presence of ethanol as co-solvent. In the view of these findings, it can be concluded that mTGase is a good choice for the site-specific PEGylation of therapeutic proteins.

In this PhD thesis the PEGylation strategies used for the synthesis of the discussed conjugates were enzymatic PEGylation via mTGase, *N*-terminal PEGylation and thiol PEGylation.

2.3 MULTICARBOXYLIC POLYMERS FOR THE DELIVERY OF PROTEINS

PEGylation lead to a great improvement of the PK profile of a given protein but usually also a reduction in biological potency after modification, due to the steric

entanglement of polymer chains during recognition of the protein with its target. Although the reduction of the binding affinity is counterbalanced by a large improvement of the systemic exposure, site-selective conjugations strategies have improved the retention of the biologic activity. Moreover, the use of new PEGylating agents (polyanionic PEG) of low molecular weight should minimize the loss of biologics potency and allow the same systemic exposure obtained with neutral and higher molecular weight PEGs.

2.3.1 Influence of ionic charge on glomerular filtration

Proteins are eliminated from the body mainly by renal excretion. The glomerular filtration rate of low molecular weight molecules is higher compared to that of high molecular weight ones, and this phenomenon is responsible for the short plasma half-life of therapeutic proteins. However, glomerular filtration rate does not depend only on the dimension of the proteins, but also on their ionic charge. It has been demonstrated that macromolecules, such as proteins, show a different elimination profile if they are charged [21].

The glomerular filtration barrier is composed of three layers: the fenestrated endothelium, the podocyte foot processes with bridging slit diaphragms and the intervening glomerular basement membrane (figure 2.17) [22]. The glomerular basement membrane consists of high-molecular weight proteins, including type IV collagen, laminins, entactin/nidogen, and sulfated proteoglycans. The major extracellular matrix-sulfated proteoglycans are collagen XVIII, perlecan, and agrin, all including heparin sulfate and chondroitin sulfate glycosaminoglycan chains. These chains, due to having sulfate radicals, impart negative charge on the glomerular basement membrane, and provide it with charge selective properties besides size-selectivity [23].

Negative charge associated with the glomerular filtration barrier is thought to retard filtration of anionic molecules due to repulsion [22]. This characteristic can be benefited to design new protein delivery systems using polyanionic polymers.

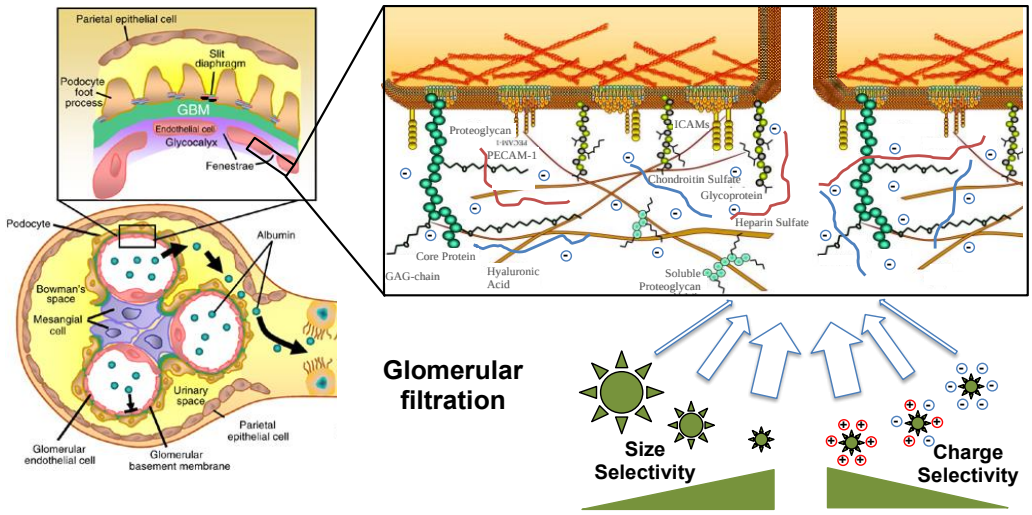

Figure 2.17: The glomerular filtration barrier and the concept of charge selectivity.

2.3.2 Multicarboxylic polymers

Multicarboxylic polymers bear on their structure carboxylic groups –COOH that confer the polyanionic characteristic to the polymeric backbone. PEG-dendron and poly(L-glutamic acid) (PLE) are among the examples of polyanionic polymers.

PEG dendron (Figure 2.18) is characterized by a heterobifunctional PEG chain. At one end it is derivatized with a symmetric bicarboxylic unit such as β-glutamic acid, which provides the polymer with a branched structure with negative charges. The other end of the heterobifunctional chain may be derivatized with a functional group suitable for the conjugation method to be employed.

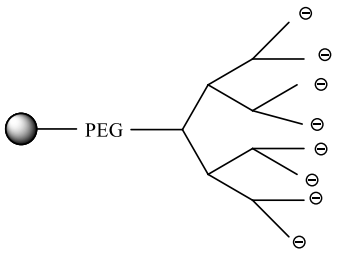

Figure 2.18: PEG-dendron structure.

PEG-dendron, $H_2N\text{-}PEG_{5k}\text{-}(COOH)_7$, was synthetized starting from Boc-NH-PEG_{5k}-NHS of 5003 Da where, at one end, the amino group was protected with t-Boc. After the removal of the protecting group to obtain the free amino group, the polymer was used for enzymatic PEGylation via tranglutaminase.

PLE (Figure 2.19) is a natural polymer obtained by polymerization of β-glutamic acid, with the formation of peptide bonds. PLE, therefore, is biodegradable and non-

toxic. It has a linear structure with a pending ϒ-carboxyl group for each repeated glutamic acid unit, conferring the polymer a polyanionic characteristic. The carboxylic groups, negative charged in phisiological condition, confer the solubility to the polymer. Moreover, the polymer has a ordered α-helical structure at pH lower than 5, while at higher pH, the ordered structure is converted in a random one.

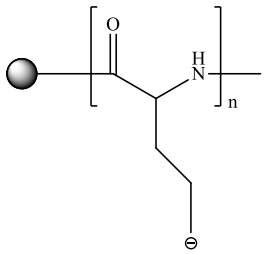

Figure 2.19: PLE structure.

The PLE used in this thesis has 50 glutamic acid units (MW 6726 Da) and an aldehyde function at one end, protected by an acetal group. After removal of the protecting group, the polymer was used for *N*-terminal conjugation via aldehyde.

The third used multicarboxylic polymers was H_2N-$PEG_{3.4k}$-b-PLE_{50}, a linear polyanionic polymer that consists of a PEG of 3.4 kDa linked to PLE made up of 50 L-glutamic acid units (Figure 2.20). Also in this case, the amino group suitable for enzymatic PEGylation, was initially protected by t-Boc.

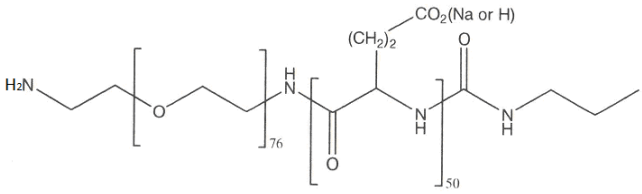

Figure 2.20: PEG-PLE structure.

2.3.3 Multicarboxylic polymers for the delivery of Granulocyte-Colony Stimulating Factor and human Growth Hormone

PEGylation, by increasing the hydrodynamic volume of a protein, decreases its renal clearance rate. However, while improving the pharmacokinetic profile of the conjugate, it may constitute a steric hindrance and reduce the binding affinity between the therapeutic protein and its target.

Therefore, in order to significantly improve the pharmacokinetic profile of proteins, polyanionic PEGs with lower molecular weights than those required with neutral PEGs may be considered as protein carriers, thus reducing the typical steric

hindrance of high molecular weight PEG that might impair the biological function of proteins. To this aim the new polyanionic polymers, previously described, can be taken into consideration for therapeutic protein delivery applications.

Moreover, polyanionic carriers should have also an impact on the pharmacodynamic behaviour of the protein. Conjugation of multicarboxylic polymers result in an increase of the final negative charge of the conjugate. The possibility to obtain the same half-life prolongation with low molecolar weight negative polymer might allows:

i) a faster diffusion of the conjugate into the tissues, thanks to the lower hydrodinamic volume of the polymer,
ii) a better preservation of the binding affinity of the protein to its receptor, thanks to the lower steric hindrance provided by the polymer and
iii) a decrease of protein aggregation due to charge repulsion.

2.4 G-CSF

G-CSF is a hematopoietic growth factor of myeloid lineage that regulates the proliferation, differentiation, and survival of granulocytes. Granulocytes (neutrophils, eosinophils, and basophils) are important mediators of antimicrobial and inflammatory responses. They are produced in bone marrow, through a process known as granulopoiesis (figure 2.21), both in health and diseased state. The productive capacity of bone marrow can increase to at least 10-fold in response to stress conditions [24].

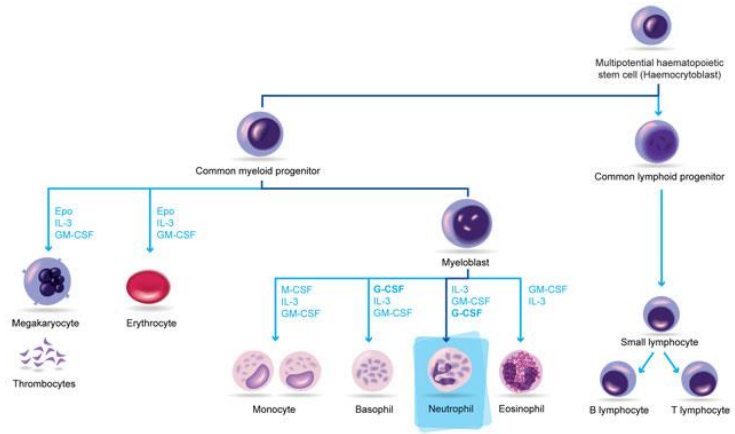

Figure 2.21: Granulopoiesis in humans.

Neutrophils represent the major subset of granulocytes, comprising 50–75% of the total circulating leukocytes. They play a fundamental role in immune response to invading bacteria, fungi, protozoa, viruses and tumor cells [24]. G-CSF is central to the production of neutrophils and is responsible for the significant increase in

neutrophil production in response to stress conditions, such as infection or offensive acts compromising bone marrow function, including anti-cancer chemotherapy.

Many tissues can produce G-CSF when appropriately stimulated with inflammatory mediators such as lipopolysaccharide (LPS), tumor necrosis factor (TNF)-α, interferon (IFN)-β, vascular endothelial growth factor (VEGF), interleukin (IL)-17 and IL-1, inducing expression in endothelial cells, macrophages, epithelial cells and fibroblasts [25]. Release of G-CSF into the bloodstream by tissues stimulates neutrophil production within the bone marrow.

G-CSF has also been shown to have an important influence on the biological functions of mature neutrophils. It stimulates phagocytic and chemotactic activity of neutrophils, increases the production of reactive oxygen intermediates in response to bacterial peptides, and enhances antibody-mediated cellular cytotoxicity (ADCC) against antibody-coated tumor target cells [26].

Additionally, G-CSF has shown to induce hematopoietic stem cell mobilization. Under normal conditions, the vast majority of hematopoietic stem/progenitors cells (HSPCs) reside in the bone marrow. The number of HSPCs in the circulation can be significantly increased in response to a number of stimuli, including hematopoietic growth factors and environmental stress such as infection [27]. A number of chemokines and cytokines have been shown to enhance migration of HSPCs into the peripheral blood [28]. This process is called hematopoietic stem cell mobilization.

2.4.1 Structure of human G-CSF

Mature human G-CSF is an 18.8 kDa protein composed of 174 amino acids (figure 2.22), cleaved from a precursor of 207 amino acids. It contains two intra-molecular disulphide bonds (Cys36-Cys42 and Cys64-Cys74) that are essential for proper folding and function, and one free cysteine residue (Cys17). Native human G-CSF has a single O-glycosylation site (Thr133) that protects the protein from aggregation but does not play a role in the biological activity of the protein [29]. G-CSF contains 17 glutamine (Q) residues.

```
TPLGPASSLP QSFLLKCLEQ VRKIQGDGAA LQEKLCATYK  40
LCHPEELVLL GHSLGIPWAP LSSCPSQALQ LAGCLSQLHS  80
GLFLYQGLLQ ALEGISPELG PTLDTLQLDV ADFATTIWQQ 120
MEELGMAPAL QPTQGAMPAF ASAFQRRAGG VLVASHLQSF 160
LEVSYRVLRH LAQP                             174
```

Figure 2.22: Aminoacid sequence of G-CSF.

X-ray crystallography of G-CSF revealed a four-α-helical bundle structure with an additional short 3_{10} helix (figure 2.23) [30].

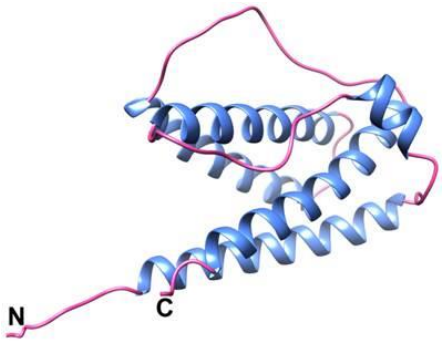

Figure 2.23: Ribbon representation of the structure of human G-CSF. Helical regions are colored in blue, coil regions in pink.

2.4.2 Recombinant human G-CSF and its therapeutic use

Recombinant human G-CSF (rhG-CSF) has been widely used as a therapeutic agent to treat chemotherapy-induced neutropenia in cancer patients, and to accelerate hematopoietic recovery following transplantation. More recently, it has also been employed to achieve hematopoietic stem cell mobilization for stem cell transplantation.

Chemotherapy is frequently accompanied by hematopoietic side effects due to the myelosuppressive character of the drugs used. These side effects generally include neutropenia (accompanied by fever and possible infection) and, to a lesser extent, thrombocytopenia and/or anemia [31]. rhG-CSF treatment reduces the duration of neutropenia and enhances hematopoietic reconstitution, and has therefore been used for recovery from chemotherapy and bone marrow transplantation.

Recombinant human G-CSF was approved by the Food and Drug Administration (FDA) for the first time in 1991, under the generic name filgrastim (brand name: Neupogen®), for use in chemotherapy-induced neutropenia. Filgrastim, produced in Escherichia coli by recombinant DNA technology, has the identical biological activity as the endogenous protein. It only differs from the endogenous G-CSF in that it contains an additional N-terminal methionine residue and is not glycosylated [32]. Another pharmaceutical analog of human G-CSF is lenograstim, which is produced in Chinese Hamster Ovary (CHO) cells, and is therefore glycosylated.

Several filgrastim biosimilars are currently in the market and are widely used. Nevertheless, filgrastim is rapidly excreted from the body due to its low molecular weight and consequent rapid renal clearance. It is also subject to proteolytic degradation. These issues result in a short half-life in vivo (1.8 - 3.5 hours), requiring multiple injections during one cycle of chemotherapy in cancer patients. In order to prolong the plasma half-life of filgrastim by decreasing its renal excretion, cellular uptake and proteolysis, a PEGylated filgrastim (Pegfilgrastim) was developed. Pegfilgrastim, obtained by N-terminal-specific chemical conjugation of the protein to

a linear PEG of 20 kDa, has demonstrated a significantly prolonged half-life (15 to 80 hours), and is currently in the market under the name of Neulasta®. Clinical studies have shown that the effect of a single subcutaneous injection of Neulasta®, administered once per chemotherapy cycle, is similar to that of daily administered filgrastim.

Scaramuzza et al [33] conjugated a PEG of 20 kDa to glutamine 135 residue of filgrastim, site-specifically, via microbial transglutaminase enzyme. The result was a new monoPEGylated filgrastim derivate, named BK0026.

2.5 hGH

hGH is a 22-kDa protein secreted by the pituitary gland. Somatotroph cells located in the anterior pituitary gland intermittently releases growth hormone (hGH), which has many physiological functions including growth promotion, protein synthesis, lipolysis and regulation of metabolic processes [34]. Although growth hormone has many biological functions, its major target organs are bone and muscle, promoting the growth of the bone and increasing the mass of the muscles [35].

hGH deficiency in children results in a condition called pituitary dwarfism, which is characterized by slowed long bone growth, younger facial features and sometimes a chubby body build. Puberty may come late or not at all in older children. It is estimated that 10,000–15,000 children in the United States have growth failure due to growth hormone deficiency [36].

2.5.1 Structure of hGH

Human growth hormone is a single-chain polypeptide. It is non-glycosylated and consists of 191 amino acid residues (Figure 2.24). hGH has three methionine residues in positions Met14, Met125, and Met170, eight tyrosine residues, one tryptophan residue (Trp86), and two disulphide bridges (Cys53–Cys165 and Cys182–Cys189). hGH contains 17 glutamine (Q) residues.

```
        10         20         30         40         50         60
PTIPLSRLFD NAMLRAHRLH QLAFDTYQEF EEAYIPKEQK YSFLQNPQTS LCFSESIPTP

        70         80         90        100        110        120
SNREETQQKS NLELLRISLL LIQSWLEPVQ FLRSVFANSL VYGASDSNVY DLLKDLEEGI

       130        140        150        160        170        180
QTLMGRLEDG SPRTGQIFKQ TYSKFDTNSH NDDALLKNYG LLYCFRKDMD KVETFLRIVQ

       190
CRSVEGSCGF
```

Figure 2.24: Aminoacid sequence of hGH.

The crystal structure studies have shown that hGH is a four helix bundle with two disulphide bonds which are located towards the C-terminal end of hGH (Figure 2.25) [37, 38].

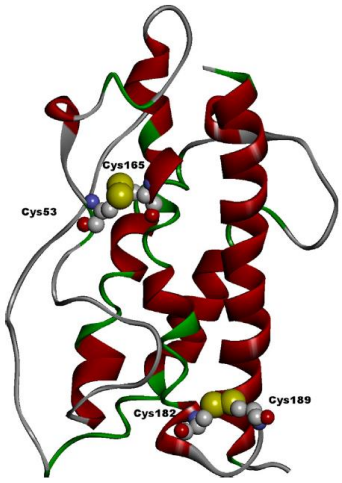

Figure 2.25: X-ray crystal structure of hGH.

Growth hormone has two binding sites (site 1 and 2) and binds to two growth hormone receptors in 1:2 complex and initiate intracellular signaling event through receptor homo-dimerization, which is critical for signalling (Figure 2.26) [39, 40]. After the signaling event, the entire receptor–ligand complex is internalized resulting in signal termination.

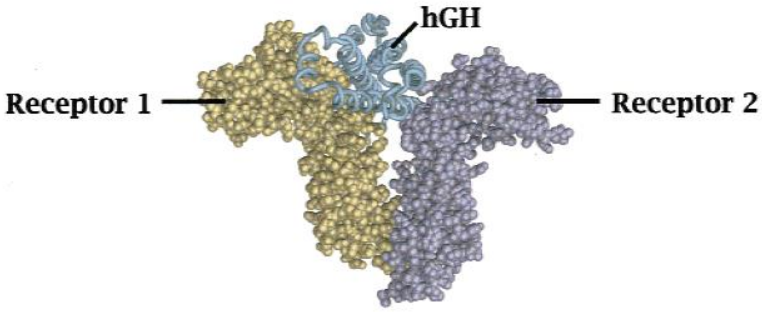

Figure 2.26: 1:2 hGH complex with its receptors.

2.5.2 Recombinant hGH and its therapeutic use

Recombinant human growth hormone (Genotropin®) is widely used to treat short stature resulting from hGH inadequacy, Turner's syndrome, and renal failure both in children and adults [41]. hGH is also used to treat metabolic complications of hGH deficiency in adults and wasting in AIDS patients. hGH is given as a daily subcutaneous injection due to its short half-life of 20–30 min. Rapid proteolysis and ligand–receptor internalization result in a short half-life. Therefore a long acting

growth hormone receptor (GHR) agonist with sufficient stability to be dosed weekly is a highly desirable alternative especially for young children.

r-hGH is produced and commercialized by several large pharmaceutical companies such as Eli Lilly (Humatrope), Genentech (Nutropin), Pfizer (Genotropin), and Serono (Saizen, Serostim). It has also become available as a biogeneric product (Sandoz's Omnitrope, Biopartners' Valtropin, and Cangene's Accretropin).

2.6 HIV-1

2.6.1 Epidemiology of HIV-1 subtype

HIV-1 is among the most genetically diverse viral pathogens described to date. Isolates can be divided into groups, subtypes, and circulating recombinant forms (CRFs) (Table 2.1). The group M viruses, which are the most widespread and account for approximately 99% of infections worldwide, can be further subdivided into nine distinct genetic subtypes, or clades. These clades show characteristic geographic localization, with clade B viruses dominating Europe, the Americas, and Australia, while clade C, which presently infects more people worldwide than any other clade, is most prevalent in southern Africa, China, and India. Despite the prevalence of subtype C, most of the antiretroviral drugs available to treat HIV-1 have been developed in the Western world using in vitro studies of subtype B isolates. However, there is a growing body of evidence that the different subtypes, and in particular the subtype C viruses, have unique antigenic, infectivity, and replicative characteristics [42, 43].

Table 2.1:Distribution of HIV-1 virus subtypes and CRFs.

Subtype	Global predominance	Main geographical distribution
A	High	Eastern Africa, Eastern Europe, Central Asia
B	High	Americas, Western Europe, Australia, Japan
C	High	South and Eastern Africa, India, China, Nepal
D	High	Eastern Africa
F	Low	South America, Central Africa, Eastern Europe
G	Low	Central Africa
H	Low	Central Africa
J	Low	Central Africa
K	Low	Central Africa
CRF01_AE	High	Southeast Asia
CR02_AG	High	West and Central Africa

2.6.2 Structure

Human immunodeficiency virus type 1 (HIV-1), the major pathogen responsible for the AIDS pandemic, is among the most genetically diverse viral pathogens described to date.

HIV-1 is composed by two strands of RNA, 15 types of viral proteins and a few proteins from the last host infected cell, all surrounded by a lipid bilayer membrane (figure 2.27). Together, these molecules allow the virus to infect cells of the immune system and force them to build new copies of the virus. Each of these molecule plays

a role in this process, from the first steps of viral attachment to the final process of budding.

The genes of HIV, that encode at least for nine proteins, are located into a cone-shaped coat. The capsid protein forms stable hexamers, which then assemble like tiles to form capsids. Moreover the nucleocapsid protein forms a stable complex with the viral RNA, to protect it [44, 45]. The encoded proteins are divided into three classes:

1. The major structural proteins, Gag, Pol, and Env
2. The regulatory proteins, Tat and Rev
3. The accessory proteins, Vpu, Vpr, Vif, and Nef

The viral enzymes, encoded by Gag gene, are: reverse transcriptase (RT), protease and integrase. The reverse transcriptase produce a DNA copy of the viral RNA genome, which is then used to build new viruses. Many of the drugs currently used are inhibitors of this enzyme. HIV protease is essential for the maturation of HIV particles as HIV proteins are formed by a long polypeptide which is cleaved in the proper functional proteins by HIV protease. Another class of drugs are protease inhibitors that are used also in combination with inhibitor of RT and integrase. The IN protein mediates the insertion of the DNA copy of the viral genome into the genomic DNA of an infected cell.

The matrix protein forms a coat on the inner surface of the viral membrane and it play a central role when new viruses bud from the surface of infected cells.

gp120 and gp41 are surface glycoproteins of enveloped viruses. They play critical roles in the initial events of viral infection, mediating virion attachment to cells and fusion of the viral and cellular membranes. Envelope glycoproteins are also major targets for the anti-viral immune response in infected hosts.

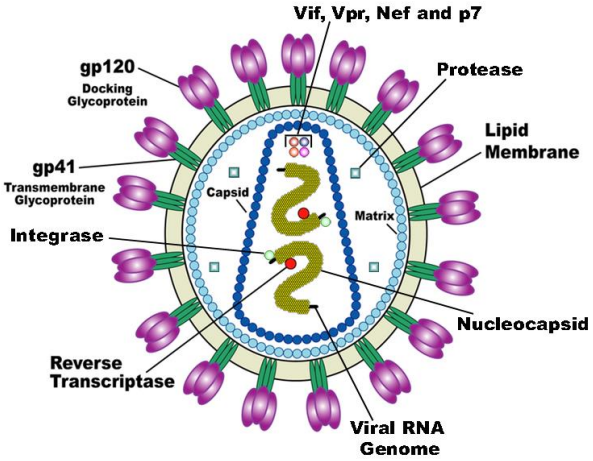

Figure 2.27:HIV-1 virus structure.

gp120 and gp41 are two non-covalently associated subunits that are generated by proteolytic cleavage of a precursor polypeptide, gp160 [46, 47]. gp120 directs target-cell recognition and viral tropism through interaction with the cell-surface receptor CD4 and one of several coreceptors (Figure 2.28) that are members of the chemokine receptor family [48]. The membrane-spanning gp41 subunit then promotes fusion of the viral and cellular membranes, a process that results in the release of viral contents into the host cell.

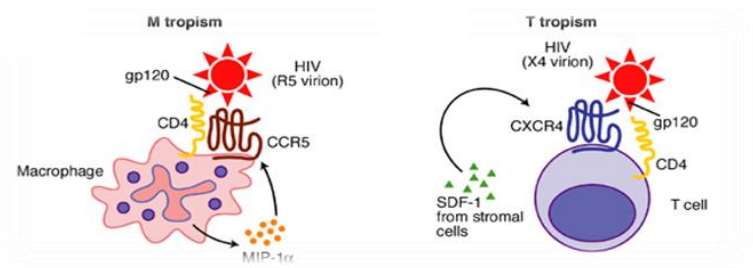

Figure 2.28:HIV-1 tropism for coreceptors.

2.6.3 Life cycle

The main several steps of HIV life cycle (Figure 2.29) consist in:

1. Receptor binding: HIV binds to receptors on the surface of a CD4 cell.
2. Fusion: the HIV envelope and the CD4 cell membrane fuse, allowing HIV to enter the CD4 cell.
3. Reverse Transcription: once inside the target cell, HIV releases the reverse transcriptase that converts the HIV RNA into HIV DNA. This conversion is necessary for the entry of HIV DNA into the nucleus.
4. Integration: integrase allows HIV DNA to enter the nucleus of the host cell. Once inside, the HIV DNA is integrated to the genetic material of the cell.
5. Transcription and Translation: the virus exploits the host cell for the production of the precursors of virus proteins.
6. Assembly: protease cuts up the precursors in order to obtain the virus proteins, that combine with HIV RNA to form a new virus.
7. Budding: the new viruses are released from the target cell.

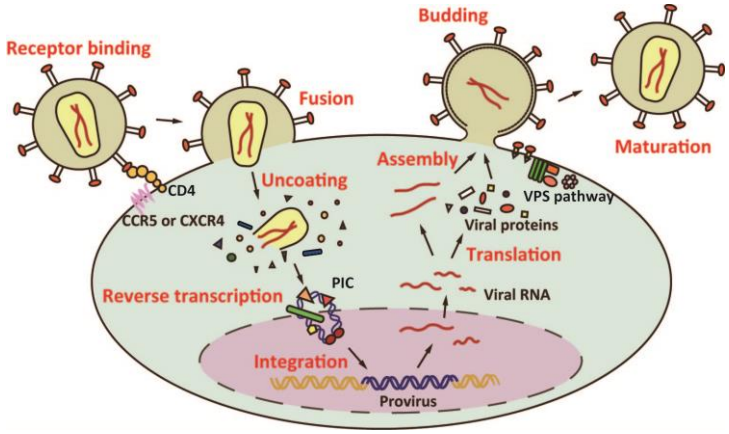

Figure 2.29:HIV-1 life cycle.

In particular, initial entry of HIV-1 into host cells is mediated by a sequence of interactions of the trimeric gp120/gp41 envelope (Env) protein complex with host cells (Figure 2.30). In the host cell entry process, these two proteins participate in a sequence of cell receptor interactions initiated by binding of gp120 to cell surface CD4. This binding event causes conformational rearrangements within gp120 that expose and stabilize a co-receptor binding site [49]. CD4 and consequent co-receptor binding result in further conformational changes in the spike assembly that expose fusogenic as well as initially cryptic helical domains of gp41 [50]. The gp41 domains participate in conformational rearrangement and cell attachment processes leading to virus-cell membrane fusion and introduction of a viral genome into the cell [51]. The various steps in viral entry are relevant targets for anti-HIV intervention.

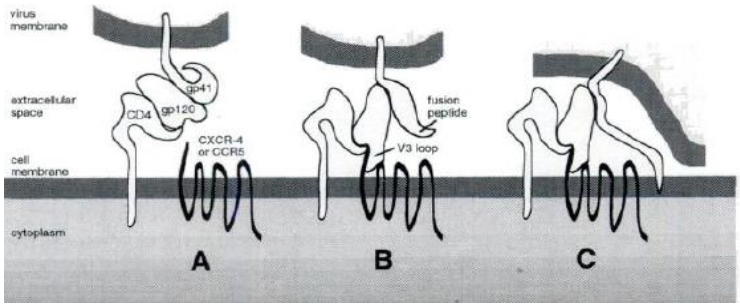

Figure 2.30: Interaction of trimeric envelope protein complex with host cell.

A part of the work reported in this thesis was developed at the Department of Biochemistry and Molecular Biology of the Drexel University College of Medicine in Philadelphia, under the supervision of Professor Irwin Chaiken, whose laboratory is focused on the design and realization of peptide drugs that inhibit the entry of HIV-1 in the target cells.

2.6.4 Triazole peptide KR14

KR14 derives from a family of peptide triazoles which have nanomolar affinity for HIV-1 envelope protein gp120, and inhibit the interactions of gp120 at both receptor CD4 and the coreceptor surrogate mAb 17b. These peptide was generated by modification of a central proline residue on a 12-mer peptide, denoted 12p1, which was originally identified as a micro-molar affinity gp120 binder from phage display library screening. It was found that the replacement of the central Pro residue by azido-Pro and it's click conjugation with ethynylferrocene led to variants with several orders of magnitude greater affinity. The resulting peptide triazole binds to gp120 with 1:1 stoichiometry, inhibit interactions at both the CD4 and co-receptor binding sites and are broadly active in neutralizing cell infection by virus subtypes from all major clades [52].
KR14 is formed by 15 amino acids with an hexanoic spacer between the glutamine and the cysteine amino acid (Figure 2.31).

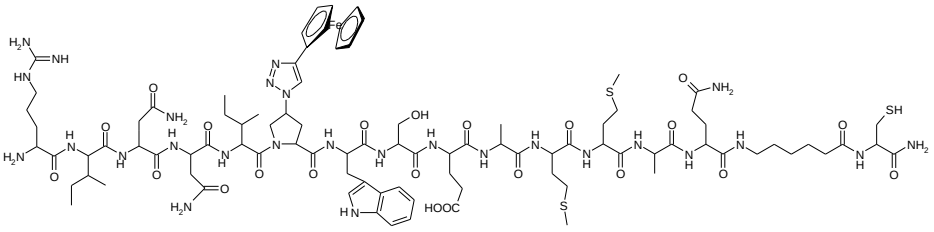

Figure 2.31: KR14 structure.

The sequence is *Arg-Ile-Asn-Asn-Ile-Azp-Trp-Ser-Glu-Ala-Met-Met-bAla-Gln-Ahx-Cys-CONH2*, where *Azp* is azidoproline and *Ahx* is the 1-amino hexanoic acid.

The pharmacophore is formed by the first 7 amino acids. The internal sequence cluster of Ftp-Trp at position 6 is required for function. In particular, that sequence provides a spatially arranged aromatic cluster, while the N-terminal extension of residues may establish hydrogen bonding interactions that help stabilize productive Env protein binding [53]. For this reason, the PEGylation was achieved at the free thiol group of the cysteine, that is far from the pharmacophore region.

3 MATERIALS AND METHODS

3.1 MATERIALS

Recombinant human G-CSF was provided by Sandoz GmbH (Kundl, Austria) in a buffer solution of 50 mM phosphate and 5% sorbitol pH 7.0. hGH was supplied by Fidia Farmaceutici (Abano Terme, Italy). BOC-NH-PEG_{5k}-NHS was from Iris Biotech GmbH (Marktredwitz, Germany). BOC-NH-$PEG_{3.4k}$-b-PLE_{50} and $PLEald_{50}$ were purchased from Alamanda Polymers, Inc. (Huntsville, Alabama, USA). mPEG_{5k}-NH_2, mPEG_{20k}-NH_2 and mPEG_{20k}-aldehyde were purchased from NOF Corporation (Tokyo, Japan). Microbial TGase (mTGase) from *Streptomyces mobaraensis* was purchased from Ajinomoto Co. (Tokyo, Japan). β-Glutamic acid, 2,4,6-trinitrobenzenesulfonic acid, Glycyl-Glycine, N-Hydroxysuccinimide (NHS), N,N-Dicyclohexylcarbodiimide (DCC), sodium sulfate anhydrous (Na_2SO4), dichloromethane (CH_2Cl_2), sodium cyanoborohydride ($NaBH_3CN$), trifluoroacetic acid (TFA), acetonitrile, methanol (MeOH), D_2O, sinapic acid, triethylamine (Et_3N), Fmoc-Osu, N,N'-diisopropylcarbodimmide (DIC), methanesulfonyl chloride, sodium azide, tetrahydrofuran (THF), ethyl acetate (EtOAc), pyridine, N,N'-Diisopropylethylamine (DIPEA), ethynylferrocene, 2-ethanedithiol, thioanisole, piperidine and salts of analytical grade were purchased from Sigma-Aldrich Co. (St. Louis, MO, USA). Precast gels were from BIO-RAD (Hercules, CA, USA). Invitrogen Human G-CSF ELISA Kit was purchased from Life Technologies (Carlsbad, CA, USA). hGH ELISA kit was from Tema ricerca Srl (Bologna, Italy). Hypophysectomized male Sprague Dawley rats were purchased from Charles River Laboratories (Lecco, Italy). All Fmoc-protected amino acids and HOBt were purchased from Novabiochem. Rink amide resin was obtained from Applied Biosystems.

3.2 ANALITICAL METHODS

Spectrophotometer analysis were performed with an Evolution 201 Spectrophotometer of Thermo Scientific (Waltham, USA). ^{1}H-NMR spectroscopy was performed with Bruker 400 MHz spectrometer and NMR data were processed using the program Topspin (Bruker GmbH, Karlsruhe, Germany). Shimadzu analytical HPLC system was used with C18 Jupiter (Phenomenex, Torrance, CA, USA; 5 μm, 300 Å, 250 x 4.60 mm) reverse phase column for analytical characterization and purification of PEG-G-CSF conjugates or with Zorbax GF-250 (Agilent Technologies, Palo Alto, CA; 4.6 × 250 mm or 9.4 × 250 mm 4 μm) size exclusion chromatography (SEC) columns for analytical characterization and purification of hGH-PLE conjugate. Centrifugation was carried out with Hettich Zentrifugen mod. MIKRO 200. The freeze-drying was performed with freeze-Hetossic Heto Lab Equipment. The dialysis tubing have been provided by Del Chimica Scientific Glassware (Naples, Italy). Aqueous and organic solutions were

evaporated with Rotavapor mod. R II BÜCHI (Switzerland). SDS-PAGE analyses were performed with Electrophoresis Power Supply 300 (Pharmacia, Sweden). Circular dichroism analyses were carried out with Jasco J-700 spectropolarimeter equipped with a Peltier temperature control unit. Mass analyses were performed with AB SCIEX MALDI-TOF mass spectrometer (Bruker-Franzen Analytik, Bremen, Germany). Pharmacokinetic profiles of PEG-G-CSF conjugates and native G-CSF were analyzed using Invitrogen Human G-CSF ELISA Kit. Pharmacokinetic profiles of hGH-PLE conjugate and native hGH were analyzed using hGH ELISA kit.

3.3 SYNTHESIS OF NH_2-PEG-(β-Glu)-(β-Glu)$_2$-(β-Glu)$_4$-(COOH)$_8$

Firstly the activation degree of Boc-NH-PEG_{5k}-NHS was determined. Then, the first step will provide the reaction between Boc-NH-PEG_{5k}-NHS and the NH_2-group of β-glutamic acid (β-Glu).

3.3.1 Determination of the activation degree of Boc-NH-PEG_{5k}-NHS

The degree of activation of Boc-NH-PEG_{5k}-NHS was determined by using a spectroscopic assay based on the so-called Glycyl-Glycine (Gly-gly) test. In this procedure, the degree of PEG activation is determined by reacting an equimolar amount of Gly-Gly with the activated PEG, followed by performing a Snyder and Sobocinsky colorimetric assay of the unreacted dipeptide [54]. This assay uses 2,4,6-trinitrobenzenesulfonic acid (TNBS), which reacts stoichiometrically with primary amino groups in an alkaline medium to give a trinitrophenyl derivative absorbing at 420 nm (Figure 3.1).

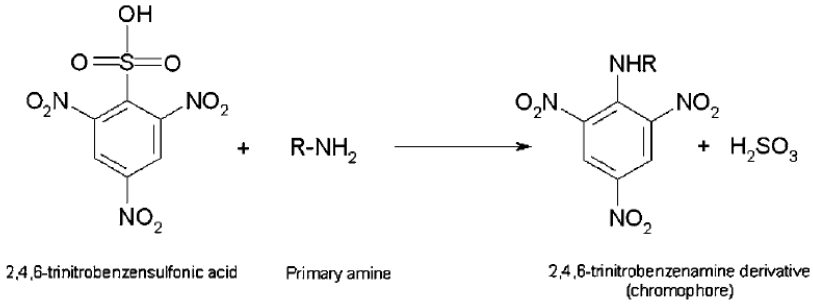

Figure 3.1: Reaction between 2,4,6-trinitrobenzensulfonic acid and a free primary amine group.

To 1 mL of 2 mM Gly-Gly solution, 1 eq. (2 µmol, MW 5000 Da) of Boc-NH-PEG_{5k}-NHS was added and the mixture was left at room temperature under continuous agitation. The TNBS assay was performed in duplicate according to Table 3.1. The reactions were incubated for 30 min before reading the absorbance at λ = 420 nm using a UV–visible spectrophotometer. The percentage of activation of Boc-NH-PEG_{5k}-NHS was calculated by using the following formula:

$$\% \text{ Activation} = [1 - (\text{AbsA} - \text{AbsB}) / (\text{AbsG} - \text{AbsB})] \times 100\%$$

where AbsA is the absorbance of PEG reaction mixture, AbsG is the absorbance of Gly-Gly standard solution and AbsB is the absorbance of the blank solution.

Table 3.1: Preparation of test solutions for the TNBS assay.

Blank	PEG reaction mixture (A)	Gly-Gly standard solution (B)
20 µL of TNBS	20 µL of TNBS	20 µL of TNBS
980 µL of borate pH 9.3	955 µL of borate pH 9.3	955 µL of borate pH 9.3
	25 µL of sample A	25 µL of sample B

3.3.2 Synthesis of Boc-NH-PEG-β-Glu-$(COOH)_2$

Boc-NH-PEG-β-Glu-$(COOH)_2$ was obtained by forming an amide bond between the activated carboxyl group of PEG and the amino group of β-glutamic acid as reported in figure 3.2.

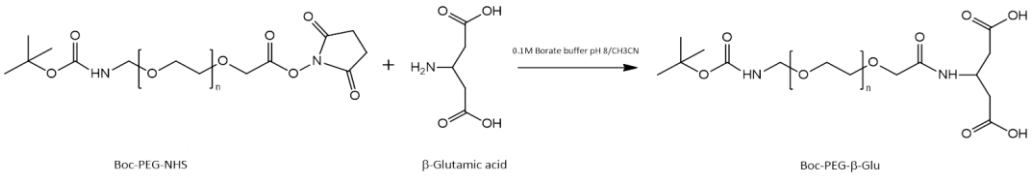

Figure 3.2: Synthesis of Boc-NH-PEG-β-Glu-$(COOH)_2$

2 g (0.4 mmol) of Boc-NH-PEG-NHS (MW 5000 Da; 84% of activated carboxylic groups) was added to 176 mg (1.2 mmol) of β-Glutamic acid (βGlu) (MW 147.1 Da; 3 equivalent in excess to activated -COOH groups of PEG), dissolved in 20 mL of 0.1 M borate buffer/CH_3CN (3:2) mixture pH 8.0. The reaction was left under stirring. After 5 h, the pH was adjusted to about 5 with HCl 0.2 N and the product was purified from the excess of βGlu by extractions with CH_2Cl_2 (6 × 200 mL). The organic phase, dried over anhydrous Na_2SO4, was concentrated under vacuum and dropped into 500 ml of cold diethyl ether under stirring. After 1 h at -20°C, the precipitate of Boc-NH-PEG-β-Glu-$(COOH)_2$ was filtered and dried under vacuum (yield: 1.75 g, 87 %). The absence of free βGlu was verified by TNBS test according to Snyder and Sabocinsky assay previously reported.

3.3.3 Activation of carboxylic groups of Boc-NH-PEG-β-Glu-$(COOH)_2$ via NHS/DCC

The carboxylic groups of Boc-NH-PEG-β-Glu-$(COOH)_2$ were activated to succinimide ester with NHS/DCC as reported in figure 3.3.

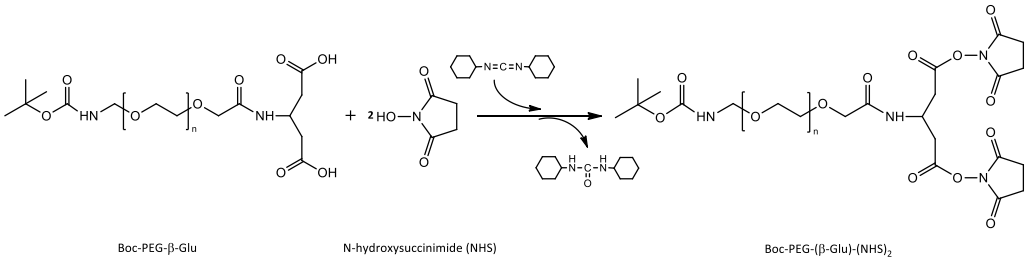

Figure 3.3: Activation of carboxyl groups of Boc-NH-PEG-β-Glu-$(COOH)_2$

430 mg (2.1 mmol) of DCC (MW 206.33 Da; 3 equivalent in excess for each carboxyl groups) and 120 mg (1.04 mmol) of NHS (MW 115.09 Da; 1.5 equivalent in excess for each carboxyl groups) were added to 1.75 g (0.35 mmol) of Boc-NH-PEG-β-Glu-$(COOH)_2$ (MW 5035 Da), previously dissolved in 20 mL of anhydrous CH_2Cl_2,. The reaction was stirred at room temperature overnight. Then the mixture was filtered and dropped into 500 mL of cold diethyl ether. After 1 h at -20°C, the precipitate of Boc-NH-PEG-(β-Glu)-$(NHS)_2$ was recovered by filtration and dried under vacuum (yield: 1.64 g, 90.5%). The degree of activation, determined according to Snyder and Sabocinsky assay, was 81.6%.

3.3.4 Synthesis of Boc-NH-PEG-(β-Glu)-$(β\text{-Glu})_2$-$(COOH)_4$

Boc-NH-PEG-(β-Glu)-$(β\text{-Glu})_2$-$(COOH)_4$ (Figure 3.4) was obtained in the same manner of Boc-NH-PEG-(β-Glu)-$(COOH)_2$ (section 3.3.2).

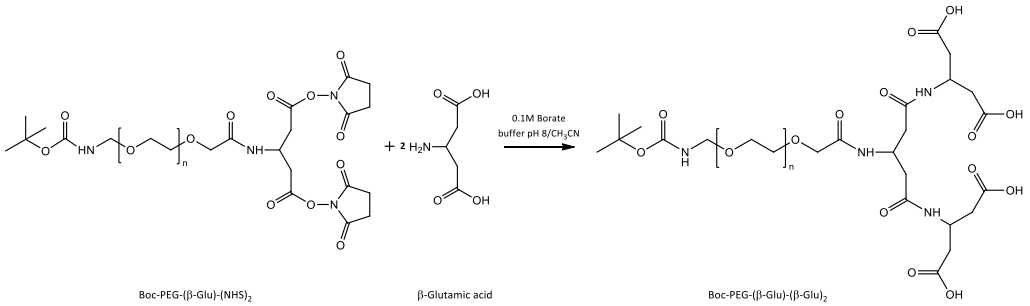

Figure 3.4: Synthesis of Boc-NH-PEG-(β-Glu)-$(β\text{-Glu})_2$-$(COOH)_4$

1.64 g (0.3 mmol) of Boc-NH-PEG-(β-Glu)-$(NHS)_2$ (MW 5229 Da; 81.6% of activated carboxylic groups) was added to 226 mg (1.5 mmol) of β-Glutamic acid (βGlu) (MW 147.1 Da; 3 equivalent in excess to activated -COOH groups of PEG), previously dissolved in 16 mL of 0.1 M borate buffer/CH_3CN (3:2) mixture pH 8.0. The reaction was conducted as explained in section 3.3.2 (yield: 1.3 g, 78.4%).

3.3.5 Activation of carboxylic groups of Boc-NH-PEG-(β-Glu)-(β-Glu)$_2$-(COOH)$_4$ via NHS/DCC

The carboxylic groups of Boc-NH-PEG-(β-Glu)-(β-Glu)$_2$-(COOH)$_4$ were activated to succinimide ester with NHS/DCC as reported in figure 3.5.

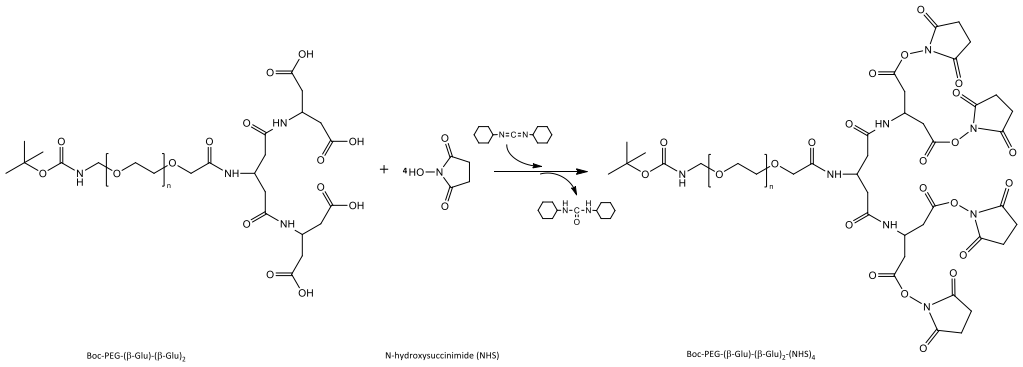

Figure 3.5: Activation of carboxyl groups of Boc-NH-PEG-(β-Glu)-(β-Glu)$_2$-(COOH)$_4$

1.3 g (0.25 mmol) of Boc-NH-PEG-(β-Glu)-(β-Glu)$_2$-(COOH)$_4$ (MW 5293 Da) were activated with 608 mg (2.9 mmol) of DCC (MW 206.33 Da; 3 equivalent in excess for each carboxyl groups) and 170 mg (1.48 mmol) of NHS (MW 115.09 Da; 1.5 equivalent in excess for each carboxyl groups) and Boc-NH-PEG-(β-Glu)-(β-Glu)$_2$-(NHS)$_4$ were recovered as reported in the section 3.3.3. The degree of activation was 83.5% (yield: 1.22 g, 88%).

3.3.6 Synthesis of Boc-NH-PEG-(β-Glu)-(β-Glu)$_2$-(β-Glu)$_4$-(COOH)$_8$

Boc-NH-PEG-(β-Glu)-(β-Glu)$_2$-(β-Glu)$_4$ (COOH)$_8$ (Figure 3.6) was obtained in the same manner of Boc-NH-PEG-(β-Glu)-(COOH)$_2$ (section 3.3.2).

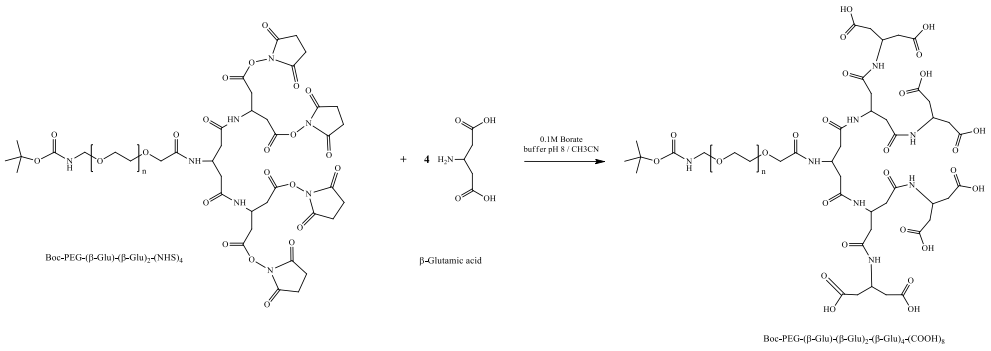

Figure 3.6: Synthesis of Boc-NH-PEG-(β-Glu)-(β-Glu)$_2$-(β-Glu)$_4$ (COOH)$_8$

1.22 g (0.2 mmol) of Boc-NH-PEG-(β-Glu)-(β-Glu)$_2$-(NHS)$_4$ (MW 5681 Da; 83.5% of activated carboxylic groups) was added to 316 mg (2.15 mmol) of β-Glutamic acid (βGlu) (MW 147.1 Da; 3 equivalent in excess to activated -COOH groups of PEG), previously dissolved in 12 mL of 0.1 M borate buffer/CH_3CN (3:2) mixture pH 8.0. The reaction was conducted as explained in section 3.3.2 (yield: 1.07 g, 85.8%).

The degree of derivatization with β-Glutamic acid was determined by ^{1}H-NMR. The signals of β-Glutamic acid are m, 4.50 ppm -NH**CH**$(CH_2)_2$-, m, 2.59 ppm -NHCH(**CH$_2$**)$_2$$(COOH)_2$ and m, 2.44 ppm -NHCH(**CH$_2$**)$_2$CONH-). The molecular weight of Boc-NH-PEG-(β-Glu)-(β-Glu)$_2$-(β-Glu)$_4$-$(COOH)_8$ was calculated by MALDI-TOF mass spectrometry.

3.3.7 Removal of protecting group t-Boc from Boc-NH-PEG-(β-Glu)-(β-Glu)$_2$-(β-Glu)$_4$-$(COOH)_8$

1.07 g of Boc-NH-PEG-(β-Glu)-(β-Glu)$_2$-(β-Glu)$_4$-$(COOH)_8$ were dissolved in 4 ml of CH_2Cl_2/CF_3COOH/H_2O (54:45:1 percent) mixture for 1 h to remove the protecting group t-Boc (Figure 3.7). The reaction mixture was evaporated to remove the TFA and the obtained oil was solubilized in CH_2Cl_2 and dropped into 300 mL of diethyl ether. The product was recovered by filtration and dried under vacuum (yield: 1.04 g, 97%).

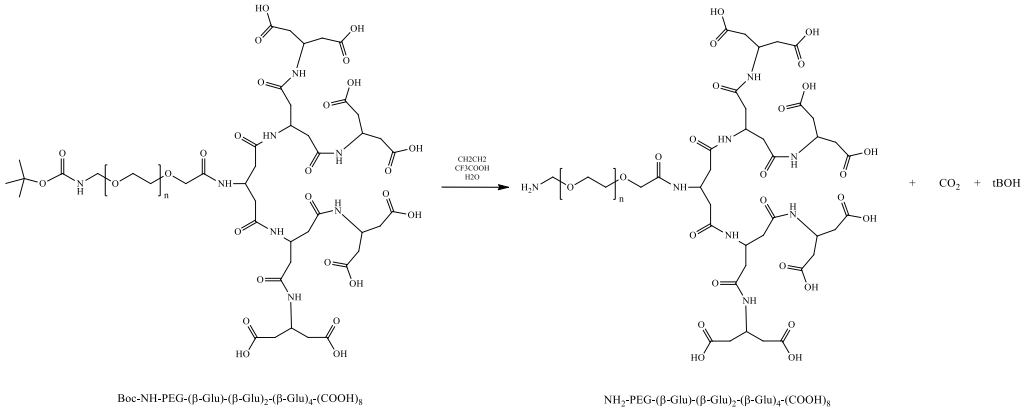

Figure 3.7: Synthesis of NH_2-PEG-(β-Glu)-(β-Glu)$_2$-(β-Glu)$_4$ $(COOH)_8$

The absence of the protecting group t-Boc was confirmed by MALDI-TOF mass spectrometry.

3.4 SYNTHESIS AND CHARACTERIZATION OF G-CSF-PEG CONJUGATES

3.4.1 Site-specific conjugation of multicarboxylic and neutral PEGs to G-CSF

G-CSF-PEG conjugates were obtained by enzymatic PEGylation, exploiting the enzyme microbial transglutaminase (mTGase). TGase(s) are a class of enzymes that catalyze an acyl transfer between two proteins involving the glutamyl group of a glutamine (acyl donor) and a primary amine (acyl acceptor), usually the ε-amino group of a lysine.

mTGase was employed for site-specific binding of PEG to G-CSF, where one of its glutamine (Gln) residue serves as acyl donor and an amino-derivative of PEG serves as acyl acceptor (Figure 3.8).

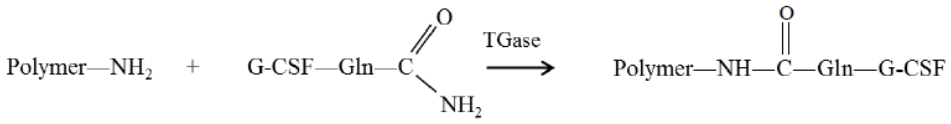

Figure 3.8: Scheme of G-CSF-PEG synthesis.

For the conjugation of G-CSF, two different multicarboxylic PEGs, PEG-dendron and H_2N-$PEG_{3.4k}$-b-PLE_{50}, and two neutral PEG-NH_2 derivatives of different molecular weight, were used.

3.4.1.1 Removal of protecting group t-Boc from Boc-$PEG_{3.4k}$-b-PLE_{50}

The Boc group of the polymer Boc-NH-$PEG_{3.4k}$-b-PLE_{50} was removed to obtain a free amine at one end of the polymer needed for the conjugation reaction (Figure 3.9).

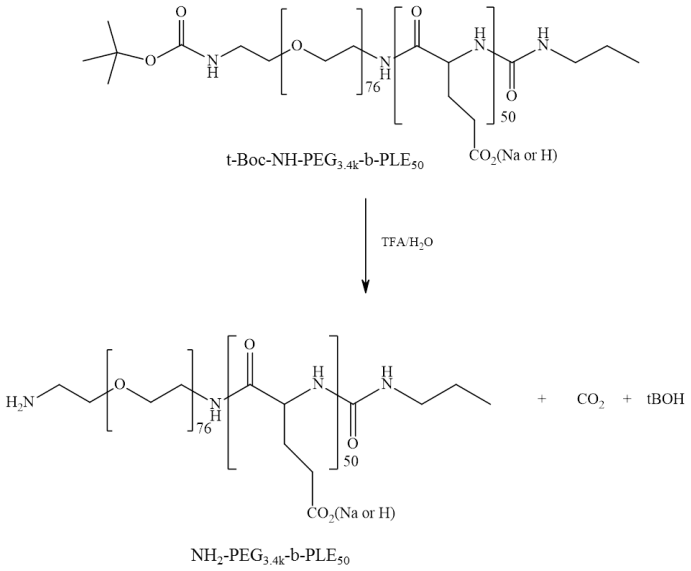

Figure 3.9: Structural formula of Boc-NH-PEG$_{3.4k}$-b-PLE$_{50}$.

73 mg of Boc-PEG$_{3.4k}$-b-PLE$_{50}$ were dissolved in 4 ml of CH_2Cl_2/CF_3COOH/H_2O (54:45:1 percent) mixture and were stirred for 1 h. The reaction mixture was evaporated to remove the TFA and the obtained oil was solubilized in Milli-Q water. The solution was neutralized and dialyzed overnight against Milli-Q water. The polymer solution was then lyophilized (yield: 69 mg, 94.5%).

The absence of the protecting group t-Boc was confirmed by MALDI-TOF mass spectrometry.

3.4.1.2 Synthesis and purification of G-CSF-PEG conjugates via mTGase-mediated PEGylation

Generally, to 975 µl (0.21 µmol, MW 18792.8 Da) of a G-CSF solution in 50 mM phosphate and 5% sorbitol, pH 7, a defined amount of PEG, previously dissolved in the reaction buffer (100 mM phosphate, pH 7.5), was added. The contents used for each PEG were shown in Table 3.2 based on the molar excess with respect the protein.

mTGase was added to the solution at an enzyme to substrate ratio (E/S) of 1:25 (w/w) in order to reach a 0.1 mM final concentration in protein. The reactions were incubated at 25°C for 4 hours and then analyzed by RP-HPLC using a Phenomenex Jupiter C18 column (250 × 4.6 mm) with a linear gradient of 40–70% (v/v) acetonitrile containing 0.01% TFA over 25 min, followed by an isocratic wash at 90% acetonitrile. The effluent was monitored by measuring the absorbance at 226 nm.

Table 3.2: Polymer contents used for the synthesis of G-CSF-PEG conjugates.

	PROTEIN/POLYMER RATIO	MW (Da)	AMOUNT OF PEG (mg)
H_2N-PEG_{5k}-$(COOH)_7$	1/50	5717	60.8
H_2N-$PEG_{3.4k}$-b-PLE_{50}	1/10	11000	23.4
$mPEG_{5k}$-NH_2	1/10	5000	10.6
$mPEG_{20k}$-NH_2	1/10	20000	42.6

The conjugates were purified by RP-HPLC using the conditions mentioned above and measuring the absorbance of the effluent at 280 nm. After the purification, the conjugates were dialyzed against 50 mM phosphate, 5% sorbitol, pH 7 and the protein concentrations were determined by UV-Vis spectrophotometry (G-CSF absorption coefficients: 0.82 mL cm^{-1}).

The purified conjugates were characterized by MALDI-TOF mass spectrometry, SDS-PAGE, and circular dichroism; and their stability studies were performed via circular dichroism, monitoring the unfolding as a function of temperature. The conjugates were aliquoted and stored in freezer for the ulterior pharmacokinetic studies in rats.

3.4.2 MALDI-TOF mass spectrometry

Mass analyses of G-CSF and its PEGylated derivatives were carried out by MALDI-TOF mass spectrometry. MALDI, matrix-assisted laser desorption/ionization, generates gas phase-ions from protein molecules, which are hit by a laser. The MALDI matrix absorbs photon energy from the laser beam and transfers it into the excitation energy of the solid system. MALDI matrices are low molecular weight organic compounds with low vapour pressure and volatile nature, mostly acidic in nature.

MALDI-MS spectra were performed on a REFLEX time-of-flight instrument equipped with a SCOUT ion source operating in positive linear mode. Ions generated by a pulsed UV laser beam (nitrogen laser, lambda 337 nm) were accelerated to 25 kV. A saturated solution of sinapinic acid in acetonitrile/water (1:1, v/v) was used as matrix and mixed with the samples dissolved in 0.1% TFA aqueous solution at a v/v ratio of 1:1.

3.4.3 SDS-PAGE

The purified conjugates G-CSF-PEG_{5k}-$(COOH)_7$, G-CSF-$PEG_{3.4k}$-b-PLE_{50}, G-CSF-PEG_{5k}, and G-CSF-PEG_{20k} were analyzed by SDS-PAGE, along with native G-CSF, to confirm the formation of the desired monoconjugates, and their purity.

For the analysis, 4 – 15% mini precast gels were used. Each well was fill with 10 µL of a solution containing 5 µg of protein, previously added of loading buffer

(containing glycerol as thickener, SDS as anionic detergent, DTT as reducer and bromophenol blue as tracer). Separations were run in 0.025M Tris, 0.192M glycine, 0.1% SDS at pH 8.3, applying 130 V for 1h. The gel was firstly stained with iodine (I_2) in the presence of $BaCl_2$ in acidic environment, to color PEG and subsequently with Coomassie blue that detect the protein bands.

3.4.4 Circular Dichroism

Circular dichroism was used to assess the effect of PEGylation on secondary structure of the protein. By comparing the far-UV CD spectra of the native protein and its PEGylated derivatives, it is possible to understand if PEGylation caused any changes in the secondary structure of the protein. In this study, native G-CSF and the G-CSF-PEG conjugates were analyzed by CD in the far-UV region. Moreover, in order to evaluate if changes were also due to the purification conditions, a native G-CSF sample was purified in the same conditions as the conjugates and analyzed as well.

CD spectra were measured on a Jasco J-700 spectropolarimeter equipped with a Peltier temperature control unit at 20 °C. Measurements of the samples were made in 50 mM phosphate, 5% sorbitol, pH 7 buffer at the concentration solutions of 0.1 mg/mL as spectrophotometrically determined at 280 nm. The spectra were collected over the wavelength range of 190–250 nm with an average of 2 scans. The data at each wavelength were averaged for 8 s. The sample cell path length was 0.1 cm. The CD data were converted to mean residue ellipticity, expressed in deg cm^2 $dmol^{-1}$ by applying the following formula:

$$\Theta = \Theta_{obs}(MRW) / 10\ L[C]$$

where Θ is the observed ellipticity in degrees, MRW is the mean residue weight of the protein (molecular weight divided by the number of residues), [C] is the protein concentration in mg/mL, and L is the optical path length in centimeters.

3.4.5 Thermal denaturation studies

Thermal stability of free and conjugated G-CSF was evaluated by circular dichroism, by monitoring the protein unfolding as a function of temperature at a fixed wavelength, in order to determine the impact of PEGylation on protein stability. Thermal denaturation was monitored on the same samples used for CD analysis by recording the decrease of the ellipticity signal at 222 nm. Thermal unfolding experiments were carried out in a 0.1 cm cell path length by heating the samples from 20 to 95°C at a rate of 5°C/min.

3.4.6 *In vivo* studies

3.4.6.1 Ethics statement

The study protocol was approved by the Ethics Committee of the University of Padova and the Italian Ministry of Health, and animals were handled in compliance with national (Italian) Legislative Decree 116/92 guidelines and with the "Guide for the Care and Use of Laboratory Animals" by the National Research Council of the National Academies.

3.4.6.2 Pharmacokinetics in rats

The pharmacokinetics of G-CSF and the conjugates were assessed in Sprague-Dawley rats (250-350 g). The rats were randomly divided into five groups, each group containing 3 rats. A dose of 100 μg/kg G-CSF (equiv) was administered via tail vein to the rats anesthetized with isoflurane gas (mixed with O_2 in enclosed cages). Blood samples were collected from the submandibular cheek bleed of the rats at pre-determined time points, centrifuged at 1500 × g for 15 min and the serum phases were separated. The G-CSF content in serum samples was quantified by human G-CSF ELISA kit (Invitrogen). The pharmacokinetic data were elaborated using *PkSolver*, applying a bicompartmental model.

3.4.6.3 ELISA

The enzyme-linked immunosorbent assay (ELISA) is a specific and highly sensitive method for quantification of proteins in solution. Sandwich ELISA assays are so-called because of the layered complex they form. The wells of the plate provided are coated with a monoclonal antibody (capture antibody) specific for the protein of interest, in this case, human G-CSF.

Samples, including standards of known protein content and unknowns, were pipetted into the wells. A biotinylated monoclonal second antibody (detection antibody) was then added and the samples were incubated. During this first incubation, the protein was bound simultaneously to the immobilized (capture) antibody on one epitope, and to the solution phase biotinylated antibody on a second epitope. After removal of excess second antibody, Streptavidin-Peroxidase (enzyme) was added, which was bound to the biotinylated antibody to complete the four-member sandwich. After a second incubation and washing to remove all the unbound enzyme, a substrate solution (in this case, tetramethylbenzidine) was added. A color reaction was developed between the enzyme and the substrate. The intensity of the

colored product was directly proportional to the concentration of the protein present in the original sample. The absorbance was read at 450 nm and the protein concentration of the analyzed samples was determined by comparison with a standard curve of known protein concentrations.

3.5 SYNTHESIS AND CHARACTERIZATION OF hGH CONJUGATES

3.5.1 Site-specific conjugation of PEG_{20kDa} to hGH

PEG-hGH conjugates, were formed by conjugation of hGH to PEG_{20kDa} in two different sites. The conjugates were obtained exploiting two different strategies according to the procedures previously reported by our lab [55]: transglutaminase (TGase) mediated enzymatic PEGylation, using $PEG_{20\ kDa}{-}NH_2$ and *N*-terminal PEGylation, based on the use of PEG_{20kDa} –aldehyde.

3.5.1.1 Synthesis and purification of PEG-Gln141-hGH

2 mg (90.4 nmol, MW 22129 Da) of hGH were diluted with 0.1 M phosphate buffer (pH 7.0) containing 50% of ethanol (v/v) in order to reach a 0.18 mM final concentration in protein. 18 mg (0.9 µmol, MW 20000 Da) of $PEG_{20\ kDa}{-}NH_2$ (10-fold molar excess) was dissolved in this solution and mTGase was added at E/S ratio of 1:20 (w/w).

The mixture was stirred at room temperature for 18 h and then analyzed and purified by RP-HPLC using a Phenomenex Jupiter C18 column (250 × 4.6 mm), detection at 280 nm, with a linear gradient of 40–80% (v/v) acetonitrile containing 0.01% TFA over 25 min, followed by an isocratic wash at 90% acetonitrile. After the purification, the solution was concentrated under vacuum and the conjugate was dialyzed against PBS solution. The protein concentration was determined by UV-VIS absorption and the conjugate was characterized by SDS-PAGE, MALDI-TOF mass spectrometry and circular dichroism.

3.5.1.2 Synthesis and purification of PEG-Nter-hGH

Conjugation with PEG-aldehyde allows modification of primary amines of proteins. The reaction was performed in acidic condition to protonate the ε-amines of the protein while the α-NH_2 group was still partially present as free base and available for reaction with aldehydes. Therefore, PEG-aldehyde selectively formed Schiff's base with the α-amino group that was after reduced to a secondary amine by sodium cyanoborohydride. The scheme of synthesis is shown in Figure 3.10.

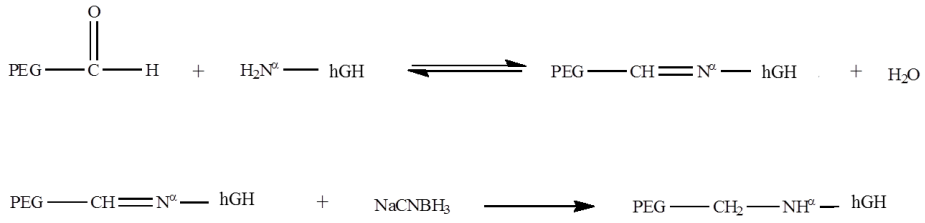

Figure 3.10: Scheme of PEG-Nter-hGH synthesis.

2 mg (90.4 nmol, MW 22129 Da) of hGH were diluted with 0.1 M acetate buffer (pH 5.0) in order to reach a 0.36 mM final concentration in protein. 9 mg (0.45 µmol, MW 20000 Da) of $PEG_{20\ kDa}$–aldehyde (5-fold molar excess) were dissolved in this solution and after 1 h $NaCNBH_3$ (50-fold molar excess) was added.

The mixture was stirred at room temperature for 5 h and then analyzed by SEC-HPLC using a Zorbax GF-250 column (250 × 4.6 mm) eluted with 0.1M phosphate buffer, 0.2 M NaCl (pH 7.2) containing 20% (v/v) of ACN. The effluent was monitored by measuring the absorbance at 280 nm. The conjugate was purified by RP-HPLC using a Phenomenex Jupiter C18 column (250 × 4.6 mm) with a linear gradient of 40–80% (v/v) acetonitrile containing 0.01% TFA over 25 min, followed by an isocratic wash at 90% acetonitrile. The effluent was monitored by measuring the absorbance at 280 nm. After the purification, the solution was concentrated under vacuum and the conjugate was dialyzed against PBS solution. The protein concentration was determined by UV-VIS absorption and the conjugate was characterized by SDS-PAGE, MALDI-TOF mass spectrometry and CD.

3.5.2 Characterization of PEG-hGH conjugates

The conjugates were characterized by MALDI-TOF mass spectrometry, SDS-PAGE, and circular dichroism as described in sections 3.4.2, 3.4.3 and 3.4.4.

Thermal denaturation of the free and conjugated hGH was monitored on the same samples used for CD analysis by recording the decrease of the ellipticity signal at 208 nm as a function of the temperature. Thermal unfolding experiments were carried out in a 0.1 cm cell path length by heating the samples from 20 to 95°C at a rate of 5°C/min. CD spectra in the full far UV range were then collected at 20°C, 95°C, and at 20°C after heating up to 95°C.

3.5.3 Site-specific conjugation of poly(L-glutamic acid) to hGH

Conjugation with poly(L-glutamic acid) is an *N*-terminal PEGylation via aldehyde. The polymer was provided with the aldehyde function protected by an acetal group. The mechanism of reaction is explained in section 3.5.1.2.

3.5.3.1 Removal of acetal group from PLE_{50ald}

The acetal group of the polymer PLE_{50ald} was removed to obtain the aldehyde at one end of the polymer (Figure 3.11).

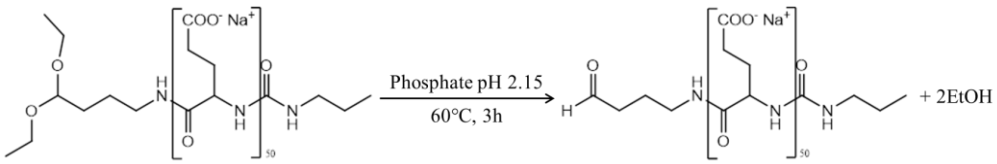

Figure 3.11: Hydrolysis of acetal group of PLE_{50ald}.

90 mg (13.2 µmol, MW 6800 Da) of PLE_{50ald} were dissolved in 2 ml of 25 mM phosphate buffer, pH 2.15 and were stirred at 60°C. After 3 h the solution was normalized and dialyzed overnight against Milli-Q water. The polymer solution was then lyophilized (yield: 72 mg, 80%).

The absence of the protecting group t-Boc was confirmed by MALDI-TOF mass spectrometry.

3.5.3.2 Selection of the synthesis conditions of hGH-PLE_{50ald}

In order to achieve the proper conditions that led to a selective formation of a monoconjugate, several options were tested. Buffer, excess of polymer and temperature were chosen as variables and were varied. In particular, the reaction buffers were 100 mM phosphate, pH 6.2 and 100 mM acetate, pH 5 and 5, 10 and 20 equivalents of polymer were used at different temperatures (5, 24, 35, 40 and 45°C).

Generally, to 500 µg (22.6 nmol, MW 22129 Da) of hGH, a defined amount of PLE_{50ald} (MW 6726 Da), previously dissolved in the reaction buffer, was added in order to reach a 0.36 mM final concentration in protein. The reactions were incubated at the temperatures over mentioned and after 1 h, $NaCNBH_3$ (50-fold molar excess) was added. After 18 hours incubation at the proper temperature, the products formation was evaluated by SDS-PAGE and the data elaboration was performed by ImageJ software in order to calculate the percentage formation of monoconjugate and biconjugate.

3.5.3.3 Synthesis and purification of hGH-PLE_{50ald}

To 5 mg (0.22 µmol, MW 22129 Da) of hGH, 7.6 mg (1.13 µmol, MW 6726 Da) of PLE_{50ald}, previously dissolved in 100 mM phosphate buffer, pH 6.2, were added in

order to reach a 0.36 mM final concentration in protein. The reaction was incubated at 35°C and after 1 h, $NaCNBH_3$ (50-fold molar excess) was added. After 18 hours incubation at 35°C, the reaction mixture was analyzed by SEC-HPLC using a Zorbax GF-250 column (250 × 4.6 mm) eluted with 0.1M phosphate buffer, 0.2 M NaCl (pH 7.2) containing 20% (v/v) of ACN. The effluent was monitored by measuring the absorbance at 280 nm.

The conjugate was purified by RP-HPLC using a Phenomenex Jupiter C18 column (250 × 4.6 mm) with a linear gradient of 40–80% (v/v) acetonitrile containing 0.01% TFA over 25 min, followed by an isocratic wash at 90% acetonitrile. The effluent was monitored by measuring the absorbance at 280 nm. After the purification, the solution was concentrated under vacuum and the conjugate was dialyzed against PBS solution. The protein concentration was determined by UV-VIS absorption (hGH absorption coefficients: 0.79 mL cm^{-1}) and the conjugate was characterized by MALDI-TOF mass spectrometry, SDS-PAGE, and circular dichroism as described in sections 3.4.2, 3.4.3 and 3.4.4.

3.5.4 Pharmacokinetic studies in rats of hGH-PLE$_{50ald}$

Pharmacokinetic profiles of free and conjugated hGH were determined in Sprague-Dawley rats (250-350 g). The rats were randomly divided into two groups of 3 animals per group. A dose of 100 µg/kg hGH (equiv.) was administered via tail vein to the rats anesthetized with 5% isoflurane gas (mixed with O_2 in enclosed cages). At predetermined times blood samples were collected from the tail vein and centrifuged at 1500 × g for 15 min. The hGH content in serum samples was quantified using the hGH ELISA kit. The pharmacokinetic data elaboration was performed by *PkSolver* program applying a bicompartmental model.

3.5.5 Pharmacodynamic Study in Hypophysectomized (HYPOX) Rats

In this study, hGH, hGH-PLE$_{50ald}$, PEG-Gln141-hGH and PEG-Nter-hGH were tested to evaluate and compared the efficacy of the conjugate and the native protein on the stimulation of somatic growth in hypophysectomized male Sprague Dawley. In hypophysectomized rats the pituitary gland was removed by surgery, therefore they can’t produce somatotropin. The considered parameters, indices of somatic growth, were the weight gain, the femoral length and the width of the tibial cortical bone tissue of diaphysis.

3.5.5.1 Weight Gain Test

Hypophysectomized male Sprague Dawley rats were purchased from Charles River Laboratories (Lecco, Italy) and weighed about 90 g at study initiation. Rats were randomized by weight in five groups (n = 6). The first group received daily, via tail vein, vehicle solution (PBS, 200 µL). A 30 µg/rat/day of native hGH was administered to the second group for 6 days. The third, the fourth and the fifth groups received a single injection (tail vein) at the beginning of the experiment of 180 µg/rat (hGH equiv.) of, respectively, hGH-PLE$_{50ald}$, PEG-Gln141-hGH and PEG-Nter-hGH. Protein solutions were prepared in vehicle solution. Animals were followed for 6 days and body weight measurements were taken at the same time every day until the end of the study.

At day 7, animals were sacrificed and their femurs and tibias harvested for the measurements as following specified. The collected femurs and tibias have been preserved in 10% neutral buffered formalin until needed.

3.5.5.2 Femoral length and width of the tibial cortical bone tissue of diaphysis measurements.

Femurs were measured with a vernier caliper to determine the length while tibias were fixed in 10% neutral buffered formalin, then decalcified in 5% formic acid for 96 h paraffin embedded. One µm sections were stained with toluidine blue. The width of the cortical bone of the tibial diaphysis was measured on the right tibia (the results were the average of at least 20 measurements per tibia).

3.6 SYNTHESIS AND CHARACTERIZATION OF PEG-KR14 CONJUGATE

3.6.1 Synthesis of azidoproline

3.6.1.1 *Mesylation of Boc-L-proline methyl ester*

The hydroxyl group of Boc-L-proline methyl ester was modified with methanesulfonyl chloride (CH_3SO_2Cl) in basic condition as reported in figure 3.12.

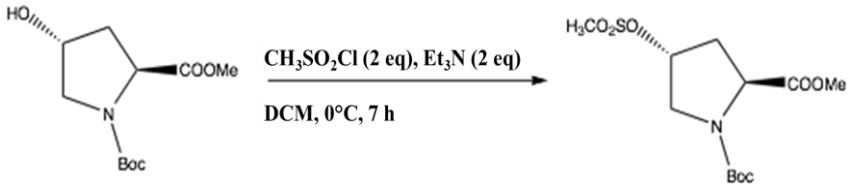

Figure 3.12: Reaction scheme of Boc-L-proline methyl ester mesylation.

5 g (0.02 moles MW 245.27 Da) of Boc-L-proline methyl ester were dissolved in ice-cold CH_2Cl_2 (100 mL) and 5.7 ml (0.041 moles, 2 equivalent, MW = 101.19 Da, d=0.726 g/ml) of Et_3N were added. 3.2 ml (0.041 moles, 2 equivalent, MW = 114.55 Da, d=1.48 g/mL) of CH_3SO_2Cl, previously diluted with 50 ml of CH_2Cl_2, were then added dropwise with funnel under ice condition.

The reaction was left under stirring and monitored with TLC. After 7 hours, the reaction was stopped adding 50 mL of H_2O and washed with 1M HCl (50 mL) (to remove the excess amount of CH_3SO_2Cl and Et_3N), then with saturated $aHCO_3$ solution (50 mL) (to remove non-reacted proline, HCl, and Et_3N.HCl) and then with saturated NaCl solution. The organic layer was dried with anhydrous Na_2SO_4 and the CH_2Cl_2 was evaporated to obtain a brown oil, left under vacuum overnight (MW 323.36 Da, yield: 5.87 g, 93.9 %).

3.6.1.2 *Nucleophilic Substitution of Mesyl by azido group*

The mesyl group was converted to an azide, needed for the following Click Chemistry to react with the alkyne ethynylferrocene. To this aim, sodium azide, which is a nucleophile, was used. The mesyl substituent was an (R) configuration and, after the nucleophilic substitution, the azide has changed in (S) (Figure 3.13).

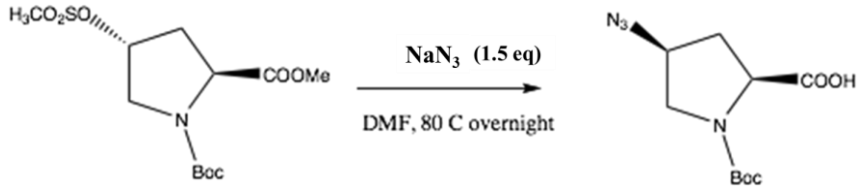

Figure 3.13: Nucleophilic substitution of mesyl group.

5.87 g of mesylated Boc-L-proline methyl ester were dissolved in 60 mL DMF and 1.75 g (0.027 moles, 1.5 equivalent, MW = 65.01 Da) of NaN_3 were slowly added. The reaction was stirred overnight under 80°C and then cooled down to room temperature. EtOAc (150 ml × 2) was used to extract the azidoproline and the organic layer was washed with saturated NaCl solution, dried with anhydrous Na_2SO_4, evaporated to obtain a brown oil and left under vacuum overnight (MW 270.13 Da, yield: 4.04 g, 85.7 %).

3.6.1.3 *Deprotection of the Methyl Ester*

The azidoproline was dissolved in 80 ml of a mixture THF/NaOH 2N (1:1 v/v), left to reflux for 2 hours and stirred overnight. After removing the organic phase under reduced pressure, 15 ml of DCM were added to extract the water layer. Concentrated HCl was used to acidify the extracted layer and then, EtOAc (20 ml) was added and the mixture was stirred overnight.

EtOAc layer was washed with saturated NaCl solution, dried with anhydrous Na_2SO_4, evaporated to obtain a light brown oil and left under vacuum overnight (MW 256.12 Da, yield: 3.17 g, 83.1 %). The scheme of reaction is reported in figure 3.14.

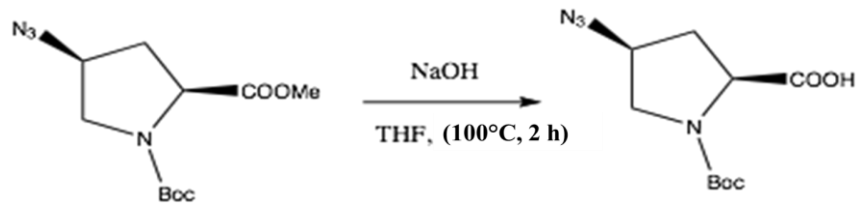

Figure 3.14: Hydrolysis reaction for the removing of the methyl.

3.6.1.4 *Substitution of N-Boc group with Fmoc*

The azidoproline was dissolved in 15 ml of DCM, 15 ml of TFA were added under ice condition and the reaction was stirred under ice for 30 min and at RT for 2 hours. The TFA was removed under gentle N_2 stream and the residue was dissolved

in 15 mL of H_2O. Na_2CO_3 was added to reach pH 9 and then 8.3 g (0.024 moles, 2 equivalent, MW = 337.3 Da) of Fmoc-Osu were added, previously solubilized in 10 ml of THF. The reaction was stirred overnight.

The water layer was extracted with ether and normalized with concentrated HCl under ice condition to achieve the formation of a white solid that was finally recovered with EtOAc extractions (20 ml × 2). The organic layer was washed with saturated NaCl solution, dried with anhydrous Na_2SO_4, evaporated to obtain a white/pink solid that was left under vacuum overnight (MW 378.38 Da, yield: 3.33 g, 79.5 %). The scheme of reaction is reported in figure 3.15.

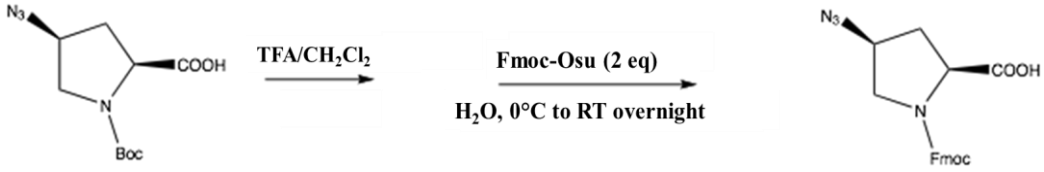

Figure 3.15: Deprotection of the N-Boc group and protection of NH group with Fmoc.

3.6.2 Synthesis of KR14 using CEM microwave synthesizer

The peptide triazole KR14 (Figure 3.16) was synthesized by CEM microwave synthesis using Fmoc chemistry on a Rink amide resin at a 0.25 mM scale.

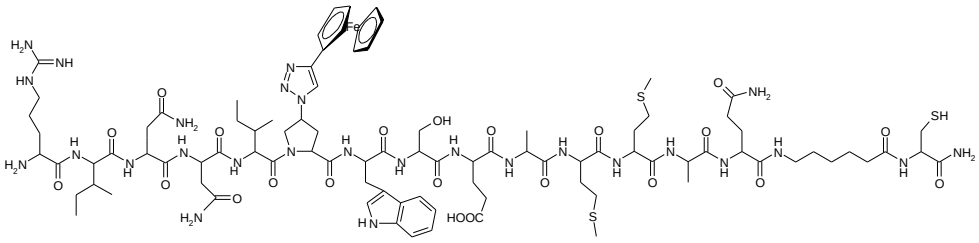

Figure 3.16: KR14 structure.

The amino acid solutions were prepared at a concentration of 0.3 M in DMF and for the 0.25 mM scale, 0.446 g of resin were used. The deprotector, the activators and the main wash solvent were a solution of piperidine 20% in DMF, DCI/HOBT (N,N'-Diisopropylcarbodimide/1-Hydroxybenzotriazole) and DMF respectively.

After the assembling of the residues, the resin was diluted in 15 ml of THF and 0.5 g of Boc-anhydride were added for the N-terminal protection. The reaction was stirred for 7 hours at RT and then the resin was filtered and washed with DCM.

After drying, a [3+2] cycloaddition reaction was completed using ethynylferrocene. For the click reaction, a mixture of 4.24 ml of acetonitrile, 4.24 ml of H_2O, 1.06 ml of DIPEA and 0.53 ml of pyridine was prepared, 20 mg of CuI and 300 mg of ethynyl ferrocene were added and the reaction was stirred at room

temperature overnight. Subsequently, the resin was filtered and taken in to cleavage cocktail of 95:2:2:1 trifluoroacetic acid (TFA)/1, 2-ethanedithiol/water/thioanisole for 2 h. Separated the resin, the solution was precipitated in cold diethyl ether. The crude peptide was recovered for centrifugation and was dissolved in 50% ACN/H2O and purified by RP HPLC (Beckmann Coulter) on a preparative C18 column (100 Å, 2.14 × 25 cm) with a linear gradient of 5–95 % of ACN/water in 0.1% TFA. The final purified peptide were lyophilized and validated by MALDI-TOF mass spectrometry.

3.6.3 Conjugation of PEG-Maleimide to KR14

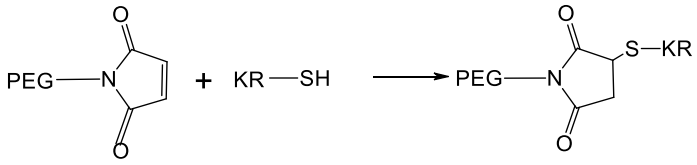

Figure 3.17: The thiol group of KR14 is conjugated to maleimide of PEG.

To 4 mL (0.94 mmol, MW 2126 Da) of a KR14 solution (0.5 mg/mL) in DMSO, 42.7 mg (2.13 mmol, 2-fold molar excess, MW 20000 Da) of PEG_{20kDa}–Mal were added and the mixture was left to stir at room temperature for 18 h (Figure 3.17). The conjugation reaction was monitored by SEC-HPLC using a Phenomenex BioSep-SEC-S 4000 column (7.8 × 300 mm) eluted with 0.1 M phosphate buffer, pH 6.8, containing 20% (v/v) of acetonitrile. The effluent was monitored by measuring the absorbance at 280 nm. Then, 3 equivalents of thioglycolic acid (TGA), with respect to each equivalent of PEG_{20kDa}–Mal, were added to the reaction mixture to block the reactive maleimide group. The conjugates were dialyzed against PBS (phosphate buffered saline), pH 7.2, using a membrane with cut-off of 14000 MWCO. The peptide concentrations were determined by UV absorption at 280 nm (absorption coefficients: 2.86 mL cm^{-1} mg^{-1}) and the characterization was carried out by SEC-HPLC and MALDI-TOF mass spectrometry.

3.6.4 Pharmacokinetic studies of KR14 and PEG-KR14

The pharmacokinetic profiles of PEG-KR14 and free KR14 were evaluated in rats by labeling the peptide moiety with fluorescein.

3.6.4.1 *Preparation of 5-FM-KR14*

KR14 was labeled with fluorescein exploiting the free thiol group (Figure 3.18). The binding of 5-FM to the free cysteine of the peptides prevented the formation of PT dimers *in vivo*.

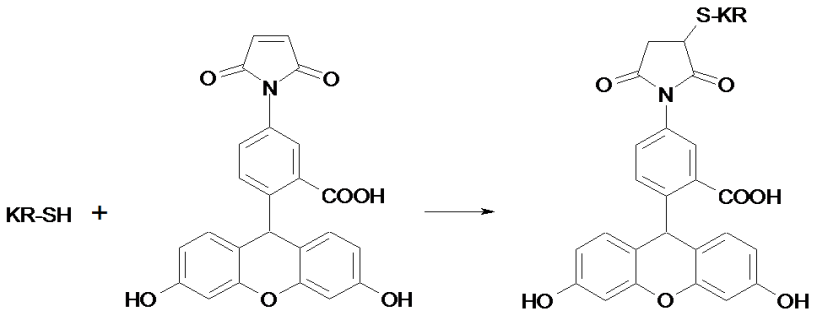

Figure 3.18: The thiol group of KR14 is conjugated to maleimide of fluorescein.

The reaction was performed at a peptide concentration of 1 mg/mL in DMSO and an excess of 0.8 eq of fluorescein-5-maleimide (5-FM). TGA was added using an excess of 1.5 eq compared to fluorescein. The reaction was monitored and purified by RP-HPLC. The product was characterized by ESI-TOF analyses and the loading of fluorescein was determined by UV-VIS absorption (absorption coefficients: 2.86 mL cm^{-1} mg^{-1}).

3.6.4.2 *Preparation of FITC-PEG-KR14*

PEG-KR14 was labeled with fluorescein through the N-terminal amino group of the peptide (Figure 3.19).

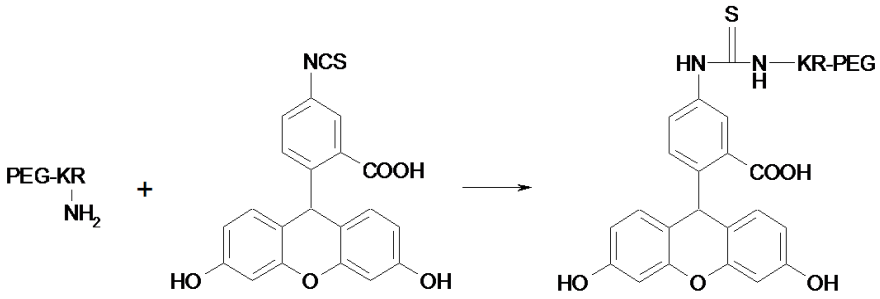

Figure 3.19: Free amino group of peptide is conjugated to isothiocyanate group of fluorescein.

The reaction was carried out at a PEG-KR concentration of 1 mg/mL in DMSO, an excess of 5 eq (0.94 mmol, MW 2126 Da) of fluorescein isothiocyanate (FITC)

and 1 eq TEA. The products were purified by dialysis and analyzed by SEC. The loading of fluorescein was determined by UV-VIS absorption using the extinction coefficient of FITC (absorption coefficients: 2.86 mL cm^{-1} mg^{-1}).

3.6.4.3 Pharmacokinetics

Pharmacokinetic profiles of free and conjugated peptide were determined in Balb/c mice. 5-MF-KR14 and FITC-PEG-KR14 were solubilized in saline buffer and were administered *via* tail vein to rats anaesthetized with isoflurane gas (mixed with O_2 in enclosed cages). At predetermined times, blood samples were withdrawn, centrifuged, PBS (Phosphate Buffer Saline) were added and then the fluorescence was determined.

3.6.5 Surface Plasmon Resonance competition experiments

Surface plasmon resonance (SPR) technique is an optical method for measuring the refractive index of very thin layers of material adsorbed on a metal. The SPR technique is based on the fact that, at certain conditions, surface plasmons on a metallic film can be excited by photons, thereby transforming a photon into a surface plasmon and it depend on the refractive index of the adsorbate. In the Biacore system the principal determinant at which the angle of incidence occurs is the refractive index close to the backside of the metal film, to which target molecules are immobilized and addressed by ligands in a mobile phase running along a flow cell. If binding occurs to the immobilized target, the local refractive index changes, leading to a change in SPR angle, which is monitored in real time by detecting changes in the intensity of the reflected light, producing a sensorgram (Figure 3.20).

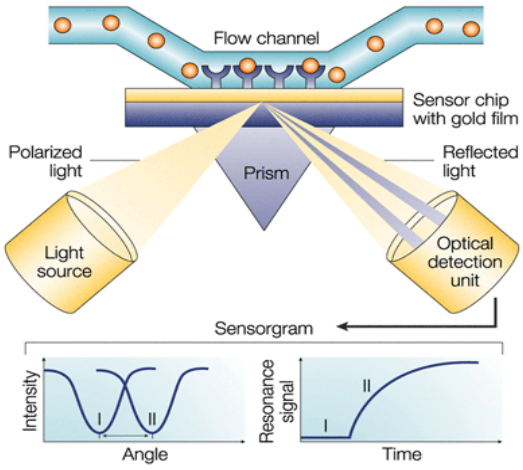

Figure 3.20: Typical set-up for an SPR biosensor.

All surface plasmon resonance (SPR) experiments were performed on a Biacore 3000 optical biosensor. A CM5 sensor chip was derivatized by amine coupling by using N-ethyl-N-(3-dimethylaminopropyl)carbodiimide/N-hydroxy-succinimide (Ishino et al., 2006) with soluble CD4, mAb 17b Fab, or as a control surface mAb2B6R (antibody to human IL-5 receptor a). For competition experiments,ligands (sCD4 and 17b mAb,) were immobilized on a surface with a density of approximately 2000 RU. Fixed solutions of gp120 were passed over the surfaces at a flow rate of 50 mL/min with 2.5 min association phase and 2.5 min dissociation phase, mixed to different amounts of native or modified peptide. Surfaces were regenerated by using 35mM NaOH and 1.3M NaCl for sCD4 and 10mM HCl for 17b surface. Data analysis was performed using BIAEvaluation1 4.0 software. The responses of a buffer injection and responses from the control surface to which the mAb 2B6R was immobilized, were subtracted to account for nonspecific binding. The inhibitor concentration at 50% of the maximal response (IC_{50}) was calculated. The inhibition curve was converted into a calibration curve by the use of a fitting function. Results were given as the percentage of gp120 bound relative to gp120 bound in the absence of peptide: $100\times[(RU-RUgp120)/RUgp120]$.

4 RESULTS

4.1 SYNTHESIS OF NH_2-PEG-(β-Glu)-(β-Glu)$_2$-(β-Glu)$_4$-(COOH)$_8$

NH_2-PEG-(β-Glu)-(β-Glu)$_2$-(β-Glu)$_4$-(COOH)$_8$, also termed PEG-dendron, is a multicarboxylic polymer characterized by the presence of carboxylic groups (─COOH) which confer the polyanionic characteristic to the polymeric chain. PEG-dendron was synthetized starting from Boc-NH-PEG$_{5k}$-NHS (MW 5003 Da) and it was derivatized at the NHS end with a symmetric bicarboxylic unit, namely β-glutamic acid, which provides a branched structure that doubles the number of negative charges at each generation. The other end of the heterobifunctional chain offers an amino group suitable for enzymatic PEGylation via tranglutaminase (Figure 4.1)

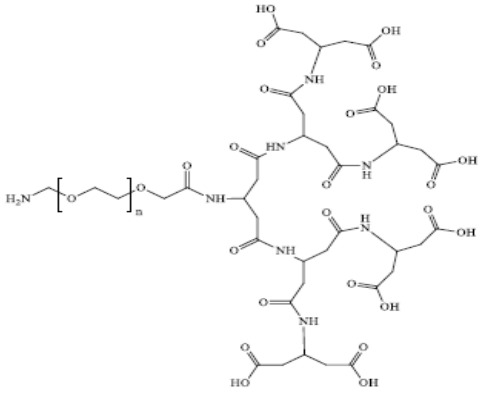

Figure 4.1: PEG-dendron.

The reaction steps have provided the formation of an amide bond between the activated carboxyl group of PEG and the amino group of β-glutamic acid, alternated to the consequently activation of the new carboxylic groups. The last step was the removal of the protecting group t-Boc to obtain the free amino group.

The results of the synthesis were reported in table 4.1.

Table 4.1: Results of the synthesis of PEG-dendron.

Synthesis step	Yield (%)	Activation degree (%)
Synthesis of Boc-NH-PEG-β-Glu-(COOH)$_2$	87	
Activation of Boc-NH-PEG-β-Glu-(COOH)$_2$		81.6
Synthesis of Boc-NH-PEG-(β-Glu)-(β-Glu)$_2$-(COOH)$_4$	78.4	
Activation of Boc-NH-PEG-(β-Glu)-(β-Glu)$_2$-(COOH)$_4$		83.5
Synthesis of Boc-NH-PEG-(β-Glu)-(β-Glu)$_2$-(β-Glu)$_4$- (COOH)$_8$	85.8	

4.1.1 Characterization of Boc-NH-PEG-(β-Glu)-(β-Glu)$_2$-(β-Glu)$_4$-(COOH)$_8$

The degree of derivatization with β-Glutamic acid was determined by ^{1}H-NMR. In figure 4.2 PEG-dendron ^{1}H-NMR spectrum was compared to Boc-NH-PEG$_{5k}$-NHS one. The signals of β-Glutamic acid are m, 4.50 ppm -NH**CH**$(CH_2)_2$-, m, 2.59 ppm -NHCH(**CH$_2$**)$_2$$(COOH)_2$ and m, 2.44 ppm -NHCH(**CH$_2$**)$_2$CONH-).

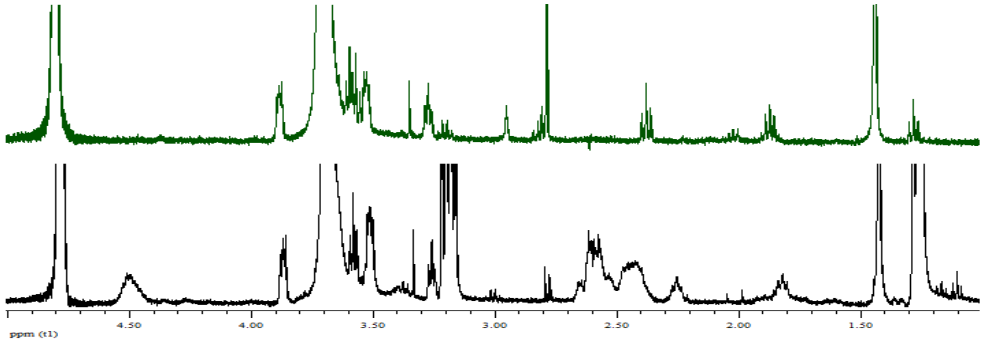

Figure 4.2: ^{1}H-NMR spectroscopy of Boc-NH-PEG$_{5k}$-NHS (green spectrum) and PEG-dendron (black spectrum).

After the integration of the signals (Table 4.2), 6 units of β-Glu were found to form the PEG-dendron, which reflect the presence of 7 carboxylic groups instead the 8 expected.

Table 4.2: Integration of the signals.

δ (ppm)	Multiplicity	Theoric integration	Sperimental integration	Attribution
4.5	m	7	3.87	-NH**CH**$(CH_2)_2$-
2.59	m	16	25.48	-NHCH(**CH$_2$**)$_2$$(COOH)_2$
2.44	m	12		-NHCH(**CH$_2$**)$_2$CONH-
1.43	s	9	9	-OC(**CH$_3$**)$_3$

4.1.2 Removal of protecting group t-Boc from Boc-PEG$_{5k}$-(COOH)$_7$

The deprotection of the amino group was performed in acidic condition where the Boc group dissociates. The absence of the protecting group was confirmed by MALDI-TOF mass spectrometry. As reported in figure 4.3, the signal at δ = 1.43 ppm (multiplicity *s*) was absent.

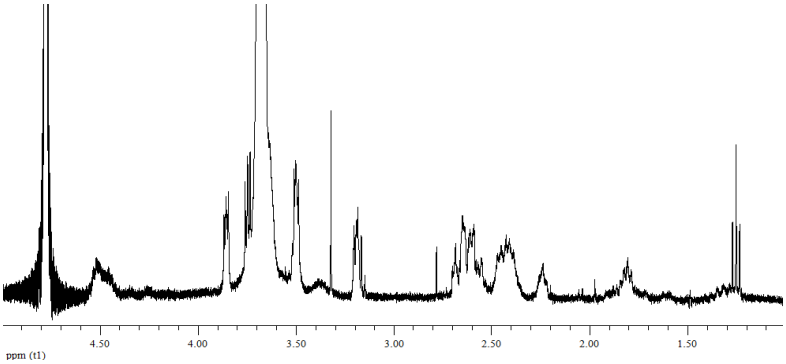

Figure 4.3: ^{1}H-NMR spectroscopy of PEG$_{5k}$-(COOH)$_7$.

The molecular weight of Boc-NH-PEG-(β-Glu)-(β-Glu)$_2$-(β-Glu)$_4$-(COOH)$_7$ was calculated by MALDI-TOF mass spectrometry and was found to be 5717 Da that corresponds to the derivatization with 6 units of β-Glu (Figure 4.4).

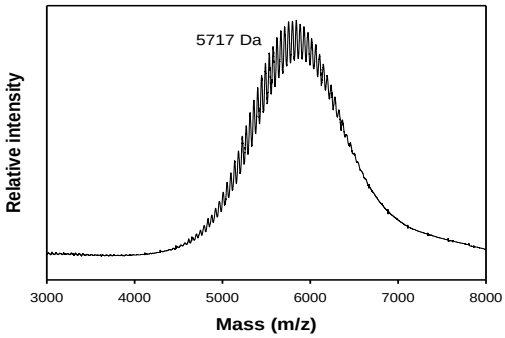

Figure 4.4: MALDI-TOF spectra of PEG$_{5k}$-(COOH)$_7$.

4.2 SYNTHESIS AND CHARACTERIZATION OF G-CSF-PEG CONJUGATES

4.2.1 Removal of protecting group t-Boc from Boc-PEG$_{3.4k}$-b-PLE$_{50}$

The absence of the protecting group was confirmed by MALDI-TOF mass spectrometry. As reported in figure 4.5, the signal at δ = 1.43 ppm (multiplicity *s*) was absent.

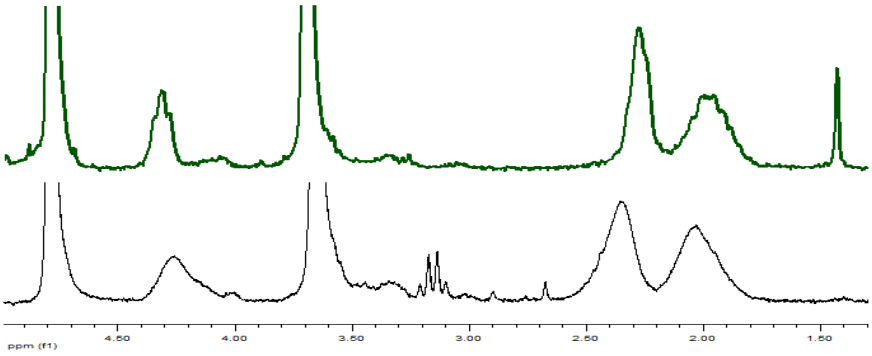

Figure 4.5: ^{1}H-NMR spectroscopy of Boc-NH-PEG$_{3.4k}$-b-PLE$_{50}$ (green spectrum) and Boc-NH-PEG$_{3.4k}$-b-PLE$_{50}$ (black spectrum).

4.2.2 Site-specific conjugation of multicarboxylic and neutral PEGs to G-CSF

G-CSF-PEG conjugates were obtained by enzymatic PEGylation, exploiting the enzyme microbial transglutaminase (mTGase). mTGase-mediated conjugations were achieved as described in section 3.4.1.2 and have allowed the site-specific binding of PEG to G-CSF, where only one of its 17 glutamines (Gln135) was the substrate for the enzyme.

The conjugates were analysed, purified and characterized by: i) RP-HPLC to remove the free rhG-CSF, ii) MALDI-TOF mass spectrometry to confirm the formation of the products, iii) SDS-PAGE to validate the purity, iv) circular dichroism to assess the effect of PEGylation on secondary structure of the protein.

4.2.2.1 HPLC profiles

The reactions were monitored by RP-HPLC at t = 0’ (before the addition of mTGase) and after 4 hours of incubation of G-CSF with the polymer in the presence

of mTGase. In figure 4.6 the chromatography profiles of G-CSF-PEG conjugates are shown.

The conjugates retention time (t_r about 21 min) were different from free G-CSF (t_r = 23 min). The yield of the reactions, calculated from the peak areas, were 74.3, 61,86 and 70% for G-CSF-PEG_{5k}-$(COOH)_7$, G-CSF-$PEG_{3.4k}$-b-PLE_{50}, G-CSF-PEG_{5k} and G-CSF-PEG_{20k} respectively.

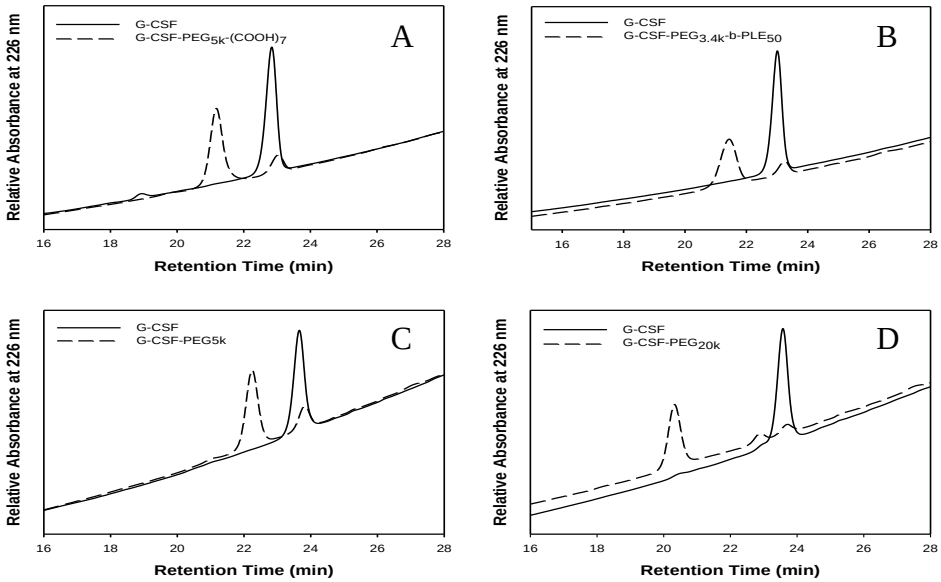

Figure 3.8: Scheme of rhG-CSF-PEG synthesis.

Figure 4.6: Chromatography profiles of G-CSF-PEG_{5k}-$(COOH)_7$ (A), G-CSF-$PEG_{3.4k}$-b-PLE_{50} (B), G-CSF-PEG_{5k} (C) and G-CSF-PEG_{20k} (D) mixture reactions.

4.2.2.2 MALDI-TOF spectra

The molecular weights of the conjugates were determined by MALDI-TOF mass spectrometry and they correspond to one molecule of G-CSF (18792.8 Da) bound to one chain of H_2N-PEG_{5k}-$(COOH)_7$ (5717 Da), H_2N-$PEG_{3.4k}$-b-PLE_{50} (11000 Da), $mPEG_{5k}$-NH_2 (5000 Da) or $mPEG_{20k}$-NH_2 (20000 Da) respectively (Figure 4.7).

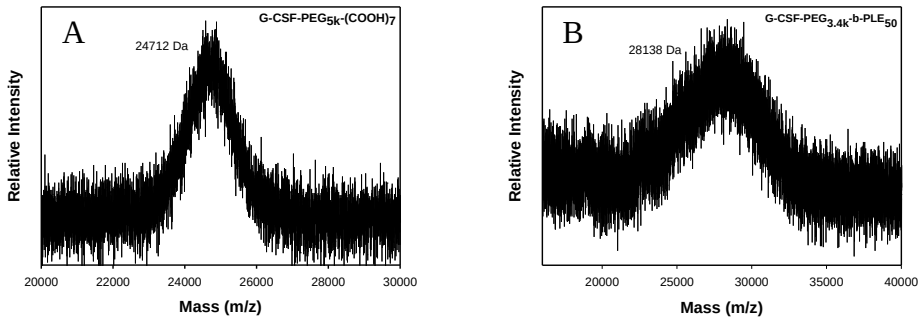

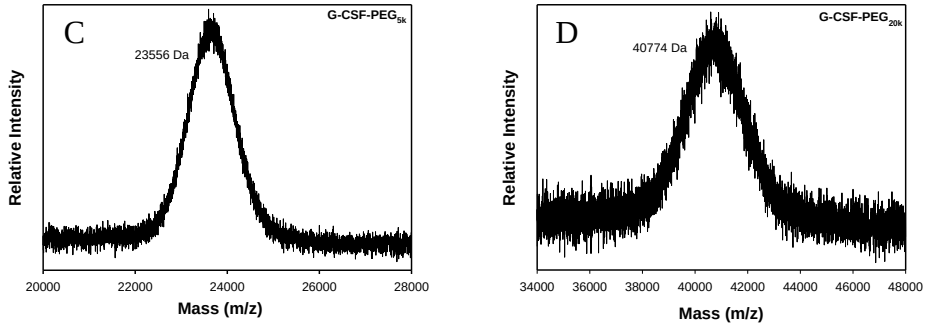

Figure 4.7: MALDI-TOF spectra of G-CSF-PEG$_{5k}$-(COOH)$_7$ (A), G-CSF-PEG$_{3.4k}$-b-PLE$_{50}$ (B), G-CSF-PEG$_{5k}$ (C) and G-CSF-PEG$_{20k}$ (D).

4.2.2.3 *SDS-PAGE*

The purified conjugates G-CSF-PEG$_{5k}$-(COOH)$_7$, G-CSF-PEG$_{3.4k}$-b-PLE$_{50}$, G-CSF-PEG$_{5k}$, and G-CSF-PEG$_{20k}$ were analyzed by SDS-PAGE (figure 4.8), along with native G-CSF, to confirm that the synthesis reactions resulted in the formation of the desired monoconjugates, and to demonstrate that the purification of the conjugates were achieved successfully.

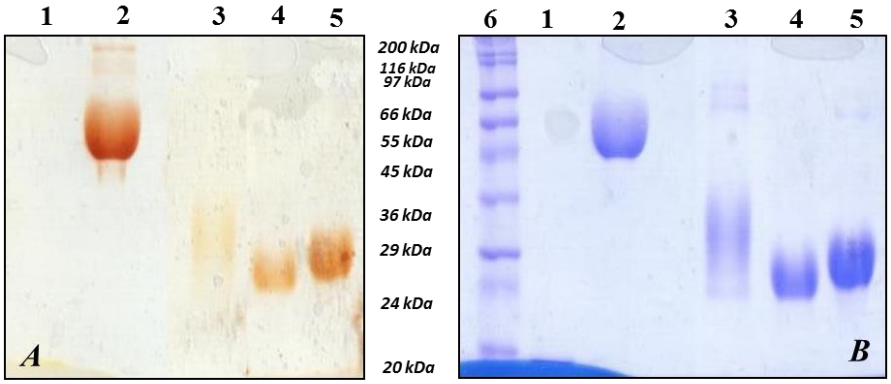

Figure 4.8: Gel electrophoresis of G-CSF (1), G-CSF-PEG$_{20k}$ (2), G-CSF-PEG$_{3.4k}$-b-PLE$_{50}$ (3), G-CSF-PEG$_{5k}$ (4), G-CSF-PEG$_{5k}$-(COOH)$_7$ (5), and marker (6). A) Colored with iodine. B) Colored with Coomassie blue.

The presence of the bands in both iodine and Coomassie blue coloration confirms that G-CSF was PEGylated in all four reactions. Molecular weights of the PEGylated conjugates on the gel are higher than their real values because PEG has a greater hydrodynamic volume than a protein of the same molecular weight. Moreover, the purified PEGylated derivatives of G-SCF are monoconjugates and pure.

4.2.2.4 *Circular Dichroism*

The investigation of the secondary structure of G-CSF and its PEGylated derivatives was carried out by far-UV circular dichroism in order to study the effect of the polymer on the protein surface. By comparing the far-UV CD spectra of a native protein and its PEGylated derivatives, it is possible to understand whether or not PEGylation caused any changes in the secondary structure of the protein.

The CD scans were carried out in 50 mM phosphate, 5% sorbitol, pH 7 buffer where the protein is more stable. The spectra showed that the G-CSF still maintained its secondary structure after conjugation as the profiles of native G-CSF and PEGylated forms were quite similar, thus suggesting that the polymer chain did not modify the protein conformation (figure 4.9).

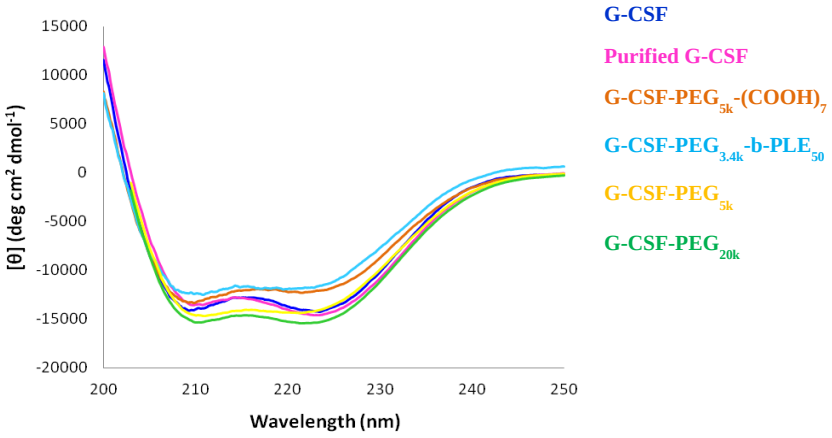

Figure 4.9: CD spectra of G-CSF and its PEGylated derivatives.

4.2.3 Stability studies

Circular dichroism can also be used to determine the thermal stability of proteins and the impact of PEGylation on protein stability, by monitoring the protein unfolding as a function of temperature at a fixed wavelength. G-CSF has 4 α-helices. Proteins with high α-helical content present peaks at 190-195 nm, 208 nm, and 222 nm and their unfolding studies are usually performed at 222 nm because α-helical proteins have a strong ellipticity signal at that wavelength, whereas unfolded proteins have no or little signal. In this CD analysis, temperature was progressively increased from 20°C to 90°C, with a temperature slope of 2°C/min.

Melting profiles of the G-CSF-PEG conjugates (Figure 4.10) showed that conjugates were slightly less stable than the native G-CSF. However, the purified G-CSF had almost the same melting profile as the conjugates, suggesting that the decrease in the stability of the protein after PEGylation is probably due to the purification conditions. Melting temperatures (the temperature where the unfolded

fraction is 50%) of the native G-CSF and its PEGylated derivatives were determined and reported in table 4.3.

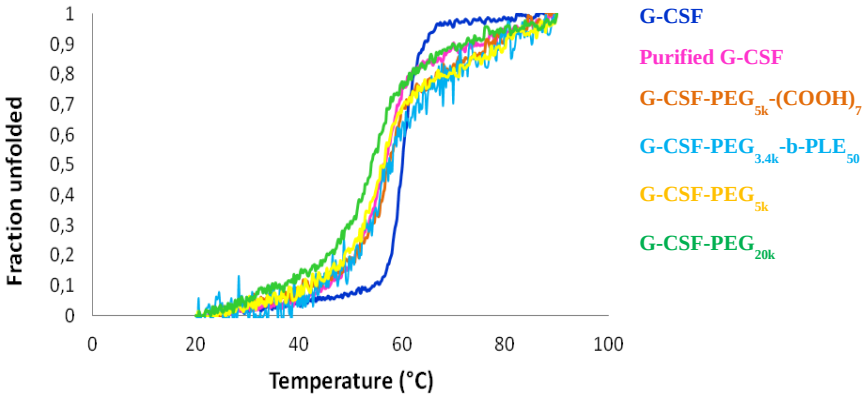

Figure 4.10: Temperature dependence of the CD intensity at 222 nm.

Table 4.3: Melting temperatures of G-CSF and its PEGylated derivatives.

Compound	T_m (°C)
Native G-CSF	60
Purified G-CSF	56.6
G-CSF-PEG$_{5k}$-(COOH)$_7$	57.4
G-CSF-PEG$_{3.4k}$-b-PLE$_{50}$	57
G-CSF-PEG$_{5k}$	56.6
G-CSF-PEG$_{20k}$	54

4.2.4 Pharmacokinetic studies

The pharmacokinetics of G-CSF and conjugates were assessed in Sprague-Dawley rats (250-350 g). The rats were randomly divided into five groups, each group containing 3 rats and a dose of 100 µg/kg G-CSF (equiv) was administered via tail vein. The G-CSF content in serum samples was quantified by human G-CSF ELISA kit (Invitrogen). The pharmacokinetic data were elaborated using *PKSolver*, applying a bicompartmental model.

As shown in figure 4.11, high plasma levels of G-CSF were recorded immediately for the native G-CSF and its PEGylated derivatives. The G-CSF level for the native protein fell below the detection limit after 7 hours, whereas the conjugates showed prolonged half-lives with detectable levels of G-CSF even after 24 hours.

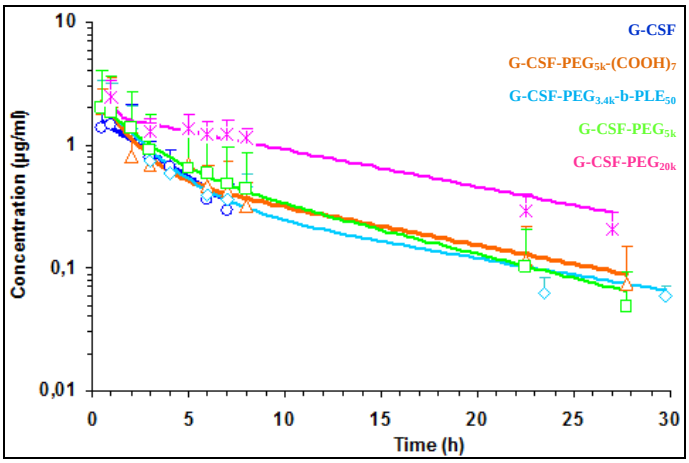

Figure 4.11: Pharmacokinetic profiles of G-CSF and its PEGylated derivatives in Sprague-Dawley rats (n=3). Data are presented as mean ±SD.

All conjugates showed an increase in elimination half-life with respect to G-CSF. The half-lives of the conjugates G-CSF-PEG$_{5k}$-(COOH)$_7$ and G-CSF-PEG$_{3.4k}$-b-PLE$_{50}$, which were coupled to multicarboxylic PEGs of 5717 Da and 11000 Da respectively, were comparable with the half-life of the conjugate G-CSF-PEG$_{20k}$, which was coupled to a neutral PEG of 20 kDa. The clearance and the apparent volume of distribution of the conjugates were significantly reduced with respect those of G-CSF. The key pharmacokinetic parameters are reported in table 4.4.

Table 4.4: Main pharmacokinetic parameters of G-CSF and its PEGylated derivatives after i.v. administration of 100 µg/kg G-CSF (equiv) to Sprague-Dawley rats.

Compounds	$t_{1/2}$ α (h)	$t_{1/2}$ β (h)	AUC$_{(0\rightarrow\infty)}$ (µg min/mL)	Cl (mL/h)	V_D (mL)
G-CSF	2.99	2.99	7.56	13.23	57.00
G-CSF-PEG$_{5k}$-(COOH)$_7$	1.00	9.80	11.54	8.14	33.72
G-CSF-PEG$_{3.4k}$-b-PLE$_{50}$	1.53	11.31	10.76	8.64	37.83
G-CSF-PEG$_{5k}$	1.48	7.72	11.60	8.15	40.81
G-CSF-PEG$_{20k}$	0.14	9.97	48.44	8.26	3.63

4.3 SYNTHESIS AND CHARACTERIZATION OF hGH CONJUGATES

4.3.1 Synthesis and characterization of PEG-Gln141-hGH and PEG-Nter-hGH

Two different site-specific mono-PEGylated forms of human growth hormone (hGH) were prepared exploiting an enzymatic PEGylation (PEG-Gln141-hGH) via transglutaminase (TGase) and a chemical *N*-terminal PEGylation (PEG-Nter-hGH). The preparation of the conjugates was accomplished as described in section 3.5.1, using 20kDa and neutral PEGs. The enzymatic PEGylation was performed in 0.1 M phosphate buffer pH 7.0 containing 50% of EtOH (v/v) in order to increase the selectivity of mTGase, according to achievements previously reported by our research group [Mero 2011]. The chemical PEGylation was conducted in 0.1 M acetate buffer pH 5 to direct the modification at the *N*-terminal, thanks to the lower *pKa* value of the α-amino group with respect to the ε-amino groups.

The conjugates were analysed and characterized by: i) RP and SEC-HPLC, ii) MALDI-TOF mass spectrometry to confirm the formation of the products, iii) SDS-PAGE to validate the purity, iv) circular dichroism to assess the effect of PEGylation on secondary structure of the protein.

4.3.1.1 HPLC profiles

The reactions were monitored by RP and SEC after 18 and 5 hours of incubation for enzymatic and chemical reaction respectively. In figure 4.12 the chromatography profiles of mixtures reaction are shown.

The yield of the reactions, calculated from the peak areas, were 45% for PEG-Gln141-hGH and 60% for PEG-Nter-hGH.

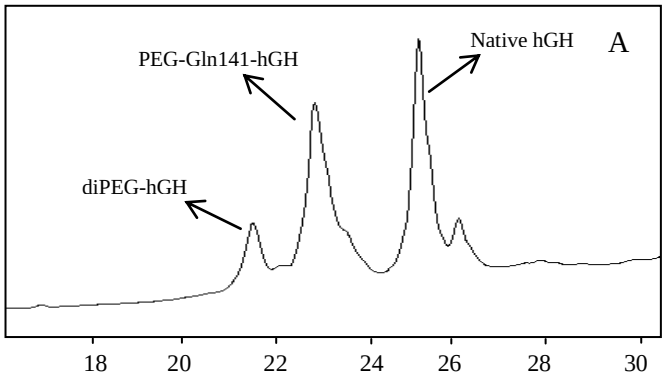

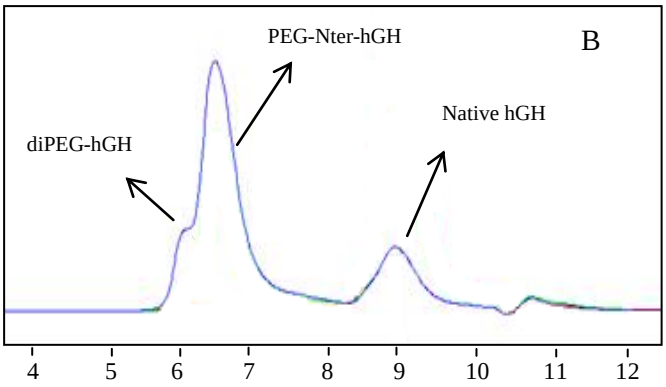

Figure 4.12: RP and SEC-HPLC analysis of PEG-Gln141-hGH (A) of PEG-Nter-hGH (B) mixture reactions.

4.3.1.2 MALDI-TOF spectra

The molecular weights of the conjugates, determined by MALDI-TOF mass spectrometry, were 44122 Da for PEG-Gln141-hGH and 44153 Da for PEG-Nter-hGH. The spectra are reported in figure 4.13.

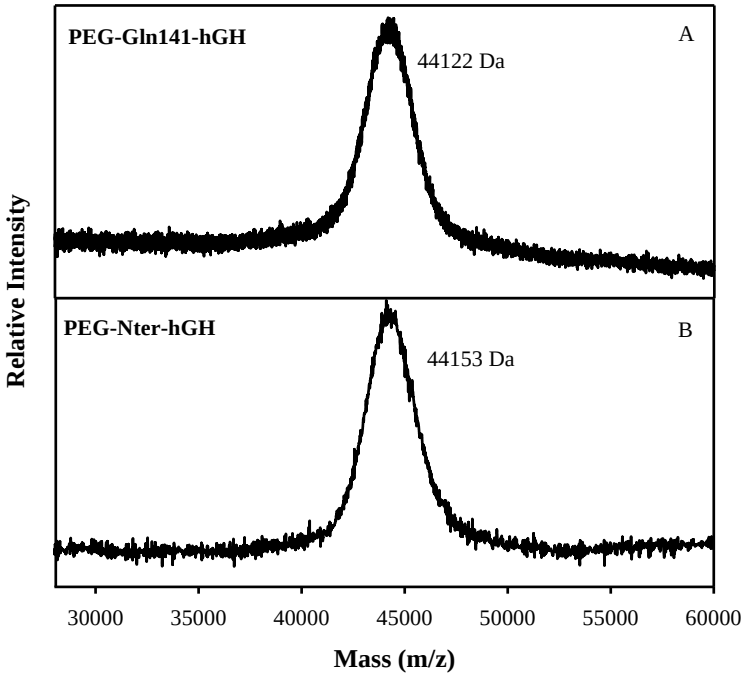

Figure 4.13: MALDI-TOF spectra of PEG-Gln141-hGH (A) and PEG-Nter-hGH (B).

4.3.1.3 SDS-PAGE

The purified conjugates were analyzed by SDS gel electrophoresis (figure 4.14), along with native hGH, to confirm that the synthesis reactions resulted in the

formation of the desired monoconjugates, and to demonstrate that the purification of the conjugates were achieved successfully.

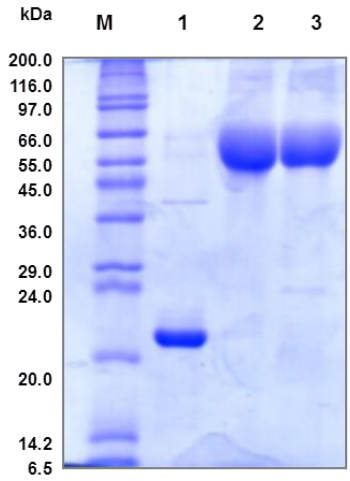

Figure 4.14: SDS gel electrophoresis of the following: M, Marker; 1, native hGH (22 kDa); 2, PEG-Gln141-hGH (~ 66kDa); 3, PEG-Nter-hGH (~ 66kDa).

4.3.1.4 Circular Dichroism

Far-UV CD spectra of native protein and PEG-hGH conjugates were compared to study the effect of the polymer on the protein surface.

The CD scans were carried out in PBS buffer and the spectra showed that the hGH in both PEG-Nter-hGH and PEG-Gln141-hGH preserved the native secondary structure (figure 4.15).

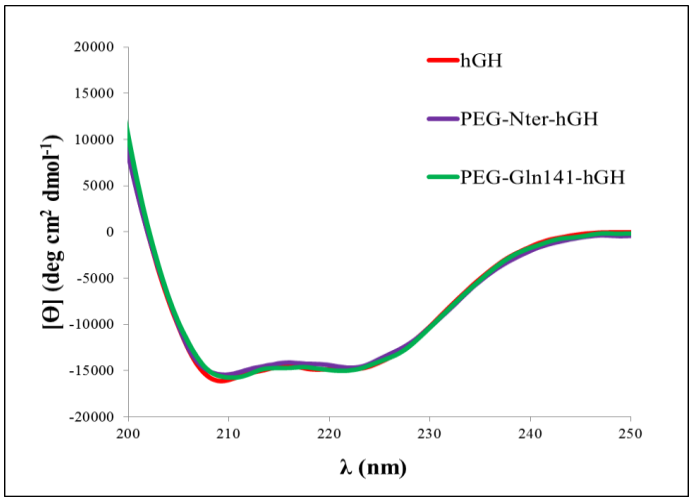

Figure 4.15: CD spectra of hGH and PEG-hGH conjugates.

4.3.2 Thermal stability studies

Thermal denaturation was carried out to investigated if the different PEGylation site caused a difference in the thermal stability of the two conjugates. Denaturation experiments of hGH and its conjugates were carried out in the temperature range of 20 – 95°C by measuring the ellipticity at 208 nm (Figure 4.16). The protein maintained its secondary structure up to 70 – 75°C and then rapidly lost its native structure with a melting temperature of 82°C. Also PEG-Gln141-hGH was found to be stable up to about 70 – 75°C and lost its secondary structure with a transition mid-point at 83.8°C. Otherwise PEG-Nter-hGH displayed a higher thermal stability, with a melting temperature of 86.1°C (Table 4.5).

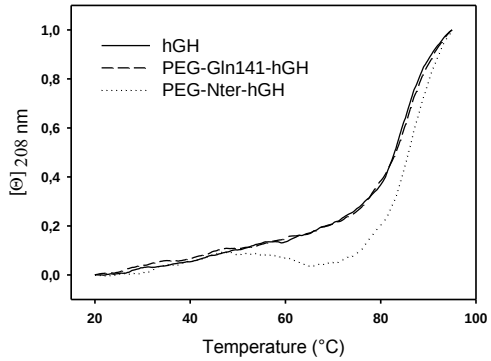

Figure 4.16: Temperature dependence of the CD intensity at 208 nm.

Table 4.5: Melting temperatures of hGH, PEG-Gln141-hGH and PEG-Nter-hGH.

Compound	T_m (°C)
hGH	82 ± 1.41
PEG-Gln141-hGH	83.8 ± 0.57
PEG-Nter-hGH	86.1 ± 0.42

Reversibility of the thermal unfolding was determined by measuring the recovery of the CD signal upon heating (95°C) and cooling (20°C) the hGH and PEGylated hGH solutions. As known, native hGH has a predominantly α-helical structure in physiological conditions with the two characteristic bands at 222 and 208 nm.

The CD spectra at 95°C show the disappearance of the bands at 222 and 208 nm, which means that the three samples lost their native α-helical structure. The conjugates, even at such high temperature, tend to preserve a certain percentage of α-helical structure with respect to hGH but more remarkably the transition was

reversible and partially reversible for PEG-Nter-hGH and PEG-Gln141-hGH, respectively, opposing to the permanent denaturation of hGH (Fig. 4.17).

In the case of PEG-Nter-hGH, after cooling the solutions to 20°C, the CD spectra showed a total recovery of the native α-helical structure (Fig. 4.17C). These results indicated that PEGylation increased thermal stability of hGH and favored the protein refolding, but for a complete recovery the site of PEG conjugation is relevant. Moreover PEG-Nter-hGH was found to be more stable than PEG-Gln141-hGH. Probably this behavior depends on the way in which the PEG chain is arranged around the protein, which in the case of protein *N*-terminus conjugation, the polymer is probably more effective in stabilizing the protein.

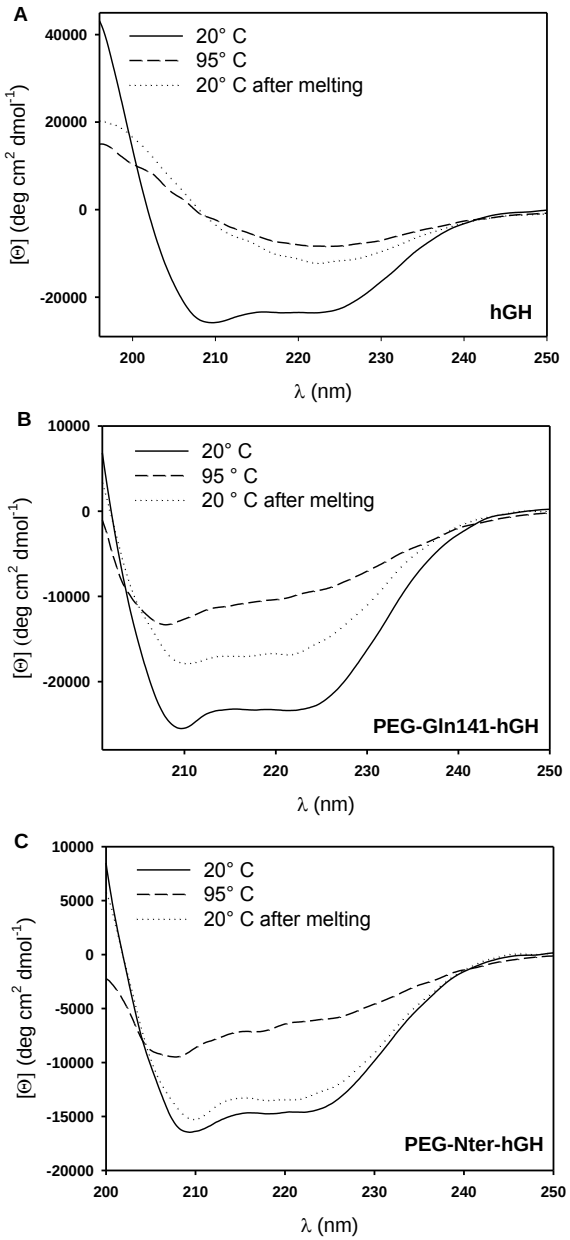

Figure 4.17: Termal stability of hGH, PEG-Gln141-hGH, and PEG-Nter-hGH by CD spectroscopy. CD spectra of hGH, PEG-Gln141-hGH, and PEG-Nter-hGH at 20°C (continuous line), 95°C (dashed line), and 20°C after heating up to 95°C (dotted line).

4.3.3 Synthesis and characterization of hGH-PLE$_{50ald}$

hGH has been site-specifically modified at the α-amino group at the protein's *N*-terminus. Conjugation with PLE$_{50ald}$ allows modification of primary amines of proteins. hGH contains ten primary amines: the *α*-amine of Phe1 and the nine *ε* amino groups of Lys residues. In order to achieve the best reaction conditions for the obtainment of a monoconjugate, a preliminary study was performed, changing some variables.

4.3.3.1 Removal of acetal group from PLE$_{50ald}$

The polymer was provided with the aldehyde function protected by an acetal group. After removal of the protecting group as describe in section 3.5.3.1, the absence of the protecting group was confirmed by ^{1}H-NMR spectroscopy. As reported in figure 4.18, the signal at δ = 1.1 ppm (multiplicity *t*) was absent.

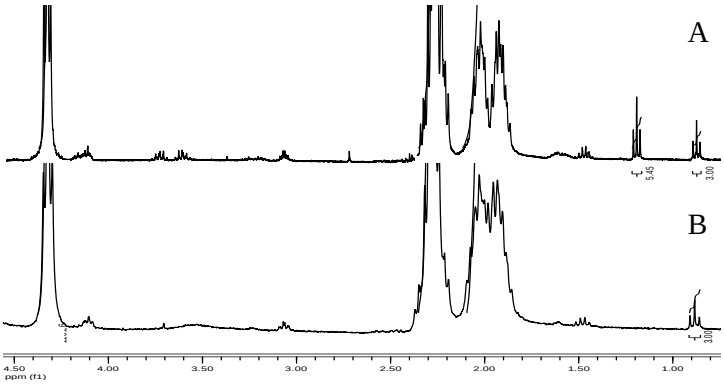

Figure 4.18: ^{1}H-NMR spectroscopy of PLE$_{50ald}$ before (A) and after (B) hydrolysis.

4.3.3.2 Study of hGH-PLE$_{50ald}$ synthesis conditions

Several reaction conditions were tested to find out the most efficient. Two reaction buffers were used (100 mM phosphate, pH 6.2 and 100 mM acetate, pH 5) and the polymer molar excess was also varied (5, 10 and 20 equivalents). Finally, the reactions were incubated at different temperatures (5, 24, 35, 40 and 45°C) and were prepared as described in section 3.5.3.2.

All the reactions were analysed by SDS-PAGE to evaluate the formation of monoconjugate and biconjugate and calculate the corresponding percentages, processing the data with ImageJ software.

The results showed that in phosphate buffer, pH 6.2 the yields of reaction were higher than in acetate buffer pH 5, as the protonation of the amines was more substantial and then they were less available for the binding to the aldehyde group.

Moreover, the increase of the polymer molar excess and also of the temperature led to an increase in the biconjugate formation (Figure 4.19).

The chosen conditions for the synthesis of hGH-PLE_{50ald} have been those that allowed the formation of only monoconjugate in the best yield.

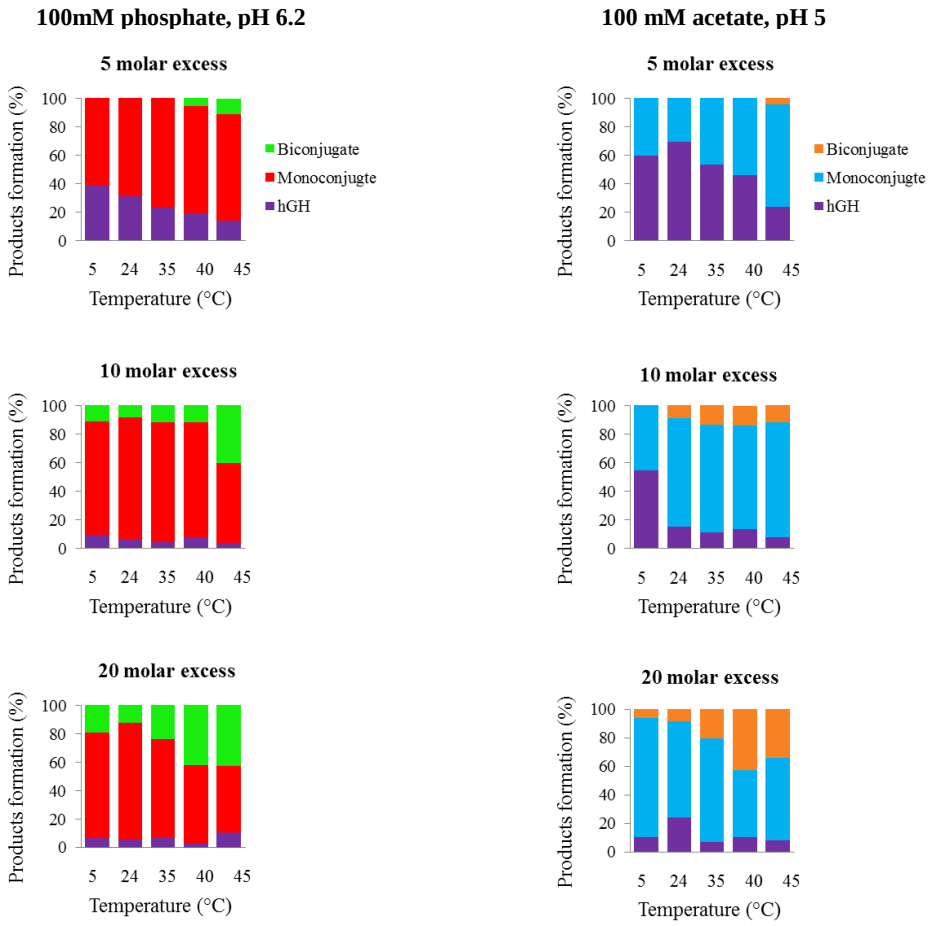

Figure 4.19: Selection of the synthesis condition.

The synthesis reaction was performed in 100 mM phosphate buffer, pH 6.2, at 35°C, using 5 equivalents of polymer as reported in section 3.5.3.3. The conjugate was then analysed and characterized by: i) SEC-HPLC, ii) MALDI-TOF mass spectrometry iii) SDS-PAGE and iv) circular dichroism.

4.3.3.3 HPLC profile

The reaction was monitored by SEC-HPLC after 18 of incubation. In figure 4.20 the chromatography profiles of mixture reaction is shown.

The conjugates retention time (t_r about 7.8 min) were different from free hGH (t_r = 9.7 min). The yield of the reactions, calculated from the peak areas, was 75%.

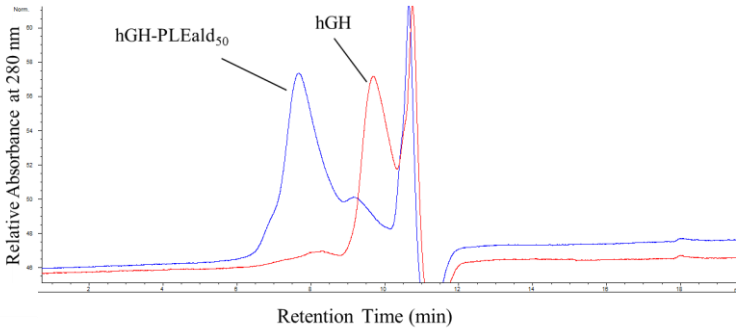

Figure 4.20: SEC-HPLC analysis of hGH and hGH-PLE$_{50ald}$.

4.3.3.4 MALDI-TOF spectrum

The molecular weight of the conjugate, determined by MALDI-TOF mass spectrometry, was 28993 Da. The spectra are reported in figure 4.21.

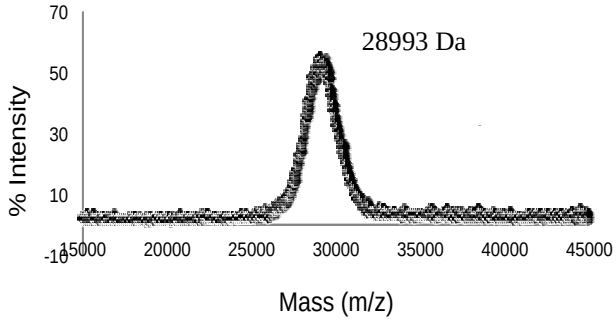

Figure 4.21: MALDI-TOF mass spectrum of hGH-PLEald$_{50}$.

4.3.3.5 SDS-PAGE

The purified conjugate were analyzed by SDS gel electrophoresis (figure 4.22), along with native hGH, to confirm that the synthesis reactions resulted in the formation of the desired monoconjugates, and to demonstrate that the purification of the conjugate was achieved successfully.

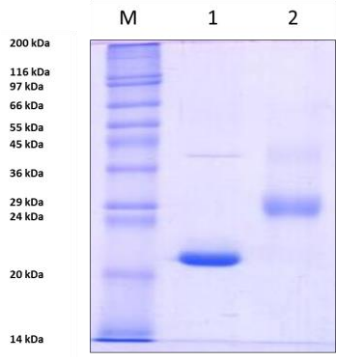

Figure 4.22: SDS gel electrophoresis of the following: M, Marker; 1, native hGH (22 kDa); 2, hGH-PLE$_{50ald}$ (29kDa).

4.3.3.6 Circular dichroism

The far-UV CD analysis (Figure 4.23), showed that hGH still maintained the native secondary structure thus suggesting that conjugation with PLE$_{50ald}$ preserved the protein conformation.

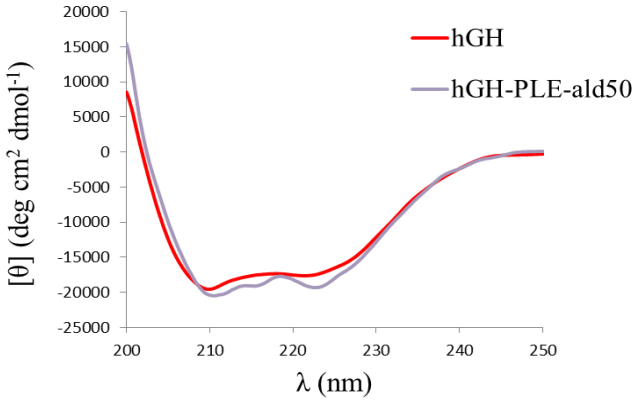

Figure 4.23: Comparison of the secondary structure of native hGH and hGH-PLE$_{50ald}$ by far-UV CD.

4.3.3.7 Pharmacokinetics

Pharmacokinetic profiles of free and conjugated hGH, reported in figure 4.24, were determined in Sprague-Dawley rats. The rats were randomly divided into two groups of 3 animals per group. A dose of 0.1 mg/kg hGH (equiv.) was administered via tail vein. The hGH content in serum samples was quantified using the hGH ELISA kit. The pharmacokinetic data elaboration was performed by *PkSolver* program applying a bicompartmental model.

The hGH level for native protein decreased rapidly at 30 min post-injection and fell to below the detection limit after 3 h. hGH-PLE$_{50ald}$ showed an higher

prolongation of the half-life, with detectable levels of hGH up to 6 h. Conjugation with PLE_{50ald} led to an increase in blood residence time. Main pharmacokinetic parameters are shown in table 4.6.

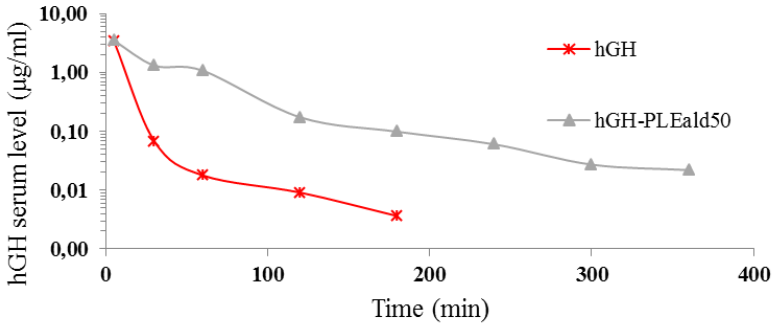

Figure 4.24: Pharmacokinetic best-fit profiles of hGH and hGH-PLE_{50ald}.

Table 4.6: Main pharmacokinetic parameters after *i.v.* administration in rats.

Compounds	$t_{1/2}$ β (min)	$AUC_{(0\rightarrow\infty)}$ (µg min/mL)	Cl (mL/min)	V_D (mL)
hGH	58.64	49.07	0.61	3.7
hGH-PLE_{50ald}	43.74	169.97	0.18	2.14

4.3.4 Pharmacodynamic of hGH, hGH-PLE_{50ald}, PEG-Gln141-hGH and PEG-Nter-hGH in hypophysectomized rats.

The bioactivity of hGH-PLE_{50ald}, PEG-Gln141-hGH and PEG-Nter-hGH was investigated in hypophysectomized rats by comparing the stimulation of somatic growth of conjugates and hGH. The free protein was administered for 6 days with a daily dose of 30 µg/rat while the conjugates were given as single injection of 180 µg/rat at first day. PEG-Gln141-hGH and PEG-Nter-hGH achieved the same weight gain as hGH and hGH-PLE_{50ald} demonstrated only a slight decrease in the potency respect to the other samples (Figure 4.25), thus confirming that the prolonged half lives of conjugates, lead to a great exposure of the protein achieving finally a good bioactive response even with a single dose per week. hGH, hGH-PLE_{50ald}, PEG-Gln141-hGH and PEG-Nter-hGH treatments promoted body weight gain with respect to the control (Table 4.7).

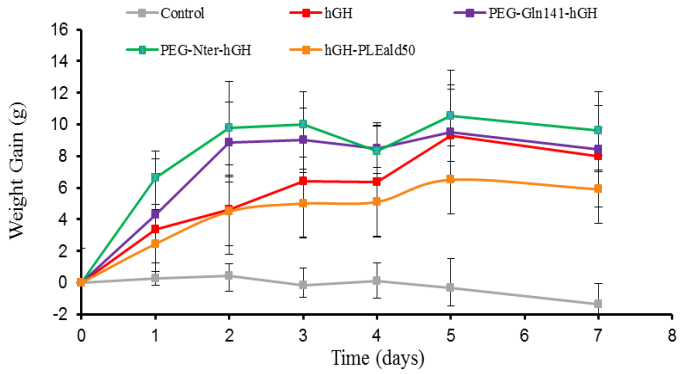

Figure 4.25: Weight gain in hypophysectomized rats given daily, via tail vein, injections of hGH (6 × 30 μg/rat) or one weekly dose of hGH-PLE$_{50ald}$, PEG-Gln141-hGH or PEG-Nter-hGH (1 × 180 μg/rat, protein equivalent).

The length of femur and the width of the tibial cortical bone tissue of diaphysis were determined in all animals at the end of the study. Compared to the control, the lengths of the femurs were significantly enhanced in hGH and hGH conjugates treated groups (Figure 4.26). In particular the increasing of bone length induced by PEG-Gln141-hGH and PEG-Nter-hGH was greater than one promoted by native protein and hGH-PLE$_{50ald}$; 3.5% and 4.4% for conjugate respectively, vs. 2.2% and 2.4% for hGH and hGH-PLE$_{50ald}$.

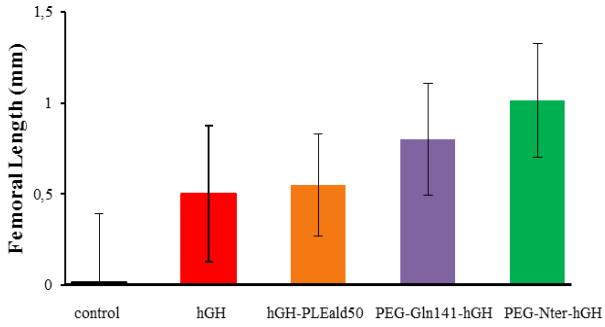

Figure 4.26: Femoral length gains in hypophysectomized rats given daily, via tail vein, injections of hGH (6 × 30 μg/rat) or one weekly dose of hGH-PLE$_{50ald}$, PEG-Gln141-hGH or PEG-Nter-hGH (1 × 180 μg/rat, protein equivalent).

The widths of tibial diaphysis demonstrated that the groups treated with hGH or hGH conjugates had a higher values with respect to the PBS-treated group. Also for this growth parameter, single injection of hGH-PLE$_{50ald}$, PEG-Gln141-hGH or PEG-Nter-hGH showed similar results with respect daily administrations of hGH. Representative stained sections of the tibial diaphysis are shown in Figure 4.27: the tibial compact bone of diaphysis is thicker in C (hGH-PLE$_{50ald}$), D (PEG-Gln141-hGH) and E (PEG-Nter-hGH) than A (vehicle) and B (hGH). The percentage growth of the width of the tibial cortical bone tissues was 8.1%, 11.6%, 13.4% and 2.1% for

hGH-PLE$_{50ald}$, PEG-Gln141-hGH, PEG-Nter-hGH and hGH treated-groups, respectively.

Cumulative body weight gain, femoral length and tibial diaphysis width measurements for the different groups are presented in Table 4.7. A weekly administration of hGH-PLE$_{50ald}$, PEG-Gln141-hGH or PEG-Nter-hGH has shown similar bioactivities with respect to daily administrations of hGH, suggesting that the conjugates have prolonged the protein exposure to this receptor. The way in which the PEG chains are arranged around the protein is fundamental for the protein/receptor recognition process and, accordingly, also the site of polymer coupling. In this case, the results suggest that the steric entanglement of the polymer chain had a similar output for both conjugates.

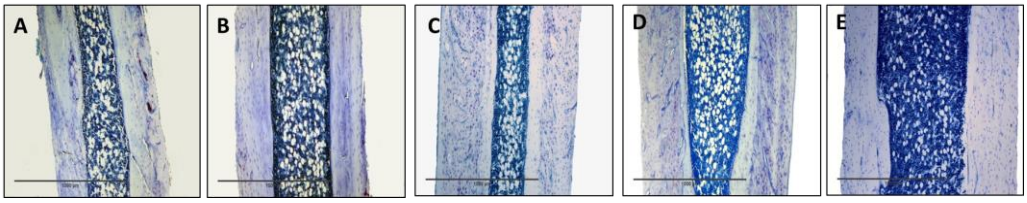

Figure 4.27: Representative stained sections of tibial diaphysis of hypophysectomized rats receiving, via tail vein, injections of A) vehicle every day; B) hGH 30 µg every day; C) hGH-PLE$_{50ald}$, D) PEG-Gln141-hGH and E) PEG-Nter-hGH 180 µg the first day.

Table 4.7: Effects of every-day (ED) administration of vehicle solution and hGH for 6 d, and first-day (FD) administration of hGH-PLE$_{50ald}$, PEG-Gln141-hGH and PEG-Nter-hGH on body weight gain, femoral length and tibial diaphyses width in hypophysectomized rats.

Compound	Dose and frequency	Cumulative body weight gain (g)	Femoral length (mm)	Width of tibial diaphysis cortical bone (µm)
Vehicle	150 µL × day	-1.37 ± 1.28	22.90 ± 0.38	334.21 ± 38.64
hGH	30 µg × day	7.98 ± 3.2	23.40 ± 0.37	341.19 ± 30.58
hGH-PLE$_{50ald}$	180 µg × week	5.9 ± 2.31	23.45 ± 0.28	361.21 ± 116.94
PEG-Gln141-hGH	180 µg × week	8.4 ± 1.4	23.70 ± 0.31	373.08 ± 44.96
PEG-Nter-hGH	180 µg × week	9.6 ± 2.49	23.92 ± 0.31	379.03 ± 25.43

4.4 SYNTHESIS AND CHARACTERIZATION OF PEG-KR14 CONJUGATE

4.4.1 Synthesis of KR14

Before to synthesized the KR14, the azidoproline was prepared according to the procedure reported in section 3.6.1 and the yield was 79.5%.

The peptide triazole KR14 was then synthesized by CEM microwave synthesis using Fmoc chemistry on a Rink amide resin at a 0.25 mM scale and after the assembling of the residues, it was undergone to *N*-terminal protection with the t-Boc group, click reaction in order to link the ethynylferrocene with a cycloaddition, cleavage from the resin and deprotection of the *N*-terminal. After the recovery, the crude peptide was dissolved in 50% ACN/H_2O and purified by RP HPLC on a preparative C18 column. The final purified peptide were lyophilized and validated by MALDI-TOF mass spectrometry (Figure 4.28)

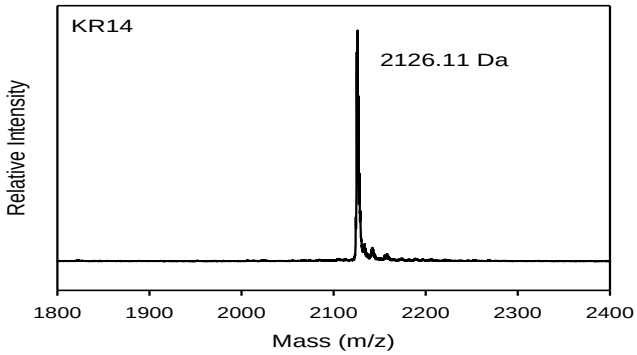

Figure 4.28: ESI-TOF mass spectrum of KR14.

4.4.2 Synthesis of PEG-KR14

KR14 was designed to contain a free thiol group at position 16. This single thiol group has been exploited to achieve selective PEGylation trough a Michael addition. This conjugation prevents the formation of peptide dimers. Moreover, the position 16 is far from the pharmacophore that is formed by the first 7 amino acids. This approach should minimize the expected activity decrease of PT after PEGylation that, as known, is due to the detrimental effect of PEG steric entanglement on the binding kinetics.

The conjugation reactions were monitored by SEC-HPLC. Figure 4.29 reported the time course of the conjugation of PEG-KR14. The disappearance over the time of the peak of free peptide (t_R= 32.31 min) corresponded to the appearance of a new peak (t_R= 19.37 min), in agreement with the formation of PEG-KR14 conjugate that has a higher hydrodynamic volume. The purification was carried out by dialysis and

was considered satisfactory when the peak of the starting peptide (t_R around 31 min) had disappeared. Conjugation of PEG-Mal to peptide led to a reaction yield of about 46%. After purification, the conjugate presented a content of free PEG of 36% and no free peptide.

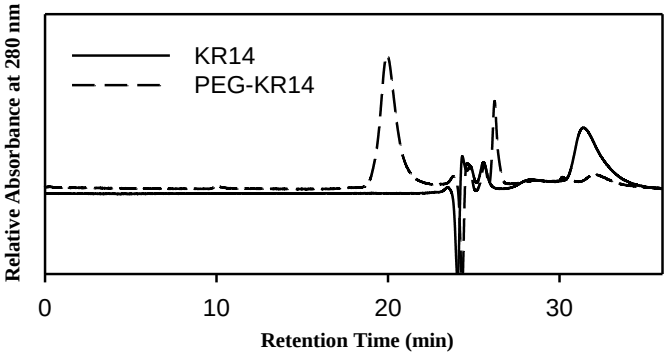

Figure 4.29: Elution profile of KR14 and PEG-KR14.

The monoconjugates were analyzed by MALDI-TOF mass spectrometry. The results showed that a monoPEGylated product was present with a MW centered at 23815 Da corresponding approximately to the sum of one chain of PEG-Mal conjugated to KR14 (Figure 4.30).

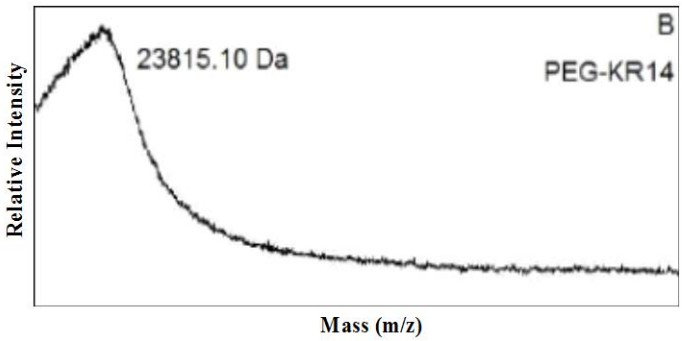

Figure 4.30: MALDI-TOF mass spectrum of PEG-KR14.

4.4.3 Pharmacokinetic studies of KR14 and PEG-KR14

The pharmacokinetic profiles of PEG-KR14 and free KR14 were evaluated in rats by labeling the peptide moiety with fluorescein.

4.4.3.1 *Preparation of 5-FM-KR14*

KR14 was labeled with fluorescein exploiting the free thiol group. The reaction was conducted as reported in section 3.6.4.1 and was monitored and purified by RP-HPLC (Figure 4.31). The product was then characterized by ESI-TOF analyses (Figure 4.32).

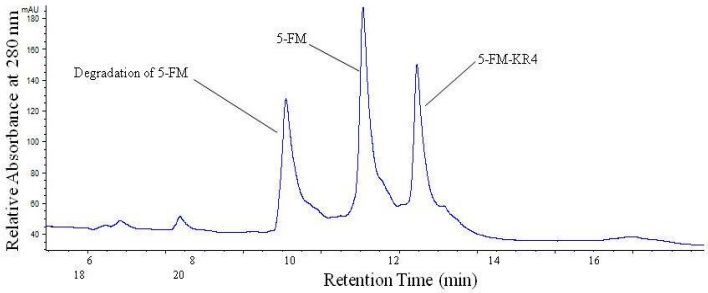

Figure 4.31: Elution profile of 5-MF-KR14 on Agilent C18 (4.6 × 250 mm). The separation was achieved by a linear gradient of 20-70% acetonitrile containing 0.1% TFA over a 25 min period. The effluent from the column was monitored at 280 nm.

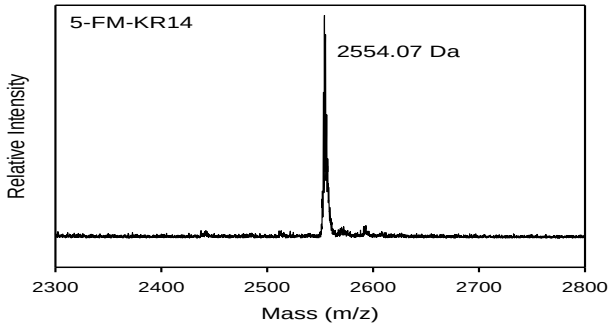

Figure 4.32: ESI-TOF mass spectrum of 5-FM-KR14.

4.4.3.2 *Preparation of FITC-PEG-KR14*

PEG-KR14 was labeled with fluorescein through the N-terminal amino group of the peptide. The reaction was conducted as reported in section 3.6.4.2 and the products was purified by dialysis and analyzed by SEC-HPLC (Figure 4.33).

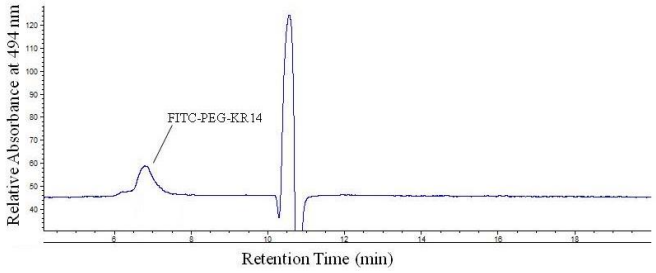

Figure 4.33: Purification profile of FITC-PEG-KR14 on Agilent Zorbax GF-250 (4.6 × 250 mm). The effluent from the column was monitored at 494 nm.

4.4.3.3 Pharmacokinetics

The pharmacokinetic profiles of free and conjugated peptide were determined in Balb/C mice after i.v administration.

As shown in figure 4.34, after administration, the plasma levels of PT decreased fast and it was not detectable (LOD = 0.8 ng/mL) after 150 min. On the contrary, PEG-KR14 showed a marked half-life prolongation with detectable levels after 360 min. PEGylation greatly increased the blood residence time. In fact, the half-life of KR14 increased from 44.42 to 288.75 min after PEGylation (Table 4.8). Also the AUC of PEG-KR14 increased 8-9 fold with respect to free PT.

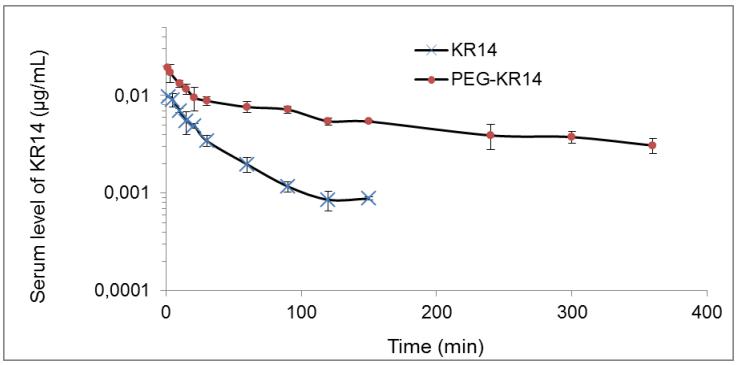

Figure 4.34: Pharmacokinetic profile of native KR14 and PEG-KR14 in mice.

Table 4.8: Main pharmacokinetic parameters of KR14 and PEG-KR14 after i.v. administration in mice.

Compounds	$t_{1/2}$ α (min)	$t_{1/2}$ β (min)	$AUC_{(0\rightarrow\infty)}$ (µg min/mL)	Cl (mL/min)	V_D (mL)
KR12	16	39.37	0.49	2.551	145.18
KR14	22.95	44.42	0.34	3.850	246.82
PEG-KR12	31.94	315	3.55	0.386	175.51
PEG-KR14	21.79	288.75	3.08	0.462	192.36

4.4.4 Surface Plasmon Resonance competition experiments

To compare the affinity of KR14 and PEG-KR14 for the gp120, surface plasmon resonance (SPR) competition experiments were conducted. The competition experiment provides the immobilization of the ligands (CD4 and 17b mAb, receptor and co-receptor) on a chip and the passage, over the surface, of a fixed solution of gp120 mixed to different amounts of native or modified peptide. 17b mAb is a co-receptor surrogate that binds a gp120 epitope that is increased in exposure following CD4 binding. The experiment has allowed to evaluate the binding of KR14 and PEGylated PT to gp120 in the presence of CD4 and 17b mAb, and the inhibitory effects of peptide and conjugate on interactions of gp120 at its CD4 and co-receptor binding sites.

In figure 4.35 is reported an example of sensorgram derived from a CD4 competition experiment for KR14 and table 4.9 shows the IC_{50} values of KR14 and PEG-KR14 for the same experiment. Table 4.10 shows the IC_{50} values of KR14 and PEG-KR14 for the mAb 17b competition experiment.

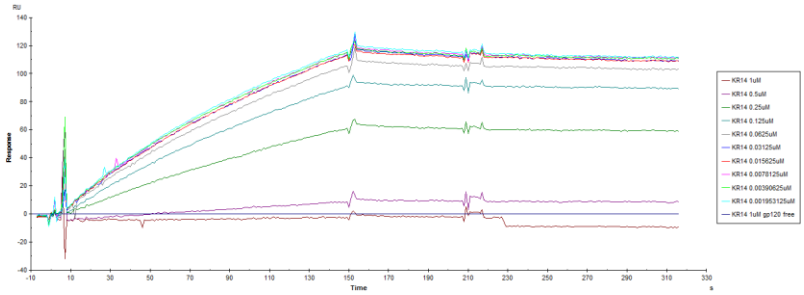

Figure 4.35: Inhibition of binding of gp120 to CD4 by KR14. CD4 was immobilized on the biosensor chip surface and gp120 was passed over the surfaces in solution with increasing concentrations of peptide.

Table 4.9: Main IC_{50} values for KR14 and PEGKR14 measured by CD4 competion experiment.

	IC_{50} (nM)
KR14	258.5 ± 14.7
PEG-KR14	387.57 ± 29.4

Table 4.10: Main IC_{50} values for KR14 and PEGKR14 measured by mAb 17b competion experiment.

	IC_{50} (nM)
KR14	246.5 ± 20.1
PEG-KR14	395.16 ± 8.6

The experiment has allowed to evaluate the binding of KR14 and PEGylated PT to gp120 in the presence of CD4 and 17b mAb, and the inhibitory effects of peptide and conjugate on interactions of gp120 at its CD4 and co-receptor binding sites. After PEGylation, no significant variations in the activity of the peptide were found, both for the CD4 and 17b mAb competition. Referring to IC_{50} values, PEG-KR14 was only about 1.5, 1.6 fold less active than free peptide. These results indicated that, after PEGylation, the peptide retained a significant activity in inhibiting the interactions of gp120 at its CD4 and co-receptor binding sites. The preservation of peptide activity after PEGylation is a promising result because usually the coupling of a such high molecular weight PEG causes a great loss of the peptide/protein activity.

5 DISCUSSION

In the last years PEGylation has become the leading approach for proteins and peptides delivery and, therefore, this technique had and will have also in the future a central role for the full exploitation of biologics.

The work reported in this thesis is focused on the design and preparation of polymer conjugates of therapeutic proteins and peptides. These systems have been studied for the obtainment of an improved balance between the pharmacokinetic and the pharmacodynamic of a conjugated biologic and for the optimization of the polymeric carrier. Any new discovered protein coming, thanks to the completion of human genome project, nowadays, might represent a new target for highly specific therapies, or might even, itself, become a new drug. Therefore the demand of protein and peptide delivery systems is expected to increase in the future. As demonstration, the number of PEGylated products on the market is continuously increasing, together with the number of new conjugates entering clinical trials.

This growing success, however, is not devoid of pitfalls, and often the therapeutic exploitation of a new protein or peptide is hampered by unexpected shortcomings. Among these potential limits it is possible to list: i) rapid renal clearance, ii) immunogenicity, iii) susceptibility to enzymatic degradation and iv) physical and chemical instabilities. In particular, a short half-life in blood is a significant problem because is reflected in frequent administration schedule of the biologic or in the injection of an high dose, to achieve the desired effect, thus also aggravating the side effects. The coupling of a polymeric carrier and in particular of PEG to a biologic drug, has demonstrated the advantage to overcome most of the aforementioned limits of biologics by acting on several aspects. For example, PEGylation reduces the rapid kidney clearance of a given protein or peptide by increasing their hydrodynamic volume, prevents immunogenicity and aggregation by shielding the protein surfaces and also increases the thermal stability. Although a reduction in biological potency is usual after PEGylation, due to the steric entanglement of polymer chains during recognition of the protein or the peptide with their targets, the advantages of this approach largely counterbalance this drawback.

The studies of this PhD has been organized into three works. The first study focused in the conjugation of common non charged or new multicarboxylic PEGs to G-CSF, a therapeutic protein presently in clinical use. G-CSF is a hematopoietic growth factor of myeloid lineage, involved in the proliferation, differentiation, and survival of granulocytes (neutrophils, eosinophils, and basophils). The aim was to extend the PK profile of the protein with polyanionic PEG that should allow a better preservation of protein activity.

The rationale of using multicarboxylic PEGs, in particular, lies in the recent understanding of the charge-selectivity concept of glomerular filtration. The idea is to exploit this concept to achieve further prolonged protein pharmacokinetics while reducing the possible impairment in protein pharmacodynamics caused by the steric hindrance of high-molecular weight PEGs.

The first part of the work was composed of two main sections: preparation of G-CSF-PEG conjugates via mTGase-mediated PEGylation, with the subsequent characterization and stability analyses, and pharmacokinetic studies of the conjugates in rats. In fact it was of paramount relevance also to understand the role of multicorboxylic PEG on the stability and physic-chemical properties of a given protein.

Four different PEGylated derivatives of G-CSF were prepared via mTGase-mediated PEGylation. The PEGs used included two multicarboxylic and two neutral PEGs. Of the multicarboxylic PEGs the following derivatives were studied: 1) H_2N-PEG_{5k}-$(COOH)_7$ (MW 5717 Da), a PEG-dendron obtained from a heterobifunctional PEG that was derivatized at one end with β-glutamic acid as branching units to provide 7 carboxyl groups, and with a primary amino group on the other end for enzyme-mediated protein conjugation, 2) H_2N-$PEG_{3.4k}$-b-PLE_{50} (MW 11000 Da), a linear PEG of 3.4 kDa linked to a PLE of 50 L-glutamic acid units. Two neutral PEGs, $mPEG_{5k}$-NH_2 and $mPEG_{20k}$-NH_2, were also used to allow comparison of the pharmacokinetic profiles between the conjugates, thus enabling to assess the influence of negatively charged polymers on protein pharmacokinetics. The yields of reaction for negatively charged PEGs were even higher with respect to neutral PEGs. The results confirmed that the conjugates were pure and mono-PEGylated as showed by SDS-PAGE and MALDI mass spectrometry. Circular dichroism was used to investigate the effect of this type of conjugation on the secondary structure of G-CSF. As the purification conditions may also affect the conformation of a protein, a G-CSF sample, purified under the same conditions of the conjugates, was also included in this study. CD investigation showed that there was no significant change in the secondary structure of G-CSF after PEGylation. Melting profiles, obtained by monitoring the protein unfolding as a function of temperature, revealed that the thermal stabilities of all conjugates were quite similar to each other and to that of G-CSF purified with the same conditions. However, they seemed to be less stable with respect to the native G-CSF. These findings suggested that the decrease in the stability of G-CSF after PEGylation may be due to the purification conditions or eventually to the different buffer, i.e. acetate pH 4.6 for native G-CSF and phosphate pH 7.4 for conjugates. Resolving this issue also by exploring more suitable purification conditions remains a future scope of this project.

The pharmacokinetic studies of the native G-CSF and its PEGylated derivatives in rats showed, firstly, that the native G-CSF had an elimination half-life of 2.99 hours, in accordance with the data reported in literature and its plasma level fell below the detection limit after 7 hours. Conversely all PEGylated G-CSF derivatives showed prolonged half-lives (up to 11 hours), with detectable serum G-CSF levels even after 24 hours, as well as markedly reduced clearance and volume of distribution. G-CSF-PEG_{5k}-$(COOH)_7$ and G-CSF-$PEG_{3.4k}$-b-PLE_{50}, obtained with the multicarboxylate PEGs of 5717 Da and 11000 Da, showed half-lives comparable to that of G-CSF-PEG_{20k}, prepared with a neutral PEG of 20 kDa.

Based on these data, it can be proposed that the presence of negative charges on the polymer results in conjugates with an increased half-life, with respect to the conjugates obtained with neutral PEGs of similar molecular weights. Therefore, in order to significantly improve the pharmacokinetic profile of proteins, polyanionic PEGs with lower molecular weights than those required with neutral PEGs may be considered as protein carriers, thus reducing the typical steric hindrance of high molecular weight PEG that might impair the biological function of proteins.

The second part of the PhD thesis focused on the comparison of the biological activity (stimulation of somatic growth) of three hGH conjugates differing for the polymeric carrier (multicarboxylic or neutral form) and for the site of polymer conjugation. hGH is a therapeutic protein involved in growth promotion, stimulation of protein synthesis, lipolysis and regulation of metabolic processes. The aim of this study was to evaluate if the protein stability and the protein/receptor recognition process were influenced by the site of conjugation of the polymer and to assess the impact of polyanionic carriers on the pharmacodynamic behaviour of the protein.

Conjugation of the multicarboxylic polymer, poly(L-glutamic acid), resulted in an increase of the final negative charge of the conjugate. The rationale of the use of negatively charged polymers for protein delivery has been above reported. The possibility to obtain the same half-life prolongation with low molecolar weight negative polymer might allow: i) a faster diffusion of the conjugate into the tissues, thanks to the lower hydrodinamic volume of the polymer, ii) a better preservation of the binding affinity of the protein to its receptor, thanks to the lower steric hindrance provided by the polymer and iii) a decrease of protein aggregation due to charge repulsion.

Two different site-specific mono-PEGylated forms of hGH were prepared exploiting an enzymatic PEGylation (PEG-Gln141-hGH) via transglutaminase (TGase) and a chemical *N*-terminal PEGylation (PEG-Nter-hGH) with neutral 20kDa PEGs. The enzymatic PEGylation was performed in presence of 50% of EtOH (v/v) in order to increase the selectivity of mTGase. Usually, only one or two glutamines, present in a highly flexible region, are substrate for the enzyme, but, it is known from literature that, incubating the protein in a proper water/organic co-solvent mixture, it is possible to increase the rigidity of the native protein, thus finally restricting the mTGase selectivity which need a glutamine inserted in a flexible bag for performing its activity. The chemical PEGylation was conducted in acidic conditions to direct the modification at the *N*-terminus, thanks to the lower *pKa* value of α-amino group with respect to the ε-amino groups. The conjugates were obtained with different yields: 40% for PEG-Gln141-hGH and 52% for PEG-Nter-hGH. The success of the synthesis was determined by RP and SEC-HPLC, MALDI-TOF mass spectrometry and SDS-PAGE. The conjugates were pure and mono-PEGylated. The sites of PEGylation were previously confirmed by our research group [Mero 2011 and Freitas 2013]. Far-UV CD spectra of native protein and PEG-hGH conjugates were compared and showed that both the *N*-terminus or the Gln141 PEGylation preserved

the protein's secondary structures, as the profiles were superimposable with that of hGH. Thermal denaturation was carried out to investigated if the different PEGylation site caused a difference in the thermal stability of the two conjugates, by evaluating the changes in the ellipticity at 208 nm. The melting temperature calculated for native protein and PEG-Gln141-hGH were 82°C and 83.8°C, respectively. PEG-Nter-hGH displayed a higher thermal stability, with a melting temperature of 86.1°C.

Reversibility of the thermal unfolding was determined by measuring the recovery of the CD signal upon heating at 95°C and cooling at 20°C the hGH and PEGylated hGH solutions. The CD spectra at 95°C showed the disappearance of the bands at 222 and 208 nm, characteristic of hGH α-helical structure in physiological conditions. This means that at 95°C the three samples lost their native α-helical structure but the conjugates, even at such high temperature, tend to preserve a certain percentage of α-helical structure with respect to hGH. Moreover the transition was reversible and partially reversible for PEG-Nter-hGH and PEG-Gln141-hGH, respectively, opposing to the permanent denaturation of hGH and in particular, PEG-Nter-hGH showed a total recovery of the native α-helical structure. These results indicated that PEGylation increased thermal stability of hGH and favored the protein refolding, but for a complete recovery, the site of PEG conjugation is relevant. Probably this behavior depends on the way the PEG chain is arranged around the protein, likely in the case of protein *N*-terminus conjugation, the polymer is more effective in stabilizing the protein.

The third site-specific monoconjugate of hGH was prepared by chemical *N*-terminal conjugation via aldehyde, using poly(L-glutamic acid) (PLE). PLE is obtained by polymerization of β-glutamic acid, therefore is biodegradable and non-toxic. It has a linear structure with a pending ϒ-carboxyl group for each repeated glutamic acid unit, conferring the polymer a polyanionic characteristic. In this case a PLE with 50 glutamic acid units and with an aldehyde function at one end (PLE_{50ald}) was chosen. After the removal of the protecting acetal group from PLE_{50ald}, several reaction conditions were tested to find out the most efficient. Reaction buffer, polymer molar excess and incubation temperature were varied. Phosphate buffer, pH 6.2 was found to be the buffer in which the yields of reaction were the highest. Moreover, the increase of the polymer molar excess and also of the temperature led to an increase in the biconjugate formation, suggesting to performed the reaction using 5 equivalents of polymer and at 35°C. The conjugate hGH-PLE_{50ald} was obtained with a yield of 55%. The success of the synthesis was determined by SEC-HPLC, MALDI-TOF mass spectrometry and SDS-PAGE. The conjugates were pure and formed by one chain of polymer attached to the protein. Far-UV CD spectra showed that hGH still maintained the native secondary structure thus indicating that the conjugation with PLE_{50ald} preserved the protein conformation.

Pharmacokinetics of the native hGH and hGH-PLE_{50ald} in rats, and subsequent evaluation of their pharmacokinetic profiles, showed a rapidly decrease, post-

injection, of the hGH level for native protein while hGH-PLE_{50ald} demonstrated an higher prolongation of the half-life, with detectable levels of hGH up to 6 h, indicating that also the conjugation with PLE_{50ald} led to an increase in blood residence time.

Pharmacodynamics allowed to compared the bioactivity of hGH, hGH-PLE_{50ald}, PEG-Gln141-hGH and PEG-Nter-hGH in the stimulation of somatic growth in hypophysectomized rats, unable to produce somatotropin. In particular, daily administrations (dose of 30 μg/rat) of hGH were compared to single injections (dose 180 μg/rat) at first day of conjugates. In the weight gain test, the body weight was measured every day for 6 days. PEG-Gln141-hGH and PEG-Nter-hGH were found to achieve the same weight gain as hGH and hGH-PLE_{50ald} demonstrated only a slight decrease in the potency respect to the other samples. This confirmed that the prolonged half lives of conjugates, lead to a great exposure of the protein reaching finally a good bioactive response even with a single dose per week. At day 7, the mean of femur lengths was also determined. Compared to the control, the lengths of the femurs were significantly enhanced in hGH and in all hGH conjugates treated groups. In particular the increase of bone length induced by PEG-Gln141-hGH and PEG-Nter-hGH was greater than one promoted by native protein and hGH-PLE_{50ald}; 3.5% and 4.4% for conjugate respectively, vs. 2.2% and 2.4% for hGH and hGH-$PLEald_{50}$. Also the evaluation of the widths of tibial diaphysis demonstrated that the groups treated with hGH or hGH conjugates had a higher values with respect to the PBS-treated group. Single injection of hGH-PLE_{50ald}, PEG-Gln141-hGH or PEG-Nter-hGH showed similar results with respect daily administrations of hGH. The percentage growth of the width of the tibial cortical bone tissues was 8.1%, 11.6%, 13.4% and 2.1% for hGH-PLE_{50ald}, PEG-Gln141-hGH, PEG-Nter-hGH and hGH treated-groups, respectively.

As conclusion of this study, it is possible to assert that: i) a weekly administration of hGH-PLE_{50ald}, PEG-Gln141-hGH or PEG-Nter-hGH had similar bioactivities with respect to daily administrations of hGH; ii) the conjugates have prolonged the protein exposure to the receptor, both in case of neutral and polyanionic conjugation. hGH-PLE_{50ald} had only a slight decrease in the performance with respect the hGH-PEG_{20kDa} conjugates but comparable to that of daily administration of the native protein; iii) the *N*-terminal PEGylation yielded a conjugate with an higher thermal stability and, in particular, it was able to recover the secondary structure after thermal denaturation, but in this case, the results suggested that the steric entanglement of the polymer chain had a similar output for both the conjugation strategies.

The way in which the PEG chains are arranged around the protein is fundamental for the protein/receptor recognition process and, accordingly, also the site of polymer coupling. This point is crucial because the protein function is known to be strictly related to the preservation of its native structure. Therefore, the possibility to obtain by PEGylation more stable proteins or even proteins that can refold spontaneously

after denaturation might represent an important achievement. Interestingly, we have also demonstrated that this stabilization is depending on the site of polymer coupling, this suggesting that PEG might have an active role in promoting the refolding.

The third part of this PhD thesis has dealt with: synthesis and characterization of KR14 peptide and its conjugation with PEG_{20kDa}-Mal, SPR affinity binding experiments and pharmacokinetic studies of the conjugate in mice. Peptide triazole KR14 bind to the envelope glycoprotein gp120 of HIV-1 with 1:1 stoichiometry inhibiting the interactions at both the CD4 and co-receptor binding sites and is broadly active in neutralizing cell infection by virus subtypes from all major clades. For the synthesis of KR14, azidoproline was previously prepared and obtained with a yield of 79.5%. Then KR14 was synthesized using a CEM microwave synthesizer, *N*-terminal protected with the t-Boc group, the ethynylferrocene was linked by click reaction, it was cleaved from the resin and deprotected at the *N*-terminus. The final purified peptide was lyophilized and validated by MALDI-TOF mass spectrometry, revealing a MW of 2126 Da. KR14 was designed to contain a free thiol group at position 16. This single thiol group has been exploited to achieve selective PEGylation through the maleimide of the 20 kDa PEG. This conjugation prevents the formation of the peptide dimer. The position 16 is also far from the pharmacophore that is formed by the triplet Ile-Azp-Trp (positions 5, 6 and 7). This approach should minimize the expected activity decrease of the peptide after PEGylation that, as known, is due to the detrimental effect of PEG steric entanglement on the binding kinetics. Conjugation of PEG-Mal to peptide led to a reaction yield of 46%. The monoconjugate was analyzed by SEC-HPLC and MALDI-TOF mass spectrometry. The results showed that a monoPEGylated product was present with a MW centered at 23815 Da corresponding approximately to the sum of one chain of PEG-Mal (MW 21000 Da) with one molecule of KR14.

The pharmacokinetic profiles of PEG-KR14 and free KR14 were evaluated in mice, after the labelling with fluorescein. After administration, the plasma levels of KR14 decreased fast and it was not detectable after 150 min. PEGylation greatly increased the blood residence time. In fact, the half-life of KR14 increased from 44.42 to 288.75 min after PEGylation and also the AUC of PEGylated PT increased 8-9 fold with respect to free peptide.

To compare the affinity of KR14 and PEG-KR14 for the gp120, surface plasmon resonance (SPR) competition experiments were conducted. The competition experiment provides the immobilization of the ligands (CD4 and 17b mAb, receptor and co-receptor) on a chip and the passage, over the surface, of a fixed solution of gp120 mixed to different amounts of native or modified peptide. 17b mAb is a co-receptor surrogate that binds a gp120 epitope that is increased in exposure following CD4 binding. The experiment has allowed to evaluate the binding of KR14 and PEGylated KR14 to gp120 in the presence of CD4 and 17b mAb, and the inhibitory effects of peptide and conjugate on interactions of gp120 at its CD4 and co-receptor binding sites. After PEGylation, no significant variations in the activity of the

peptide were found, both for the CD4 and 17b mAb competition. The CD4 competition IC_{50} values for KR14 and PEG-KR14 were, respectively, 258.5 ± 14.7 nM and 387.57 ± 29.4 nM, while the IC_{50} calculated after the 17b mAb competiton experiment were 246.5 ± 20.1 nM for the peptide and 395.16 ± 8.6 nM for the PEGylated KR14. PEG-KR14 was only about 1.5, 1.6 fold less active than free peptide. This results indicated that, after PEGylation, the peptide retained a significant activity in inhibiting the interactions of gp120 at its CD4 and co-receptor binding sites. The preservation of peptide activity after the PEGylation, is a promising result because usually the coupling of a such high molecular weight PEG causes a great loss of the peptide/protein activity.

6 REFERENCES

[1] B. Leader, Q.J. Baca, D.E. Golan, Protein therapeutics: a summary and pharmacological classification, *Nat. Rev. Drug Discovery* 7 (2008) 21–39.

[2] D. Platis, N.E. Labrou, Chemical and genetic engineering strategies to improve the potency of pharmaceutical proteins and enzymes, *Curr. Med. Chem*. 15 (2008) 1940–1955.

[3] L. Jorgensen, H.M. Nielson, Delivery Technologies for Biopharmaceuticals: Peptides, Proteins, Nucleic Acids and Vaccines, *JohnWiley & Sons, Ltd.,West Sussex* (U.K, 2009.

[4] Veronese FM and Pasut G, PEGylation: Posttranslational bioengineering of protein biotherapeutics, *Drug Discovery Today: Technologies* 5 (2-3) (2008), 57-64.

[5] C. Dhalluin, A. Ross, L.A. Leuthold, S. Foser, B. Gsell, F. Müller, H. Senn, Structural and biophysical characterization of the 40 kDa PEG-interferon-alpha2a and its individual positional isomers, *Bioconjug. Chem*. 16 (3) (2005) 504–517.

[6] A. Basu, K. Yang, M. Wang, S. Liu, R. Chintala, T. Palm, H. Zhao, P. Peng, D. Wu, Z. Zhang, J. Hua, M.C. Hsieh, J. Zhou, G. Petti, X. Li, A. Janjua, M. Mendez, J. Liu, C. Longley, Z. Zhang, M. Mehlig, V. Borowski, M. Viswanathan, D. Filpula, Structure-function engineering of interferon-beta-1b for improving stability, solubility, potency, immunogenicity, and pharmacokinetic properties by site-selective mono-PEGylation, *Bioconjug. Chem*. 17 (2006) 618–630.

[7] F. Meng, B.N. Manjula, P.K. Smith, S.A. Acharya, PEGylation of human serum albumin: reaction of PEG-phenyl-isothiocyanate with protein, *Bioconjug. Chem.* 19 (2008) 1352–1360.

[8] F.M. Veronese, A. Mero, F. Caboi, M. Sergi, C. Marongiu, G. Pasut, Site-specific pegylation of G-CSF by reversible denaturation, *Bioconjug. Chem.* 18 (2007)1824–1830.

[9] Giorgi ME, Agusti R, and Lederkremer RM, Carbohydrate PEGylation, an approach to improve pharmacological potency, *Beilstein J. Org. Chem.* 10 (2014), 1433–1444.

[10] L. Mariniello, R. Porta, Transglutaminases as biotechnological tools, in: K. Mehta, R. Eckert (Eds.), Transgluatminase, Prog. Exp. Tum. Res., vol. 38, Karger, Basel, 2005, pp. 174–191.

[11] D. Aeschlimann, M. Paulsson, Transglutaminases: protein cross-linking enzymes in tissues and body fluids, *Thromb. Haemost*. 71 (1994) 402–415.

[12] R. Griffin, R. Casadio, C.M. Bergamini, Transglutaminases: natures biological glues, *Biochem. J.* 368 (2002) 377–396.

[13] Rachel NM and Pelletier JN, Biotechnological Applications of Transglutaminases, Biomolecules 3 (2013), 870-888.

[14] T. Kashiwagi, K. Yokoyama, K. Ishikawa, K. Ono, D. Ejima, H. Matui, E. Suzuki, Crystal structure of microbial transglutaminase from Streptoverticillium mobaraense, *J. Biol. Chem*. 277 (2002) 44252–44260.

[15] K. Yokoyama, N. Nio, Y. Kikuchi, Properties and applications of microbial
transglutaminase, *Appl. Microbiol. Biotechnol*. 64 (2004) 447–454.

[16] H. Sato, Enzymatic procedure for site-specific PEGylation of proteins, *Adv. Drug Deliv. Rev*. 54 (2002) 487–504.

[17] Mero A, Spolaore B, Veronese FM, and Fontana A, Transglutaminase-Mediated PEGylation of Proteins: Direct Identification of the Sites of Protein Modification by Mass Spectrometry using a Novel Monodisperse PEG, *Bioconjugate Chem* 20 (2009), 384–389.

[18] Coussons PJ, Price NC et al, Factors that govern the specificity of transglutaminase-catalysed modification of proteins and peptides, *Biochem J* 282 (1992), 929-930.

[19] Fontana A, Spolaore B, Mero A, and Veronese FM, Site-specific modification and PEGylation of pharmaceutical proteins mediated by transglutaminase, *Advanced Drug Delivery Rev* 60 (2008), 13–28.

[20] Mero A, Schiavon M, Veronese FM, and Pasut G, A new method to increase selectivity of transglutaminase mediated PEGylation of salmon calcitonin and human growth hormone, *J of Controlled Release* 154 (2011), 27–34.

[21] Maddox DA, Deen WM, Brenner BM, Glomerular filtration. In *Handbook of Physiology. Renal Physiology*. Bethesda, MD: Am Physiol Soc, sect. 8, vol I, 13, (1992), 545-638.

[22] Miner JH, Glomerular filtration: the charge debate charges ahead, *Kidney International* 74 (2008), 259–261.

[23] Kanwar YS, Danesh FR, and Chugh SS, Contribution of Proteoglycans Towards the Integrated Functions of Renal Glomerular Capillaries, *American J of Pathology* 171-1 (2007), 139-143.

[24] Crea F, Giovannetti E, Zinzani PL, and Danesi R, Pharmacologic rationale for early G-CSF prophylaxis in cancer patients and role of pharmacogenetics in treatment optimization, *Critical Rev in Oncology/Hematology* 72 (2009), 21–44.

[25] Bendall LJ and Bradstock KF, G-CSF: From granulopoietic stimulant to bone marrow stem cell mobilizing agent, *Cytokine & Growth Factor Rev* (2014).

[26] Barreda DR, Hanington PC, and Belosevic M, Regulation of myeloid development and function by colony stimulating factors, *Developmental and Comparative Immunology* 28 (2004), 509–554.

[27] Greenbaum AM and Link DC, Mechanisms of G-CSF-mediated hematopoietic stem and progenitor mobilization, *Leukemia* 25 (2011), 211–217.

[28] Nervi B, Link DC, and DiPersio JF, Cytokines and Hematopoietic Stem Cell Mobilization, *J of Cellular Biochem* 99 (2006), 690–705.

[29] Oh-eda M, Hasegawa M et al, O-linked sugar chain of human granulocyte colony-stimulating factor protects it against polymerization and denaturation allowing it to retain its biological activity, *J Biol Chem* 265 (1990), 11432-11435.

[30] Hill CP, Osslund TD, and Eisenberg D, The structure of granulocyte-colony-stimulating factor and its relationship to other growth factors, Proc Natl Acad Sci USA 90 (1993), 5167-5171.

[31] Zhuge C, Lei J, and Mackey MC, Neutrophil dynamics in response to chemotherapy and G-CSF, *J Theoretical Biology* 293 (2012), 111–120.

[32] Vanz ALS, Renard G et al, Human granulocyte colony stimulating factor (hG-CSF): cloning, overexpression, purification and characterization, *Microbial Cell Factories* (2008) 7:13.

[33] Scaramuzza S, Tonon G et al, A new site-specific monoPEGylated filgrastim derivative prepared by enzymatic conjugation: Production and physicochemical characterization, *J of Controlled Release* 164 (2012), 355–363.

[33] Scaramuzza S, Tonon G et al, A new site-specific monoPEGylated filgrastim derivative prepared by enzymatic conjugation: Production and physicochemical characterization, *J of Controlled Release* 164 (2012), 355–363.

[34] Strobl, J. S.; Thomas, M., Growth hormone rapidly activates rat serine protease inhibitor 2.1 gene transcription and induces a DNA-binding activity distinct from those of Stat1,-3, and-4. *J. Pharmacol. Rev*. 1994, 46, 1.

[35] Rosen, T.; Bengtsson, Growth hormone therapy in elderly people, *B. A. Lancet* 1990, 336, 285.

[36] http://www.hgfound.org/pub_growth.html.

[37] Chantalat, L.; Jones, N. D.; Korber, F.; Navaza, J.; Pavlovsky, A. G., The crystal-structure of wild-type growth-hormone at 2.5 angstrom resolution, *Protein Pept.* Lett. 1995, 2, 333.

[38] De Vos, A. M.; Ultsch, M.; Kossiakoff, A. A., Human growth hormone and extracellular domain of its receptor: crystal structure of the complex, *Science* 1992, 255, 306.

[39] Ilondo, M. M.; Damholt, A. B.; Cunningham, B. A.; Wells, J. A.; De Meyts, P.; Shymko, R. M., Receptor dimerization determines the effects of growth hormone in primary rat adipocytes and cultured human IM-9 lymphocytes, *Endocrinology* 1994, 134, 2397.

[40] Pearce, K. H., Jr.; Cunningham, B. C.; Fuh, G.; Teeri, T.; Wells, J. A., Growth hormone binding affinity for its receptor surpasses the requirements for cellular activity, *Biochemistry*, 1999, 38, 81.

[41] Blethen, S. L.; Baptista, J.; Kuntze, J.; Foley, T.; LaFranchi, S.; Johanson, A., Adult height in growth hormone (GH)-deficient children treated with biosynthetic GH. The Genentech Growth Study Group. *J. Clin. Endocrinol. Metab.* 1997, 82, 418.

[42] Hu DJ, Subbarao S, Vanichseni S, et al. Frequency of HIV-1 dual subtype infections, including intersubtype superinfections, among injection drug users in Bangkok, Thailand. *AIDS*, 19, 303–308, 2005.

[43] Anna Maria Geretti, HIV-1 subtypes: epidemiology and significance for HIV management. *Current Opinion in Infectious Diseases*, 19, 1-7, 2006.

[44] Kwong, P. D., Human immunodeficiency virus: refolding the envelope. *Nature*, 433, 815–816, 2005.

[45] Chan, D. C., Fass, D., Berger, J. M., Kim, P. S., Core structure of gp41 from the HIV envelope glycoprotein. *Cell*, 89 (2), 263–273, 1997.

[46] Wyatt, R., Sodroski, J., The HIV-1 envelope glycoproteins: fusogens, antigens, and immunogens. *Science*, 280 (5371), 1884–1888, 1998.

[47] Gardner MB1, Luciw PA, Sawai ET, Marthas ML, Miller CJ, McChesney MB, Lerche NW, Pedersen NC., Simian retrovirus vaccines: simian retrovirus and simian immunodeficiency lentivirus, *AIDS Res Hum Retroviruses*. 1996 Mar 20;12(5):399-401.

[48] Lijun Wu, Norma P. Gerard, Richard Wyatt, Hyeryun Choe, Cristina Parolin, Nancy Ruffing, Alessandra Borsetti, Angelo A. Cardoso, Elizabeth Desjardin, Walter Newman, Craig Gerard, Joseph Sodroski, CD4-induced interaction of primary HIV-1 gp120 glycoproteins with the chemokine receptor CCR-5. *Nature*, 384, 179-183, 1996.

[49] Christopher C. Broder* and Ronald G. Collmant, Chemokine receptor and HIV. *Journal of Leukocyte Biology*, 62, 20-29, 1997.

[50] Cocchi F., De Vico AL, Garzino-Demo A, Cara A, Gallo RC, Lusso P., The V3 domain of the HIV-1 gp120 envelope glycoprotein is critical for chemokine-mediated blockade of infection. *Nat Med*, 2, 1244-1247, 1996.

[51] Willett B J, Hosie M J, Nell JC, Turner JD, Hoxie JA, Common mechanism of infection by lentiviruses. *Nature*, 385, 587, 1997.

[52] Umashankara M, McFadden K, Zentner I, Schon A, Rajagopal S, Tuzer F, Kuriakose SA, Contarino M, Lalonde J, Freire E, et al: The active core in a triazole peptide dual-site antagonist of HIV-1 gp120. *ChemMedChem* 2010, 5(11):1871–1879.

[53] Gopi H1, Cocklin S, Pirrone V, McFadden K, Tuzer F, Zentner I, Ajith S, Baxter S, Jawanda N, Krebs FC, Chaiken IM., Introducing metallocene into a triazole peptide conjugate reduces its off-rate and enhances its affinity and antiviral potency for HIV-1 gp120, *J Mol Recognit*. 2009 Mar-Apr;22(2):169-74. doi: 10.1002/jmr.892.

[54] Snyder, S. L. and Sobocinski, P. Z. (1975) An improved 2,4,6,-trinitrobenzenesulfonic acid method for the determination of amines. *Anal. Biochem.* 64, 284–288.

[55] Silva Freitas D1, Mero A, Pasut G., Chemical and enzymatic site specific PEGylation of hGH, *Bioconjug Chem.* 2013 Mar 20;24(3):456-63. doi: 10.1021/bc300594y. Epub 2013 Mar 4.